

Deciphering Novel Modes of Action of Lead Compounds with Antibacterial or Anti-virulence Activity against *Mycobacterium tuberculosis*



Inaugural-Dissertation

zur

Erlangung des Doktorgrades

der Mathematisch-Naturwissenschaftlichen Fakultät

der Universität zu Köln

vorgelegt von

Raphael Gries

aus St. Ingbert

Die vorliegende Arbeit wurde im Zentrum für Molekulare Medizin Köln (ZMMK) in der Abteilung für Bakterielle Pathogenese und Antibiotika-Entwicklung (Klinik I für Innere Medizin, Uniklinik Köln) angefertigt und wurde durch die Deutsche Forschungsgemeinschaft (DFG) und das Deutsche Zentrum für Infektionsforschung (DZIF) gefördert.

Gutachter: Prof. Dr. Oliver Cornely

Prof. Dr. Karin Schnetz

Tag der mündlichen Prüfung: 06.12.2023

„Bei dir fangt's jo frieh an!“

- Hiltrud Gries

„Some things just need to be done for the Peanut.“

1 Acknowledgements

Zuallererst möchte ich mich bei Herrn PD Dr. Dr. Jan Rybniker bedanken, der es mir ermöglicht hat, diese Arbeit und alle erforderlichen Experimente in der Abteilung für Bakterielle Pathogenese und Antibiotika-Entwicklung der Klinik I für Innere Medizin des Universitätsklinikums Köln durchzuführen.

Ebenfalls möchte ich Prof. Karin Schnetz und Prof. Oliver Cornely ganz herzlich für die Betreuung während der experimentellen Phase meiner Promotion als „Thesis advisory Committee“ und für die Übernahme der Begutachtung dieser Dissertation danken. Herzlichen Dank auch an Prof. Jürgen Dohmen für die Übernahme des Vorsitzes meines Prüfungskomitees.

Dr. Michael Dal Molin gilt mein Dank für die Betreuung und tatkräftige Unterstützung im Labor und bei wissenschaftlichen Fragestellungen. Neben Michael möchte ich auch Dr. Sebastian Theobald für angeregte wissenschaftliche Diskussionen und Unterstützung danken.

Ein besonderer Dank gilt auch Edeltraud van Gumpel, die mir alles Wichtige für das sichere Arbeiten in einem Labor der biologischen Sicherheitsstufe 3 beigebracht hat. Neben Edel gilt auch Jason Chhen mein Dank, da ihr mich immer direkt bei all meinen, zum Teil etwas verrückten Ideen, tatkräftig unterstützt habt. Auch Sandra Winter gehört mein Dank, die mich neben Edel direkt liebevoll im Labor aufgenommen und unterstützt hat.

Ich möchte hiermit auch den Kollegen aus der DZIF TTU Tuberkulose für die standortübergreifende Kooperation danken. Insbesondere möchte ich hier Prof. Stefan Niemann, Dr. Viola Dreyer, Dr. Lindsay Sonnenkalb und Dr. Christian Utpatel nennen. Mein Dank gilt weiterhin meinen internationalen Kollegen, mit deren Zusammenarbeit über Ländergrenzen hinweg exzellente Forschung möglich war. Besonderer Dank gilt hier Prof. Alain Baulaud, Dr. Kamel Djaout, Dr. Zainab Edoon und Prof. Kevin Pethe.

Selbstverständlich möchte ich auch allen weiteren Mitgliedern der TRU-ID danken, allen voraus Julie Mudler, Dinah Lange, Dr. Alexander Simonis und Dr. Alexandra Albus.

Dank geht außerdem an alle meine Freunde für ihre Unterstützung und Verständnis, allen voran natürlich meinen Peoplez, Dr. Dennis Schulze und Aileen Herrmann. Auch bei meinen Eltern und meiner Schwester möchte ich mich recht herzlich bedanken. Sie waren es, die mich in meiner Jugend und während meines Studiums unterstützt und ermutigt haben. Zu guter Letzt möchte ich mich bei Dr. Sabine Urban bedanken, ohne die ich jetzt nicht wüsste, wo ich wäre.

2 Table of Content

1	Acknowledgements.....	3
2	Table of Content	4
3	Introduction.....	6
3.1	<i>Mycobacterium tuberculosis</i> and Host Cell Infection	6
3.2	An Overview of Currently Employed Anti- <i>Mtb</i> Drugs and Drug Targets.....	8
3.2.1	The Mycobacterial Cell Wall Synthesis as Potential Target.....	12
3.2.2	The Amino Acid Biosynthesis as Potential Target	14
3.2.3	The Respiratory Chain as Potential Target	14
3.3	An Overview of Anti-virulence and Promising Anti-virulence Targets	15
3.3.1	The ESX-1 Type VII Secretion System	18
3.4	Objectives	21
4	Materials and Methods.....	22
4.1	Cultivation Conditions.....	22
4.2	Fibroblast Survival Assay (FSA).....	23
4.3	Resazurin Microtiter Assay (REMA)	23
4.4	L-tryptophan Rescue Experiment.....	23
4.5	Thermal Stability	24
4.6	Generation of Resistant Mutants	24
4.7	Whole Genome Sequencing	24
4.8	Determination of Intracellular Growth in THP-1-derived Macrophages	25
4.9	Secretome Assay.....	25
5	Results.....	27
5.1	Screening for Small Molecules with Anti-mycobacterial Activity	27
5.2	Hit Compounds with Growth Inhibitory Activity against <i>Mtb</i>	29
5.2.1	B5 – a Potential Inhibitor of L-tryptophan Biosynthesis	33

2 Table of Content

5.2.2	Characterization of Two Novel Inhibitors of the <i>Mycobacterium tuberculosis</i> Cytochrome bc ₁ Complex	35
5.3	Hit Compounds with Potential Anti-virulence Activity against <i>Mtb</i>	49
5.3.1	Discovery of dual-active ethionamide boosters inhibiting the <i>Mycobacterium tuberculosis</i> ESX-1 secretion system.....	53
6	Discussion	89
6.1	Screening for Small Molecules with Anti-mycobacterial Activity	89
6.2	Hit Compounds with Growth Inhibitory Activity against <i>Mtb</i>	91
6.3	Hit Compounds with Potential Anti-virulence Activity against <i>Mtb</i>	95
6.4	Concluding Remarks	99
7	Literature.....	101
8	Summary	117
9	Zusammenfassung.....	118
10	List of Abbreviations	120
11	List of Tables	124
12	List of Figures	124
13	Affidavit / Eidesstattliche Erklärung.....	125
14	Appendix.....	127

3 Introduction

Tuberculosis (TB) is a communicable disease that poses significant health challenges worldwide. It is caused by the inhalation of airborne *Mycobacterium tuberculosis* (*Mtb*), which is expelled into the air through activities such as coughing, singing or speaking¹. This mycobacterium primarily infects the lungs, leading to pulmonary TB, but can also affect other parts of the human body, such as lymph nodes, bones, joints and the central nervous system, resulting in extrapulmonary TB². Before the COVID-19 pandemic, TB was the leading cause of death caused by a single infectious agent, even surpassing HIV. In 2021, an estimated 10.6 million people were diagnosed with an active TB, leading to 1.6 million deaths. Furthermore, the World Health Organization estimates that roughly a quarter of the global population is potentially infected with *Mtb*, showing an asymptomatic, latent TB³.

3.1 *Mycobacterium tuberculosis* and Host Cell Infection

Throughout history, TB has afflicted humanity and earned a variety of different names, including ‘Scrofula’, ‘the King’s Evil’ and ‘the white plague’. By the 19th century, it was commonly referred to as ‘consumption’, even though Johann Schönlein had already identified and classified it as “tuberculosis”⁴⁻⁷. In 1882, Robert Koch's groundbreaking work isolated *Mtb* as the causative agent of TB⁸. He was also able to extract the microorganism from patients and inoculate laboratory animals such as guinea pigs⁹.

Today, it is known that the *M. tuberculosis* complex includes *Mtb* and other mycobacteria such as *M. bovis*, *M. caprae*, *M. microti*, *M. canetti*, *M. africanum* and *M. pinnipedii*¹⁰. Phylogenetic analysis classifies *Mtb* into the following genealogy: the southeast Asian and Oceanian clades (lineage 1), the Eurasian clades (lineages 2-4), the African clades (lineages 5 and 6), and the Ethiopian clade (lineage 7)¹¹. Interestingly, split-offs of lineage 1 can be correlated with the first and second wave of human migration, which matches the dispersal of this organism throughout Eurasia¹¹. *Mtb* is an aerobic, nonmotile, rod-shaped and acid-fast microorganism with a guanine and cysteine-rich, 4.4 million base pair long genome containing 3,924 genes (strain H37Rv)^{12,13}. Mycobacteria are especially robust microorganisms, mainly because of their unique and impermeable cell wall, containing an unusual additional layer of cross-linked mycolic acids¹⁴.

After inhalation of airborne droplets containing mycobacteria, the pathogen is transported to the lower respiratory tract, where macrophages and dendritic cells phagocytose the foreign

3 Introduction

organism¹. During phagocytosis the membrane of the macrophage indents and thus absorbs the target cell into a novel compartment, the phagosome¹⁵. Inside the phagosome the mycobacterium is then exposed to gradually decreasing pH to then be delivered to the lysosome where the degradation process is finalized¹⁶. As a defense mechanism *Mtb* developed the ability to escape the phagosome by utilizing the type VII secretion system ESX-1 (see chapter 5.3.1)¹⁷. The secretion of virulence factors by *Mtb* hinders phagosomal maturation, allowing the pathogen to escape the phagosome and to enter the nutrient-rich cytosol^{17,18}. By escaping the phagosome, *Mtb* induces a highly inflammatory form of host cell death: necrosis. This form of cell death is not intended by the host cell and manifests in three prominent ways: necroptosis, pyroptosis and ferroptosis¹⁹. Necroptosis is triggered through the activation of specific cell surface receptors, such as the tumor necrosis factor receptor 1 (TNFR1)²⁰. Upon activation, TNFR1 engages the receptor-interacting protein kinase 1 (RIPK1) and RIPK3, forming the necrosome complex²⁰. Activation of the necrosome leads to phosphorylation of mixed lineage kinase domain-like protein (MLKL), which subsequently translocates to the cell membrane, causing disruption and cell lysis²⁰. Pyroptosis, on the other hand, involves the activation of intracellular protein complexes, such as the NLRP3 inflammasome^{21,22}. NLRP3 activates caspase-1, which cleaves pro-inflammatory cytokines like pro-interleukin-1 β (pro-IL-1 β) and pro-interleukin-18 (pro-IL-18) into their active forms: IL-1 β and IL-18. Simultaneously, caspase-1 cleaves gasdermin D, leading to the formation of membrane pores and eventual cell swelling and rupture. Ferroptosis is characterized by the accumulation of lipid peroxides and iron in host cells, which can potentially be induced by *Mtb* and is mediated by decreased levels of glutathione peroxidase-4 (Gpx4).²³ Iron is an essential nutrient for *Mtb*, and the pathogen employs various strategies to acquire iron from the host²³. This competition for iron may result in cellular iron overload, promoting lipid peroxidation and eventual cell death²³.

3 Introduction

3.2 An Overview of Currently Employed Anti-*Mtb* Drugs and Drug Targets

The currently applied standard treatment regimen for drug-sensitive *Mtb*, which includes the administration of multiple antibiotics (isoniazid, rifampicin, pyrazinamide and ethambutol) for 6 months, is effective but unwieldy²⁴. Incompetent treatment regimens promote the development of antibiotic resistance, necessitating direct supervision, which in turn leads to an increased burden on medical infrastructure and financial resources²⁵. Notably, the highest incidence per capita is observed in economically weak or highly populated countries, such as central and south Africa, as well as of southeast Asia²⁵. The lack of medical infrastructure in low-income countries complicates case detection and successful treatment of active tuberculosis, further promoting the emergence of resistant *Mtb* (Figure 1).

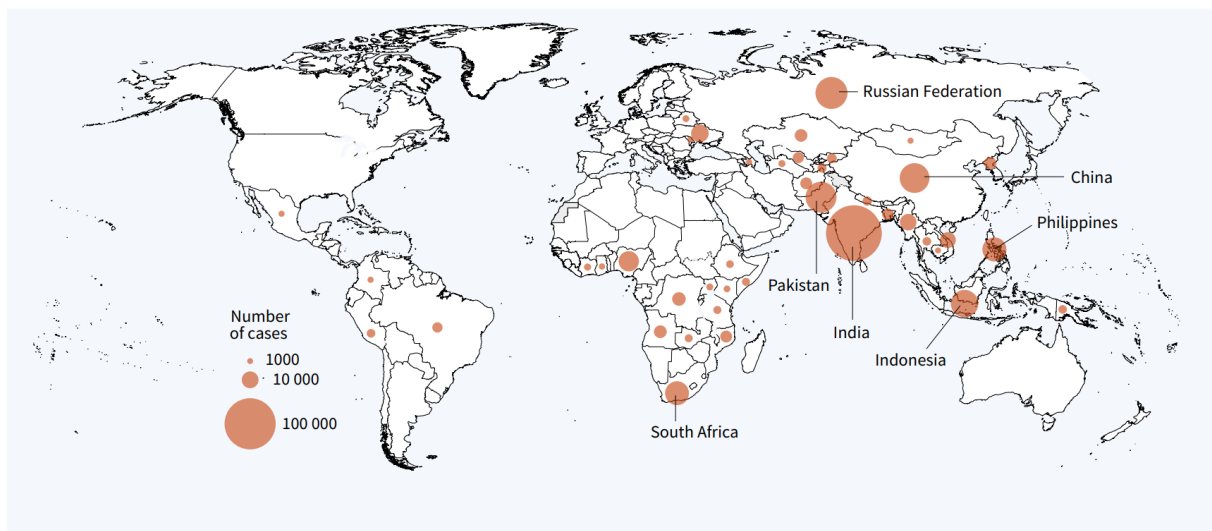


Figure 1: Estimated number of incident cases of MDR/RR-TB in 2021 for countries with at least 1000 incident cases. The seven countries with the highest burden in terms of numbers of MDR/RR-TB cases, and that accounted for two thirds of global MDR/RR-TB cases in 2021, are labelled. Used with permission³.

An individual infected with an *Mtb* strain that is resistant to isoniazid and rifampicin, referred to as a multidrug-resistant (MDR) strain, is practically incurable using the standard treatment regimen²⁶. In 2021, 450 000 cases of MDR or at least rifampicin-resistant (RR) strains were reported³. The WHO recommends a 6-month treatment regimen for MDR-TB, consisting of bedaquiline, pretomanid, linezolid and moxifloxacin²⁷. MDR-strains that are additionally resistant to any fluoroquinolone and capreomycin, kanamycin or amikacin, are classified as extensively drug resistant (XDR) strain²⁶. Approximately 20% of isolated MDR-strains are at least resistant to fluoroquinolones (pre-XDR), putting them at high risk of evolving into XDR-strains³. Treating pre-XDR and XDR strains is extremely challenging, as they exhibit resistance against most major treatment options and complex personalized treatment regimen

3 Introduction

need to be applied ²⁶. Drug susceptibility testing is crucial here to identify second-line antibiotics to which the XDR-strain is still sensitive. This information is essential for developing a personalized treatment regimen, which should consist of four different second-line anti-tuberculous drugs, making treatment of XDR-strains even more expensive ²⁵. However, it's important to note that this combination may result in more adverse side effects ^{26,28}.

The currently exploited molecular targets of anti-mycobacterial drug are essential for mycobacterial propagation or metabolic maintenance (Figure 2). This includes the inhibition of DNA replication by targeting the DNA gyrase, most notably done by fluoroquinolones (e.g. moxifloxacin, ciprofloxacin, levofloxacin) ²⁹, or the inhibition of the DNA-dependent RNA polymerase (e.g. rifampicin, sorangicin, myxopyronin, streptolydigin) ³⁰⁻³³. An alternative target involves the disruption of protein biosynthesis through the alteration of the ribosome ³⁴, which is the mode of action for the substance classes such as macrolides (e.g. erythromycin, telithromycin, clarithromycin) ^{35,36}, aminoglycosides (e.g. streptomycin, kanamycin, amikacin, gentamicin) ^{37,38} and oxazolidinones (e.g. linezolid) ³⁹. Furthermore, the synthesis of the unique mycobacterial cell wall is a highly utilized target of several (first-line) anti-tuberculous compounds (e.g. isoniazid, ethionamide, ethambutol, delamanid and pretomanid, see chapter 3.2.1) ⁴⁰⁻⁴². In addition, attenuation of the mycobacterial metabolism by inhibiting the cholesterol metabolism ⁴³ or amino acid biosynthesis ⁴⁴ are essential targets (see chapter 3.2.2). The recent discovery of bedaquiline has identified the disruption of the mycobacterial energy supply as a novel promising anti-mycobacterial target (bedaquiline, imidazoipyridines (Q203) and lansoprazole sulfide, see chapter 3.2.3) ⁴⁵⁻⁴⁷.

3 Introduction

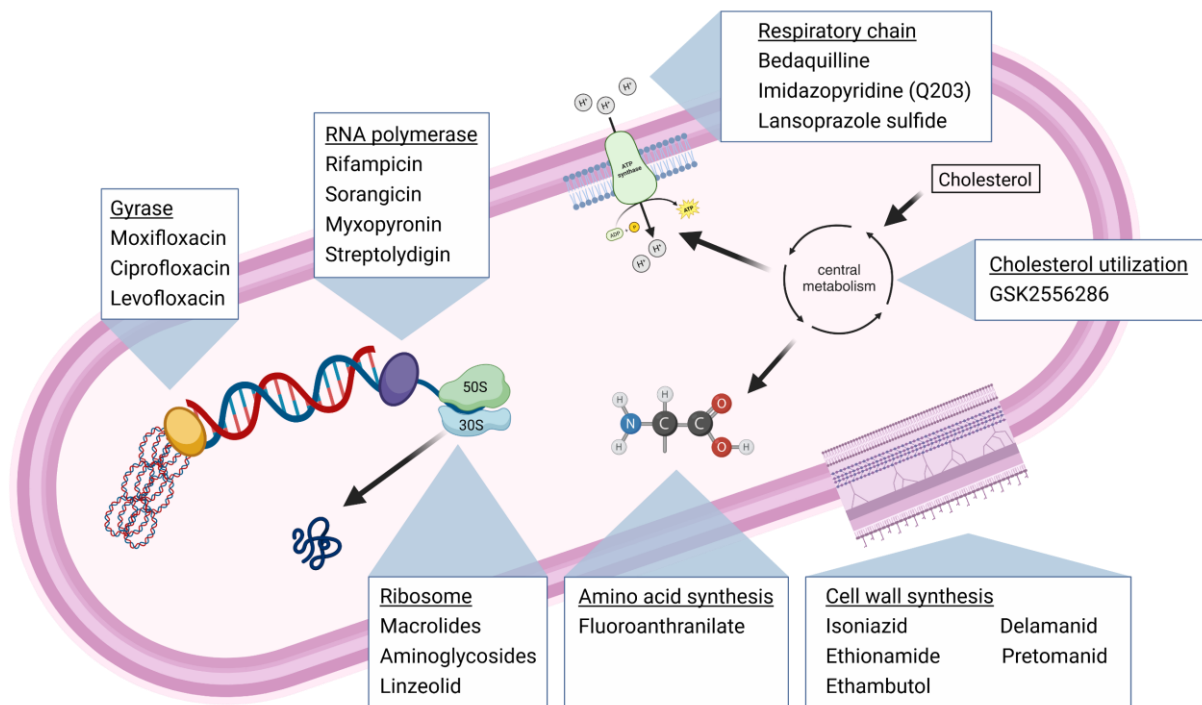


Figure 2: Schematic overview of antibiotic targets in *Mycobacterium tuberculosis*. The most common mycobacterial targets of well-described antibiotics include the gyrase, the RNA polymerase, the respiratory chain, the cholesterol metabolism, the ribosome, the amino acid synthesis and the cell wall synthesis. Scheme was created with BioRender.com.

Although several compounds are currently in clinical phase I and II trials with promising progresses, all lead substances act on the targets described above (Table 1). Nevertheless, these current advances in drug development against *Mtb* do not provide fundamentally new concepts. Most compounds focus on either on disrupting the genetic translation or transcription, the cell wall synthesis or the mycobacterial cell supply. This demonstrates the urgent need for the discovery of novel modes of action.

3 Introduction

Table 1: Overview of the global clinical development pipeline for new anti-*Mtb* drugs in 2022. Name, main characteristics and target category of drugs currently investigated in clinical studies are described ⁴⁸.

Phase	Name	Description	Target category
I	Macozinone ⁴⁹	Benzothiazinone; BTZ-403 derivative; DprE1 inhibitor	Cell wall synthesis
	BVL-GSK098 ⁵⁰	Amino piperidine; Ethionamide booster	Cell wall synthesis
	GSK-286 ⁵¹	Inhibitor of cholesterol catabolism in <i>Mtb</i>	Metabolism
	TBAJ-587 ⁵²	Diarylquinoline; inhibitor of <i>Mtb</i> ATP synthase	Energy metabolism
	TBAJ-876 ⁵³	Diarylquinoline; inhibitor of <i>Mtb</i> ATP synthase	Energy metabolism
	TBI-166 ⁵⁴	Riminophenazine; clofazimine derivative; inhibits the translation of DNA	DNA transcription
	TBI-223 ⁵⁵	Oxazolidinones; inhibits the transcription of mRNA	mRNA translation
II	BTZ-043 ⁵⁶	Benzothiazinone; DprE1 inhibitor	Cell wall synthesis
	GSK303665 ⁵⁷	Inhibitor of <i>Mtb</i> leucyl-tRNA synthetase	mRNA translation
	OPC-167832 ⁵⁸	carbostyryl derivative; DprE1 inhibitor	Cell wall synthesis
	SPR720 (Fobrepodacin) ⁵⁹	aminobenzimidazole; inhibits <i>Mtb</i> DNA gyrase	DNA transcription
	Telacebec (Q203) ⁶⁰	imidazopyridine amide; QcrB inhibitor, inhibits <i>Mtb</i> ATP synthase	Energy metabolism
	TBA-7371 ⁶¹	Azaindole; DprE1 inhibitor	Cell wall synthesis
	Delpazolid ⁶²	Oxazolidinone; inhibits 23S ribosomal subunit	mRNA translation
	SQ109 ⁶³	Ethylenediamine; inhibits MmpL3	Cell wall synthesis
	Sutezolid ⁶⁴	Oxazolidinone; inhibits the transcription of mRNA	mRNA translation
Sudapyridine (WX-081) ⁶⁵	Diarylquinoline; Bedaquiline derivative; inhibits ATP synthase	Energy metabolism	
III	Treatment regimens of bedaquiline in combination therapies		
	Treatment regimens of established antibiotics for use against resistant strains		

3.2.1 The Mycobacterial Cell Wall Synthesis as Potential Target

The cell wall biosynthesis of *Mtb* is a highly utilized target for antibiotics. The unique mycobacterial cell wall consists of the cytoplasmic membrane, the cell wall and the cell envelope (Figure 3) ^{66,67}. The cytoplasmic membrane is similar to other bacteria, providing structural integrity and being involved in transport, cell signaling and energy generation ^{68,69}. Surrounding the membrane is the cell wall, consisting of cross-linked peptidoglycans that form covalent complexes with arabinogalactans and lipoarabinomannan ^{68,70}. The cell wall provides additional integral support and acts as a permeability barrier ⁷¹. Outwards connected is the outer cell envelope consisting of a mycolic acid layer unique to mycobacteria and responsible for the high robustness and natural resistance of mycobacteria to antibiotic compounds ⁷². Mycolic acids are long chain α -alkyl β -hydroxyl fatty acids that are either linked to the arabinogalactans in the cell wall or exist as unlinked trehalose or glycerol esters ⁷³. The biosynthesis of mycobacterial cell wall and mycolic acid layer is essential for mycobacterial growth and requires highly coordinated and localized protein machineries, making their disruption unique targets for highly specific anti-mycobacterial drugs ⁷⁴.

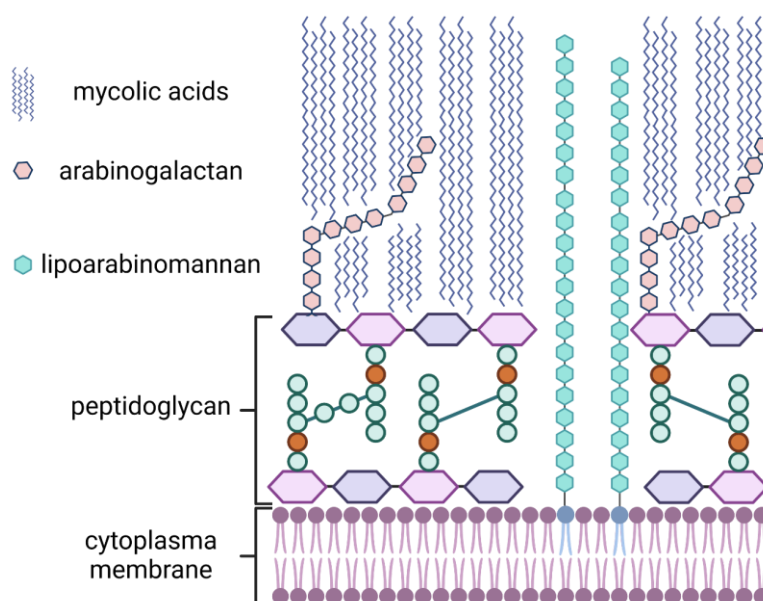


Figure 3: Schematic overview of the plasma membrane, cell wall and cell envelope of *Mycobacterium tuberculosis*. The unique cell wall of mycobacteria consists of peptidoglycans connected with lipoarabinomannan, arabinogalactans and an outer envelope of mycolic acids. Scheme was created with BioRender.com.

The most notable targets of the cell wall synthesis include the decaprenylphosphoryl- β -D-ribofuranose-2-epimerase DprE1/DprE2 complex ⁷⁵⁻⁷⁷, the NAD-dependent Enoyl-acyl carrier protein (ACP) reductase InhA ⁷⁸, the membrane-bound transporter MmpL3 (mycobacterial

3 Introduction

membrane protein *Large 3*)⁷⁹, the type I polyketide synthase 13 (*Pks13*)⁸⁰, and the arabinosyltransferases (*AmbA*, *AmbB* and *AmbC*)⁸¹. *DprE1* and *DprE2* are essential in the cell wall synthesis as they are directly responsible for producing the arabinan component of arabinogalactan and lipoarabinomannan⁷⁵. The most prominent inhibitors of the decaprenyl-phosphoryl- β -D-ribose epimerization are the 1,3-benzothiazin-4-ones (BTZs)^{56,82}. *InhA* is part of the fatty acid synthase type II system, which is essential in mycolic acid biosynthesis⁷⁸. This central enzyme can be targeted by several antibiotics, including the clinically used isoniazid (INH) and ethionamide (ETH). Both of these drugs are so called prodrugs, which are not bioactive against *Mtb* in their applied form but need prior bioactivation by the pathogen's own enzymatic machinery. For INH and ETH, this activation is catalyzed by *KatG* or a specific Bayer-Villiger monooxygenase (*EthA*, *EthA2* or *MymA*), respectively^{83,84}. These enzymes convert the previously inactive drug into the active NAD adduct, INH-NAD or ETH-NAD, which then directly inhibits the activity of the essential enzyme *InhA*⁷⁸.

The transporter *MmpL3* belongs to the resistance-nodulation-division superfamily (RND) and is centrally involved in the translocation of trehalose monomycolate to the periplasm where it is used for mycolic acid synthesis⁸². Although the concerns that *MmpL3* might also allow efflux-mediated drug-resistance have been discerned by the discovery of the inhibitor SQ109⁶³, there is still a certain promiscuity associated with unspecific effects of *MmpL3* inhibitors on the proton motive force⁸⁵. *MmpL3* represents one of the more common anti-tuberculous targets identified during anti-*Mtb* drug screening in recent years^{82,86}. Besides the ethylenediamine derivative SQ109, several other classes of compounds, such as several carboxamide derivatives, adamantly ureas, pyrroles and pyrazoles, benzimidazoles, spiropiperidines and piperidinoles have been found to inhibit *MmpL3*^{82,86-88}. The multi-domain polyketide synthase *Pks13* is also essentially involved in mycolic acid production. Utilizing the thioesterase activity of *Pks13*, trehalose molecules are processed into the monomycolate precursors used for mycolic acid biosynthesis⁸⁹. Compounds with antibiotic activity targeting *Pks13* include several thiophene and benzofuran scaffolds^{82,90,91}. In addition, the arabinosyltransferases *EmbA*, *EmbB* and *EmbC* are also involved in the cross-linking of the highly branched arabinogalactan and thus are essential for mycobacterial growth⁷³. The activity of the arabinosyltransferases can be disrupted by inhibitors such as the first-line antibiotic ethambutol, leading to abrogated cell wall biogenesis and therefore preventing cell division^{81,92,93}.

3 Introduction

Overall, recent drug discovery attempts have shown that the mycobacterial cell wall provides several essential targets, resulting in a pleiotropy of diverse chemical scaffolds with promising anti-tuberculous activity for further drug development.

3.2.2 The Amino Acid Biosynthesis as Potential Target

Amino acid biosynthesis pathways are a novel approach to deal with (drug-resistant) *Mtb*⁴⁴ as they are naturally essential for metabolic maintenance and growth. Although *Mtb* can use certain amino acids from intracellular macrophages as a nitrogen source (aspartate, glutamate, glutamine, glycine, alanine, leucine, valine and isoleucine), *de novo* synthesis of amino acids is still required. As the biosynthesis pathways for tryptophan (trp), histidine, leucine and cysteine are not present in humans, enzymes utilized in these are promising antibiotic targets⁴⁴. For example, the tryptophan biosynthesis employs several consecutive enzymatic steps, which provide potential interaction points with bioactive molecules. This can be done by allosteric inhibition, for example, by indole propionic acids or anthranilate derivatives, which bind to the anthranilate synthase TrpE^{94,95}. Another example is the allosteric inhibition of the TrpAB holoenzyme by the azetidine derivative BRD4592⁹⁶. This highly specific inhibition of an essential metabolic pathway might result in a high potential of patient tolerance, allowing administration of sufficient concentrations to reduce development of resistance.

3.2.3 The Respiratory Chain as Potential Target

Although *Mtb* can survive in an anaerobic environment as obligate aerobic bacterium, it thrives in the presence of oxygen as terminal electron acceptor. The electron transfer from electron donors, such as NADH and succinate, to oxygen is utilized to translocate H⁺ from the mycobacterial cytoplasm to the periplasm (Figure 4)^{69,97,98}. The thus created gradient of H⁺ concentrations between both sides of the inner membrane is called the proton-motive force and is utilized by the F₁F₀ ATP synthase for the oxidative phosphorylation of ADP to ATP^{69,98}. This electron transport chain in *Mtb* is composed of a number of different enzyme complexes, including NADH dehydrogenase (also known as complex I), succinate dehydrogenase (complex II) and the two proton-pumping, terminal oxidases cytochrome-bc₁-aa₃ (complex III and IV) and cytochrome *bd*⁹⁹. Under aerobic conditions the cytochrome-bc₁-aa₃ supercomplex is by far more efficient as a terminal oxidase and is thus primarily utilized by *Mtb* to maintain the proton gradient necessary for ATP synthesis. Because of this, optimal growth of *Mtb* is

3 Introduction

dependent on cytochrome-bc₁-aa₃ functionality, although it is not essential for growth as cytochrome *bd* can act as compensatory system.

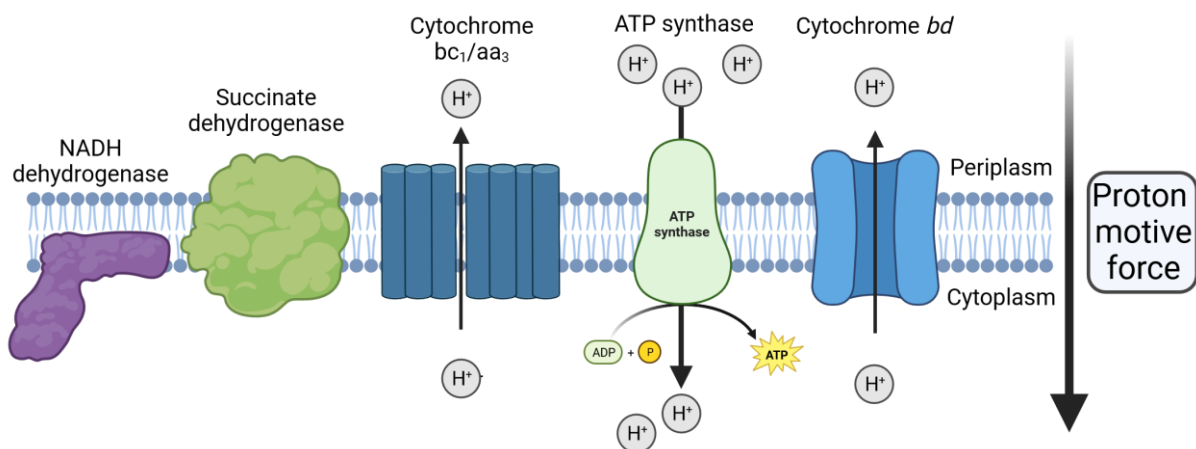


Figure 4: Schematic overview of the respiratory chain of *Mycobacterium tuberculosis*. In order to generate the membrane spanning H⁺ gradient which is responsible for the proton motive force, several multiprotein complexes including the NADH dehydrogenase, the succinate dehydrogenase, cytochrome bc₁/aa₃ and cytochrome *bd* are utilized. The proton motive force is then used by the ATP synthase to catalyze the reaction of adenosine diphosphate (ADP) and phosphate (P) to adenosine triphosphate (ATP). This scheme was inspired by Bald et al., 2017⁹⁹ and recreated under the creative commons attribution 4.0 international license. Scheme was created with BioRender.com.

The identification of bedaquiline (BDQ) was the first time since the 70s that a drug was approved which targeted *Mtb* in a novel way⁴⁵. BDQ directly inhibits the F₁F₀ ATP synthase, thus disrupting the ATP synthesis. This discovery marked the start of the investigation of the membrane-bound energy metabolism of *Mtb* as potential molecular target, resulting in the discovery of compounds inhibiting the ATP synthase (BDQ, squaramides)^{100,101}, NADH dehydrogenase (clofazimine)¹⁰², the cytochrome-bc₁-aa₃ (Q203, lansoprazole sulfide)^{47,60} and the proton motive force (pyrazinamide, SQ109)^{103,104}.

3.3 An Overview of Anti-virulence and Promising Anti-virulence Targets

In addition to well-established antibiotics, there are different concepts to battle pathogens, such as host-directed or anti-virulence approaches. Host-directed therapies are designed to target either the host cell or a specific mechanism of the host-pathogen interaction, thereby supporting the host organism in dealing with the infection^{105,106}. On the other hand, anti-virulence compounds directly target the pathogen to significantly reduce its effectiveness in infecting the host cell (virulence) potentially even render it avirulent^{82,107}. In comparison to conventional antibiotics, both of these approaches are predicted to have a drastically reduced evolutionary pressure on the pathogen hence diminishing the development of potential resistance

3 Introduction

mechanisms against these drugs¹⁰⁷. Furthermore, these compounds vastly increase the number of potentially druggable molecular targets and thus increase the possibility of discovering substances with novel modes of action against *Mtb*.

Currently investigated strategies for host-directed therapies include the promotion of phagosome maturation and enhancing autophagy¹⁰⁵. There are several promising compounds regarding these targets like rapamycin, which inhibits mTOR, a negative regulator of autophagy¹⁰⁸; Metformin, as inductor of mitochondrial reactive oxygen species¹⁰⁹ and tyrosine kinase inhibitors such as Imatinib¹¹⁰, which acidify lysosomes and thus attenuate mycobacterial multiplication. In addition, Vitamin D has shown to increase the response of monocytes to interferon- γ (IFN- γ) which in turn promotes autophagy and phagosomal maturation¹¹¹. An emerging and promising field in host-directed therapy focuses on inhibition of *Mtb*-induced inflammation and host cell death by investigation of necrosis (ferroptosis, pyroptosis)¹¹²⁻¹¹⁴, TNF mediated signaling¹¹⁵, the p38 mitogen-activated protein kinase¹¹⁶⁻¹¹⁸ or the NLRP3 inflammasome²².

Investigation of bacterial-associated targets also unveiled various promising anti-virulence approaches (Figure 5), including the identification of compounds that inhibit the formation or secretion of a diverse set of molecules, so-called virulence factors. These factors are important for mycobacteria as they enable the pathogen to successfully infect its host, to obtain necessary nutrition while doing so, and to evade or suppress the immune system¹¹⁹. The activity of a small molecule or protein to disrupt these properties is therefore called “anti-virulence”¹²⁰. While compounds with anti-virulence activity significantly affect a pathogen’s ability to infect and propagate inside its host cell, they should not show growth inhibitory or bactericidal activity directly against the microorganism¹²¹. By avoiding to directly disrupt mycobacterial growth these compounds are less likely to provide sufficient evolutionary pressure to promote resistance¹²².

Already postulated anti-virulence targets of *Mtb* include the PhoPR regulon¹²³, inhibition of phagosomal regulation and maturation as well as inhibition of protein secretion that is essential for virulence¹²⁴. The two-component system PhoPR consists of the response regulator protein PhoP and the sensor protein PhoR and is centrally involved in various regulation processes of *Mtb*^{124,125}. A recent microarray-based transcriptomic study has shown that roughly 2% of the *Mtb* genome is regulated by PhoP¹²⁶. In addition, the PhoP deletion mutant (*ΔphoP-H37Rv*) represents a dysregulation of the synthesis of cell wall components specific to pathogenic

3 Introduction

mycobacteria¹²⁷, whereas a SNP (S219L) in *phoP* was shown to negatively affect ESX-1 gene expression¹²⁸. One promising small molecule targeting the PhoPR regulatory system is the carbonic anhydrase inhibitor ethoxzolamide, for which inhibition of PhoPR-facilitated virulence of *Mtb* has been demonstrated¹²³. Phagosomal regulation and maturation is currently investigated by inhibitors targeting the *Mtb* protein-tyrosine-phosphatase B (MptpB)¹²⁹, the secreted acid phosphatase M (SapM)¹³⁰ or the zinc peptidase Zmp1¹³¹. The most promising example of an anti-virulence target remains the ESX-1 secretion system, which is crucial for the secretion of several virulence-associated proteins and therefore for the high virulence of *Mtb*. In addition, ESX-1-facilitated export of virulence factors has already been shown to be druggable^{17,132}.

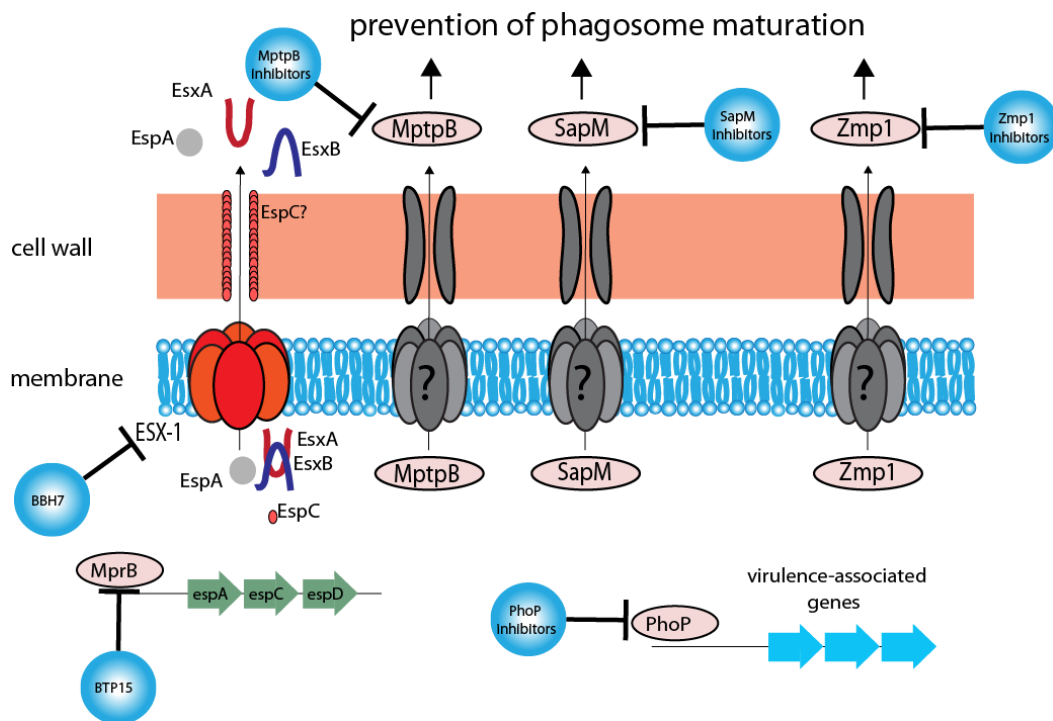


Figure 5: Schematic overview of anti-virulence targets in *Mycobacterium tuberculosis*. Prevention of phagosomal maturation is caused by the *Mtb* protein-tyrosine-phosphatase B (MptpB), secreted acid phosphatase M (SapM) and the zinc peptidase Zmp1. The ESX-1 secretion system is centrally involved in the secretion of proteins important for infection (EsxA/EsxB). Expression of ESX-1 is regulated by MprB and, like other virulence-associated genes, by PhoP. Reprinted with permission from Gries et al., 2020¹⁰⁵.

3.3.1 The ESX-1 Type VII Secretion System

Several mycobacterial secretion systems are involved in the host-pathogen interaction between *Mtb* and its host cell. This includes Sec-mediated secretory pathways (Sec2) or twin-arginine translocation (TAT) systems, but most importantly, type VII secretion systems¹³³. Mycobacteria developed five different type VII secretion systems ESX-1, ESX-2, ESX-3, ESX-4 and ESX-5, with each transporter system being involved in a different biological task¹³⁴. The ESX-1 secretion system for example is well-known to be centrally responsible for *Mtb* virulence. Attenuation of this secretion system by deletion of key components was shown to result in an avirulent phenotype. The most famous example of this phenotype is the attenuated *Mycobacterium bovis* BCG vaccine strain¹³⁵. This *M. bovis* strain lacks, among others, the so-called “region of difference 1” (RD1) genomic locus, which includes two of the ESX-1 substrates in addition to several ESX-1 components, resulting in significantly reduced virulence^{135,136}. The genetic RD1 deletion (Δ RD1) similarly affects *Mtb*, also resulting in an avirulent phenotype¹³⁷. *Mtb* therefore requires a fully functional ESX-1 secretion system in order to optimally infect host cells^{133,138}. This avirulent phenotype can be utilized in *in vitro* infection models, such as fibroblast survival assays based on MRC-5 human lung fibroblasts¹³². In these experimental setups wild type *Mtb* strains are easily distinguishable from strains that show an avirulent phenotype, either caused by genetic deficiencies or by exposure to compounds with anti-virulence activity¹³².

The ESX-1 secretion system is a highly conserved, yet complex system that employs several specialized proteins to transport a multitude of substrates across the cytoplasmic membrane (Figure 6)¹³⁹. The core structure of ESX-1 consists of various membrane-bound ESX conserved components (Eccs) EccB, EccCa, EccCb, EccD, EccE and MycP^{134,140}. The unique multidomain structure of EccC consists of a short domain of unknown function (DUF) and three ATPase domains that potentially provide the energy for the secretion of EsxB^{140,141}. This substrate presumably acts as a chaperone protein for the strictly co-secreted major ESX-1 effector protein EsxA¹⁴². Other substrates of ESX-1 include the ESX-associated proteins (Esp) EspA, EspB, EspC, EspE, EspF, EspJ, EspK, the Pro-Glu family protein PE35 and the Pro-Pro-Glu family protein PPE68^{134,140}. The final ESX-1 components, espG and EccA, are located in the cytosol and exhibit activity as a chaperone or ATPase, respectively¹⁴³.

The most important ESX-1 substrates, EsxA and EsxB, also called early secreted antigenic target 6 kDa (ESAT-6) and culture filtrate protein 10 kDa (CFP-10), are directly associated with virulence of *Mtb*^{17,144}. While both proteins are strictly co-secreted, it is believed that EsxA

3 Introduction

is the virulence effector protein that plays an important role during infection, and EsxB is more likely to be a stabilizing carrier protein, as the EsxAB heterodimer shows a higher melting temperature as EsxA alone^{17,138,142,145,146}. In addition, EsxA is proposed to mediate the phagosomal escape of *Mtb*, meaning the translocation of *Mtb* from the maturing phagosome into the cytosol of the host cell^{147,148}. The acidic-pH-dependent membrane-permeabilizing activity of EsxA potentially disrupts the lipid membranes of the phagosome at low pH, allowing the cytosolic translocation of the pathogen^{147,148}. Additionally, EsxA is described as a strong immunoregulator that binds to cellular proteins and stimulates the secretion of several cytokines. Treatment of peripheral blood monocyctic cells (PBMCs) from *Mtb*-infected donors with EsxA showed significantly increased secretion of IFN- γ , IL-2, IL-6, IL-8, IL-10, the monocyte chemoattractant protein-1 (MCP-1), the macrophage inflammatory protein-1 α (MIP-1 α) and TNF- α ¹⁴⁹. The abundance of EsxA and EsxB is often used *in vitro* as a molecular probe. This is done by detecting or quantifying the amount of secreted protein, which indicates inhibition of the ESX-1 secretion system^{132,150}.

From a genetic perspective, it is important to note that the *espACD* operon, which encodes EspA, EspC and EspD, is located outside of the RD1 locus. Although EspD is not a substrate of ESX-1, it is necessary to stabilize the substrates EspA and EspC¹⁵¹. The expression of the ESX-1 system's operon is associated with the two-component regulatory system PhoPR and the transcription factors WhiB6 and EspM¹⁵²⁻¹⁵⁴. Concerning the expression of ESX-1 substrates, several proteins have been shown to bind to the *espACD* promoter region, including EspR, MprA and *lsr2*¹⁵⁵⁻¹⁵⁷. All of these regulators are essential for a fully functional ESX-1 secretion system^{134,139,158}. All in all, the ESX-1 secretion system is a highly complex multi-protein complex that has proven to play a central role in *Mtb* virulence. Thus, it is a promising target for novel anti-mycobacterial compounds suitable for combination treatments of existing and novel antibiotics⁸².

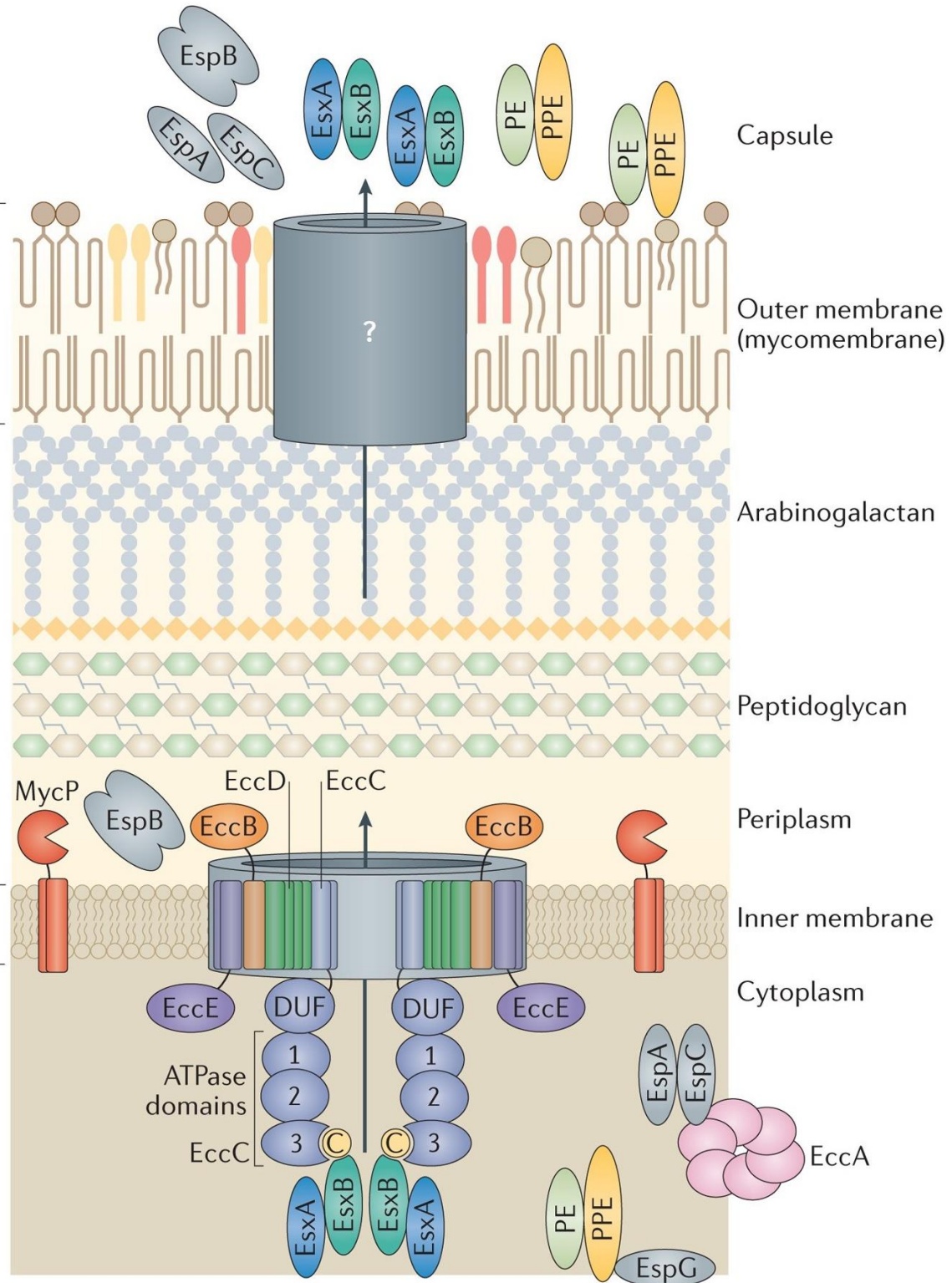


Figure 6: Conserved aspects of ESX-1 protein transport in *M. tuberculosis*. This schematic overview shows localization and interaction of ESX-1 conserved components (EccA, EccB, EccC, EccD and EccE) and ESX-1 associated proteins (EspA, EspB, EspC and EspG) as well as associated Pro-Glu (PE) family protein and Pro-Pro-Glu (PPE) family protein and the membrane-bound MycP. Reprinted with permission from Gröschel et al., 2016¹⁴⁰.

3.4 Objectives

The increasing prevalence of drug-resistant *Mtb* is a persisting and exacerbating global health problem. This issue is further aggravated by the lack of identification of novel molecular targets which could be exploited to combat drug-resistant *Mtb* or to improve currently employed treatment regimens. Although great combined efforts of academia and industry are currently being undertaken, they have not yet produced a satisfactory amount of novel lead structures, as attrition rates for bioactive compounds to be considered as anti-*Mtb* drug are extraordinarily high. In addition to conventional antibiotics with activity against *Mtb*, there is also the emerging field of anti-virulence drugs. These compounds potentially abrogate infection by *Mtb* via several promiscuous targets and thus may benefit anti-*Mtb* regimens as adjunct therapy. In order to scientifically contribute to solving these drug discovery issues in the future, the following major objectives were set for this thesis:

- (I) Identification and characterization of compounds of interest with growth inhibitory or anti-virulence activity against *Mtb* to potentially derive molecular structures as promising lead compounds
- (II) Identification of putative molecular targets of above-mentioned compounds to decipher the respective mode of action

4 Materials and Methods

Since this monograph is structured similarly to a cumulative dissertation, two manuscripts are included as chapter 5.2.2 and 5.3.1. Therefore, this materials and methods section will only list materials and methods used in experimental setups described outside of these publications. The material and methods used in the publications are described separately in the respective chapters.

4.1 Cultivation Conditions

Mycobacterium tuberculosis

The *Mycobacterium tuberculosis* Erdman strain (provided by S.T. Cole, Institut Pasteur Paris) was grown in two different growth media. The first medium consisted of BD Difco™ Middlebrock 7H9 broth (Becton Dickinson, Franklin Lakes, USA) supplemented with 0.2% glycerol (Th. Geyer GmbH & Co. KG, Renningen, Germany), 10% albumin dextrose catalase (ADC Middlebrook; Becton Dickinson, Franklin Lakes, USA), and 0.05% Tween80 (Carl Roth GmbH + Co. KG, Karlsruhe, Germany). The second medium used was Sauton's medium, which is protein-free and consists of the following ingredients per 1 liter: 0.5 g monopotassium phosphate (Carl Roth GmbH + Co. KG, Karlsruhe, Germany), 0.5 g magnesium sulfate (Thermo Fisher Scientific, Waltham, USA), 4 g L-asparagine (Sigma-Aldrich, St. Louis, USA), 0.05 g ammonium ferric citrate (Thermo Fisher Scientific, Waltham, USA), 2 g citric acid (Th. Geyer GmbH & Co. KG, Renningen, Germany), 100 µL 1% zinc sulfate (Sigma-Aldrich, St. Louis, USA), and 60 mL glycerol.

MRC-5 human lung fibroblasts

MRC-5 human lung fibroblasts (obtained from the Coriell Institute for Medical Research, Camden, USA) were cultured in Gibco Minimum Essential Medium (Thermo Fisher Scientific, Waltham, USA). This culture medium was further enriched with 10% heat-inactivated fetal bovine serum (FBS; sourced from Thermo Fisher Scientific, Waltham, USA), 1% Gibco nonessential amino acids (Thermo Fisher Scientific, Waltham, USA), and 1 mM Gibco sodium pyruvate (Thermo Fisher Scientific, Waltham, USA). The cell line was maintained at a temperature of 37°C with a 5% CO₂ atmosphere.

4 Materials and Methods

THP-1 human monocytes and THP-1-derived macrophages

THP-1 cells and THP-1-derived macrophages were cultivated in Gibco RPMI 1640 medium (Thermo Fisher Scientific, Waltham, USA), supplemented with 10% FBS (Pan-Biotech, Aidenbach, Germany). The cells were maintained at a temperature of 37°C with a 5% CO₂ atmosphere. Differentiation into macrophages was done in the presence of 200 nM phorbol 12-myristate 13-acetate (PMA; Sigma-Aldrich, St. Louis, USA) for 24 h. Experiments using THP-1-derived macrophages were performed after a 24 h rest period in medium without PMA.

4.2 Fibroblast Survival Assay (FSA)

Assessment of cytoprotection was conducted by utilizing the Fibroblast Survival Assay using MRC-5 human lung fibroblasts¹³². A total of 4,000 cells were placed in 384-well plates. These cells were then subjected to a pre-incubation period of 3 hours with the relevant test compounds. Following this, they were exposed to *Mtb* at a Multiplicity of Infection (MOI) of 10 and allowed to incubate for 72 hours. To determine cell viability, the luminescence-based reagent CellTiter-Glo (Promega, Fitchburg, USA) was used and analyzed using a Biotek3 microplate reader (Agilent technologies, Santa Clara, USA).

4.3 Resazurin Microtiter Assay (REMA)

In this experiment frozen *Mtb* samples were thawed and their concentration adjusted to an optical density (OD₅₆₀) of 0.0003. Subsequently, 90 µL of this suspension was mixed with 10 µL of the test substance, which had been serially diluted (1:2), within the testing plates. These plates were then placed in an incubator set at 37°C for a duration of 7 days. After this incubation period 10 µL of resazurin (obtained from Sigma-Aldrich, St. Louis, USA) were introduced into each plate and they were incubated for an additional 24 hours. To quantify the growth of mycobacteria, the amount of catalyzed resorufin was analyzed using a plate reader measuring absorbance at 560 nm and 590 nm.

4.4 L-tryptophan Rescue Experiment

This experimental setup is based on a growth associated assay such as REMA in with the final product of the putative enzymatic pathway, which is potentially targeted by the test compound, is added to the broth in sufficient surplus. In this case 0.1 % L-tryptophan were added to the 7H9c broth used a REMA.

4.5 Thermal Stability

Separate microtiter plates were prepared containing 10 μL of a ten-times concentrated, serial dilution (1:2) of the respective test compound for each time point. The plates were then airtight sealed using SealPlate® film (Sigma-Aldrich, St. Louis, USA) and incubated at 37°C. After the specific time period the airtight seal was removed, a fresh serial dilution of reference compound and controls were added and the microtiter plate was then subjected to a REMA. MIC was calculated using GraphPad Prism 8.

4.6 Generation of Resistant Mutants

Mtb was cultured in 7H9c medium at 37°C under aerobic conditions. To generate spontaneous mutants resistant to the test compounds, a range of 3×10^7 to 3×10^9 bacteria were plated on 7H10 agar plates containing five to ten times the MIC of the respective test compounds. Following an incubation period of 14 to 28 days, colonies were selected and subsequently subcultured on 7H10 agar plates both with and without the respective compound. Subsequent cultivation of these mutants was conducted in 7H9c medium, followed by testing for resistance in microtiter plates (REMA), both in the presence and absence of the respective compound.

4.7 Whole Genome Sequencing

Mutants were rendered nonviable through heat treatment and subsequently suspended in TE buffer. These samples were then dispatched to the Leibniz Research Center Borstel. Chromosomal DNA (gDNA) extraction was carried out using the cetyltrimethylammonium bromide (CTAB) method, a procedure previously described¹⁵⁹. For the preparation of libraries intended for next-generation sequencing (NGS), gDNA underwent processing using a modified Nextera protocol, as briefly described below: The input DNA was fragmented using tagmentation, and indexed adapters were incorporated through a reduced-cycle amplification process. Sequencing of DNA libraries was performed using a paired-end sequencing strategy with 2×150 bp reads on an Illumina NextSeq 500 platform, following the manufacturer's guidelines (Illumina, San Diego, CA). Raw read data (fastq files) were subjected to sequencing analysis using MTBseq v1.0.3, a semi-automated bioinformatics pipeline tailored for the examination of *Mycobacterium tuberculosis* complex isolates, as referenced in¹⁶⁰. In summary, the raw reads were aligned to the reference genome of *M. tuberculosis* H37Rv (GenBank accession number NC_000962.3) employing the BWA-MEM algorithm, with subsequent

4 Materials and Methods

refinement through the GATK software package. To be considered confident variant calls, variants (including single nucleotide polymorphisms [SNPs] and insertions and deletions [indels]) needed to meet specific criteria: a minimum coverage of 4 reads in both forward and reverse orientations, a minimum of 4 reads supporting the allele with a Phred score of at least 20, and an allele frequency of 75%. Consecutive SNP calls within a 12-base pair window, which could potentially signify artificial variant calls around indels or within regions associated with drug resistance genes and repetitive sequences (such as PPE/PGRS genes), were excluded from the analysis.

4.8 Determination of Intracellular Growth in THP-1-derived Macrophages

For this experiment 50,000 THP-1-derived macrophages were differentiated in 96-well plates (see above). These cells were then subjected to a pre-incubation period of 2 hours, followed by infection with an eGFP-expressing *Mtb* strain at a Multiplicity of Infection (MOI) of 2. The cells were allowed to incubate for a total duration of 48 hours. To assess the intracellular growth of *Mtb* the cells were fixated with 4% paraformaldehyde, washed with PBS and subsequently counted, after staining the cell nuclei with 4',6-diamidino-2-phenylindole (DAPI; sourced from Thermo Fisher Scientific, Waltham, USA). Intracellular growth of *Mtb* was determined by fluorescence microscopy. For this at least two pictures were taken at the central region of each well. The amount of infected THP-1-derived macrophages was determined using ImageJ by overlaying the respective DAPI image with the fluorescence image¹⁶¹. Thus, the general region of *Mtb* location can be found and infected cells can be counted.

4.9 Secretome Assay

Mycobacteria were cultured initially as a pre-culture until reaching the mid-logarithmic growth phase (OD₅₆₀ 0.8) in Sauton's medium supplemented with 0.05% Tween80. Subsequently, they were transferred to a main culture in Tween80-free Sauton's medium containing the respective test compound, commencing at OD₅₆₀ 0.4. After 72 hours of incubation, both the supernatant and cell pellet were harvested. For the analysis of intracellular proteins, the cell pellet was resuspended in Dulbecco's Phosphate Buffered Saline (PBS; Thermo Fisher Scientific, Waltham, USA), supplemented with a protease inhibitor (cOmplete mini EDTA-free; Roche, Basel, Switzerland). The cell suspension was then lysed by subjecting it to five cycles of beating with glass beads (150-212 µm; Sigma-Aldrich, St. Louis, USA) using a cell disruptor (Disruptor Genie; Scientific Industry, Bohemia, USA). Each cycle consisted of 1 minute of beating at

4 Materials and Methods

maximum speed, with 1-minute cooling intervals in between. Subsequently, the supernatant, free of beads, was filtered through a 0.22 μm filter (Carl Roth GmbH + Co. KG, Karlsruhe, Germany). For Western blotting, supernatant samples were filtered again (0.22 μm) and concentrated 100-fold using Vivaspin20 centricons (Sartorius, Göttingen, Germany). During the concentration process, larger proteins were removed using 100 kDa cutoff centricons, followed by further concentration using 5 kDa cutoff centricons for the collected flow-through. Concentrated samples were then separated using TruPAGE™ Precast Gels 4-12% (Sigma-Aldrich, St. Louis, USA) and semi-dry blotted using iBlot2 (Invitrogen, Waltham, USA). Immunodetection was carried out using antibodies, including anti-ESAT6 HYB 076-08 (Santa Cruz, Dallas, USA), anti-Myco bacterium tuberculosis HSP65 (Invitrogen, Waltham, USA), and anti-AG85 NR-13800 (BEI Resources, Manassas, USA). These primary antibodies were paired with the respective secondary antibodies (anti-mouse or anti-rabbit; Cell Signaling Technology, Cambridge, UK). The quantification of band intensities was performed using ImageJ ¹⁶¹.

5 Results

Since this monograph shows structural characteristics of a cumulative dissertation, the results section presents experimental concepts and data from unpublished work, as well as finished manuscripts that are either already published or currently under peer review. These manuscripts are included along with their respective supplementary data and a brief complementary summary in chapter 5.2.2 and chapter 5.3.1. The accompanying summaries of the manuscripts briefly describe the context of each manuscript and my respective contribution to them.

5.1 Screening for Small Molecules with Anti-mycobacterial Activity

The first step of top-down drug discovery consists of identification of potentially active substances by screening large quantities of diverse chemical structures ¹⁶². To identify substances active against *Mtb*, a dual screening platform was employed, combining the resazurin microtiter assay (REMA) ¹⁶³, a standardized growth inhibitory assay, with the host cell-based fibroblast survival assay (FSA) ¹³². In a REMA, the NADH-dependent conversion of the blue resazurin to the highly-fluorescent, pink resorufin is catalyzed in the presence of bacteria, and can thus be used to measure bacterial growth. Based on this, compounds that inhibit mycobacterial growth can be identified. Growth inhibitory effects include direct interaction with *Mtb*, which reduces mycobacterial propagation but could also indicate general cytotoxicity of the tested substance. To exclude cytotoxic effects and validate activity in a host cell-associated context, the complementary FSA is employed to assess anti-mycobacterial activity in a host cell-based infection model. Here, MRC-5 human lung fibroblasts are infected with a high *Mtb* load (MOI 10; multiplicity of infection of 10) and host cell survival will be determined three days post infection by viability measurement (CellTiterGlo). Furthermore, growth inhibitory effects on *Mtb* are cross-verified through microscopy. In the following, this dual screening platform was applied to two molecule libraries totaling 60,000 small molecules in order to identify compounds with novel anti-mycobacterial activities. Depending on the project the dual screening platform was applied in a different manner. In project I, 50,000 compounds from a library provided by the Leibniz Forschungsinstitut für Molekulare Pharmakologie (Berlin, Germany) were analyzed to specifically identify molecules with novel antibiotic activity. Therefore, the screening was optimized to promptly exclude compounds with no growth inhibitory effect in the REMA (Figure 7). Furthermore, excluding structures already described in the literature and compounds lacking activity in the host cell context (FSA) resulted in a high attrition rate, with only eleven compounds (a hit rate of 0.022 %) selected for

5 Results

further investigation. In contrast, in project II, 10,000 small molecules from the World Diversity Set 3 library provided by SPECS (Zoetermeer, Netherlands) were analyzed. In this case, the dual screening platform was utilized to identify compounds with either antibiotic or anti-virulence activity. Therefore, all 10,000 compounds were initially tested in both the REMA and the FSA, resulting in two (0.020%) compounds with antibiotic activity and 43 (0.43 %) compounds with anti-virulence activity. The characterization and investigation of the respective targets of hit compounds identified in both screening attempts are further described for compounds showing antibiotic activity in chapter 3.2 and for compounds showing anti-virulence activity in chapter 3.3.

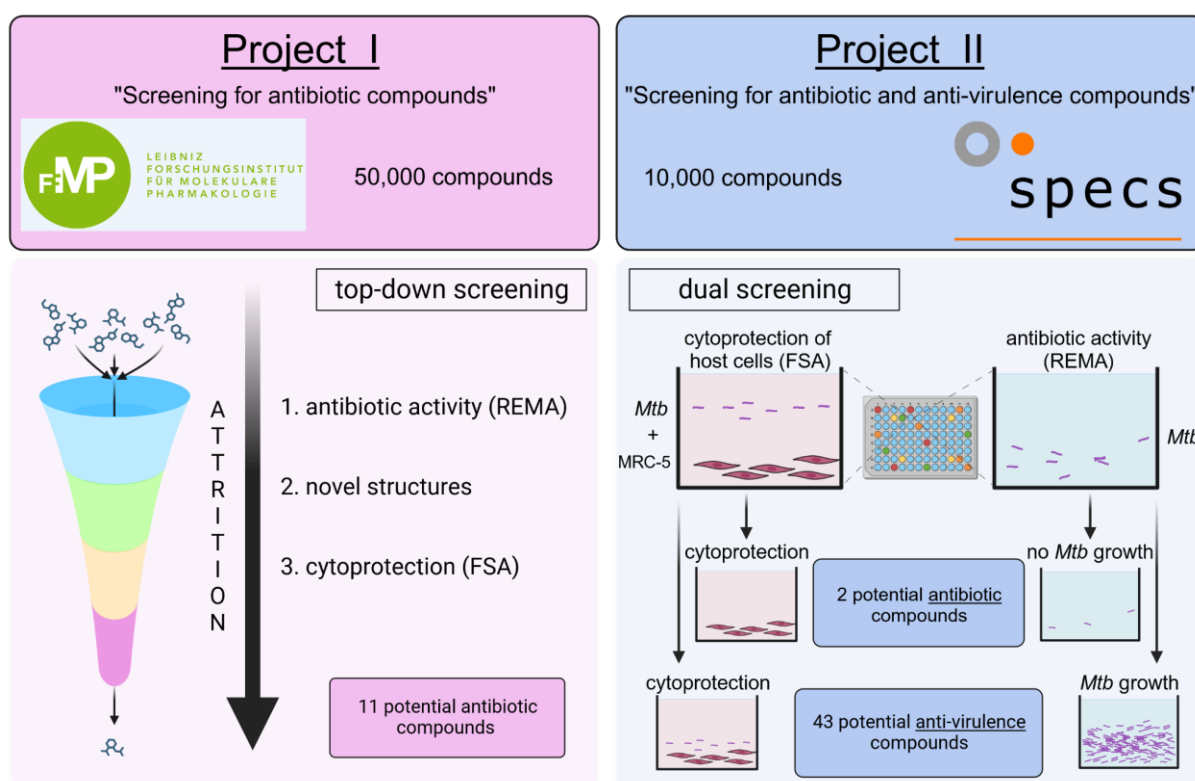


Figure 7: Schematic overview of the utilized screening approaches. This medium-throughput screening included 60,000 compounds divided in two separate projects. Project I (left) was focused on identifying antibiotic compounds, thus utilizing top-down screening processes, by which compounds from the library were excluded if they showed less favorable attributes during antibiotic (REMA) testing, if they provided novel structures and if they showed activity in a host cell model (FSA). During the II. screening project (right) all compounds were directly cross-screened utilizing the experimental setup for testing for antibiotic activity (REMA) and simultaneously the experimental setup screening for cytoprotection (FSA). This allows the categorization of potential hit compounds into two groups: potential antibiotics and potential anti-virulence compounds. Scheme was created with BioRender.com.

5.2 Hit Compounds with Growth Inhibitory Activity against *Mtb*

The combined screening efforts of both projects yielded 12 compounds that exhibited promising antibiotic activity and were commercially available. For these hit substances, new powder was ordered, the activity was re-confirmed in the respective assays. Additionally, potential molecular targets were further investigated. In order to gain insights into the molecular mode of action, the evolutionary pressure induced by the antibiotic activity of the test compounds was harnessed to generate spontaneous resistant mutants for each compound (Figure 8). As *Mtb* generally exhibits a relatively low genomic mutation rate^{164,165} and contains only a relatively small number of multi-drug exporters¹⁶⁶, mutants displaying Single Nucleotide Polymorphisms (SNPs) and showing a less susceptible phenotype are likely to indicate a target that is essential for mycobacterial growth. These SNPs potentially represent the molecular target for the respective compound, which may include genes essential for mycobacterial propagation, such as those encoding enzymes involved in the central carbon metabolism, extended energy metabolism, protein biosynthesis, cell wall synthesis and any gene associated with the regulation thereof^{91,167}.

Subsequent testing started with plating high bacteria numbers (10^8 - 10^{10}) on 7H10 agar plates containing the respective compounds at concentrations five to ten times the MIC (Table 2). After two weeks of incubation, visible colonies were picked, subcultivated on medium without compound and subsequently tested in REMA to confirm resistance. Mutants that exhibited reduced growth inhibitory efficacy of the test substance were labelled as resistant mutants and further investigated. Since resistance is caused by gene modifications, the identification of these alterations might indicate genes that facilitate resistance and, consequently, potential molecular targets. To identify SNPs, confirmed resistant mutants were selected and sent in for whole genome sequencing at the Leibniz Research Center in Borstel. A summary of hit compounds with growth inhibitory activity and their putative target can be found in Table 2.

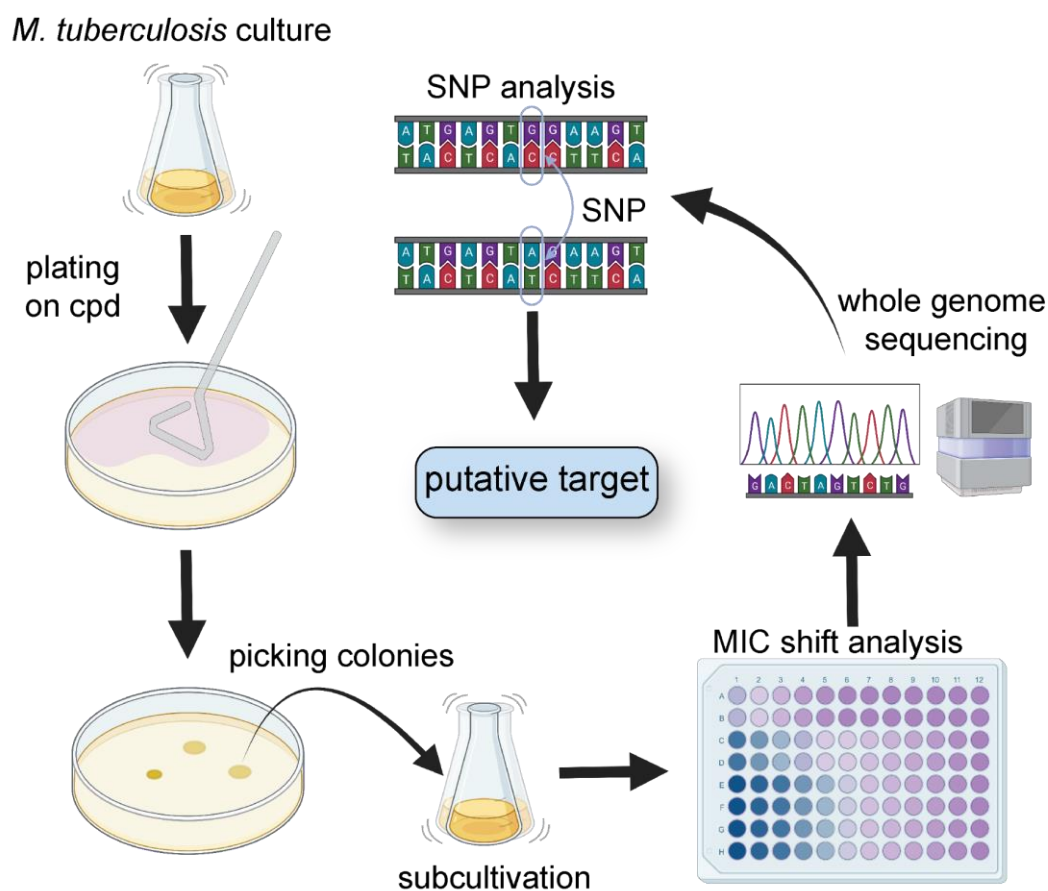


Figure 8: Schematic overview of utilized pipeline for target identification. *Mycobacterium tuberculosis* cultures were plated on 7H10 agar plates containing the test compound in concentrations five to ten times the MIC₉₀. After two to four weeks single colonies were picked from these plates, separately cultivated on agar plates with and without the test compound (not shown) and then subcultivated in liquid culture. The sensitivity of the potentially resistant strains was then tested in a REMA to evaluate the shift in MIC₉₀. Confirmed resistant strains were then harvested, inactivated and sent for whole genome sequencing. The following analysis of single nucleotide polymorphisms (SNPs) identified potential molecular targets. Scheme was created with BioRender.com.

For compounds B1-B4, B8 and B10, this approach did not yield any resistant mutants. Colonies picked from mycobacteria exposed to the compounds B1, B2 and B8 showed no reduced sensitivity to the respective compound in REMA validation. Additionally, a retrospective investigation of bacterial growth on plates containing the respective compound revealed an increased abundance of colonies compared to other compounds. This occurrence was similar to *Mtb* exposed to the bacteriostatic compound LPZS, which were used as a control. Hence, it is conceivable that B1, B2 and B8 are potentially also bacteriostatic, but no specific target could be identified. Mycobacteria exposed to B3, B4 and B810 at various concentrations above the MIC did not show any colonies until roughly three to four weeks after plating. At that point, an increasing number of colonies started to appear. To verify if these compounds suffered from thermal degradation, which could explain a sudden loss of activity, they were preincubated at 37°C for one to four weeks and subsequently tested in REMA (Figure 9). This experimental

5 Results

setup clearly visualizes the drastic loss of efficacy even after one or two weeks of pre-incubation at 37°C. Therefore, the compounds were labeled thermally instable and no target could be identified.

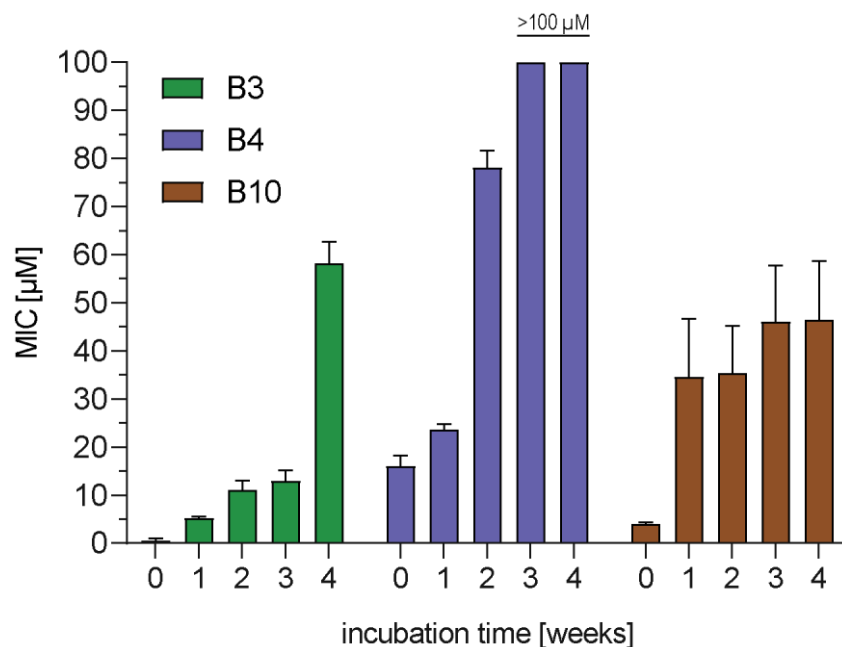


Figure 9: MIC shift of compounds after pre-incubation at 37°C. Test compounds were pre-incubated in the assay plate for a specific time-period before performing REMA. The respective minimal inhibitory concentration (MIC) was calculated for each plate. Shown are the mean and standard deviation of the mean of at least two replicates.

Using this pipeline, alterations in genes coding for various essential genes were found for the remaining six compounds: B5, B6, B7, B9, S7 and S32. Identified targets by this approach include alterations in genes associated with cell wall synthesis: *katG* (Rv1908c; B7), *dprE1* (Rv3790; B9), *mmpL3* (Rv0206c; S7) and *ethA* (Rv3854c; S32). In addition, compounds B5 and B6 favored resistance-conveying mutations in the genes *trpA* (Rv1613)/*trpB* (Rv1612) and *qcrB* (Rv2106), respectively. The enzyme complexes encoded by *trpA/trpB* are essential in the biosynthesis of L-tryptophan and the protein encoded by *qcrB* is centrally involved in the ATP-synthesis. These two targets were subsequently further investigated (see chapter 5.2.1 and chapter 5.2.2.).

5 Results

Table 2: Overview of hit compounds with growth inhibitory activity. 90% Minimal inhibitory concentration (MIC₉₀) was determined by REMA, whereas 50% effector concentration (EC₅₀) was calculated based on host-survival in FSA. Targets represent single nucleotide polymorphisms found in resistant mutants.

ID	MIC ₉₀ [μ M]	EC ₅₀ [μ M]	Target	Comment
B1	5.4	12.06	n/a	potentially bacteriostatic
B2	0.4	2.6	n/a	potentially bacteriostatic
B3	0.6	3.6	n/a	thermally instable
B4	16.0	0.4	n/a	thermally instable
B5	1.0	0.8	TrpA/TrpB	aminoacid biosynthesis
B6	1.12	0.78	QcrB	ATP synthesis
B7	6.25	1.4	KatG	prodrug activation
B8	3.1	2.2	n/a	potentially bacteriostatic
B9	1.3	1.8	DprE1	cell wall synthesis
B10	4.0	2.3	n/a	thermally instable
S7	6.8	5.21	MmpL3	cell wall synthesis
S32	10.63	5.79	EthA	cell wall synthesis prodrug activation

5.2.1 B5 – a Potential Inhibitor of L-tryptophan Biosynthesis

The compound B5 showed growth inhibitory activity in broth, as was demonstrated in a growth inhibition assay (REMA), where it exhibited an MIC of 1 μM (Figure 10 A). In addition, the presence of B5 resulted in cytoprotection of MRC-5 fibroblasts during infection with a high abundance of *Mtb* (MOI 10; Figure 10 B). Furthermore, infection experiments of THP-1-derived macrophages with eGFP-expressing *Mtb* showed reduction of intracellular mycobacterial growth in the presence of 10 μM B5, comparable to the control 10 μM rifampicin (Figure 10 C). The control antibiotic gentamycin (10 μM), which cannot permeate the macrophage membrane, on the other hand, only slightly reduced intracellular growth of mycobacteria. This indicates that B5 potentially permeates eukaryotic membranes and can also act as a growth inhibitor inside the host cell. In order to identify a putative target for B5, WT *Mtb* were exposed to 5 μM B5 on 7H10 agar plates for two weeks according to the target identification protocol (Figure 8). During this selection process for resistant mutants, twelve colonies could be selected, resulting in a mutation frequency of 4×10^{-7} . All mutants showed an increased resilience against B5 compared the wild type parental strain in a REMA. The MIC shifted from 1 μM for the WT to roughly 52 μM for the mutants. The shift in MIC of one representative mutant is shown in Figure 10 A, whereas growth inhibition curves of all mutant are displayed in Appendix Figure 1. WGS of all twelve resistant Mutants identified SNPs in either *trpA* (Rv1613; 50%) or *trpB* (Rv1612; 50%). Both SNPs always occurred at the respectively same position as P65T (*trpA*) or P321L (*trpB*). These genes encode for the proteins TrpA and TrpB, which together form an $\alpha\beta\beta\alpha$ heterotetramer that is essential for the final step of the L-tryptophan biosynthesis (Figure 10 D). As a follow-up step to validate the trpA/B complex as a potential target of B5, a rescue experiment in which L-tryptophan, the product of this enzymatic step, was added to cultures exposed to different concentrations of B5 (Figure 10 E). In the presence of 0.1% L-tryptophan, the wild type lost sensitivity to the compound B5 at concentrations well above the MIC (100 times the MIC, 100 μM). Therefore, it is conceivable that the compound B5 potentially inhibits the trpA/B heterotetramer.

5 Results

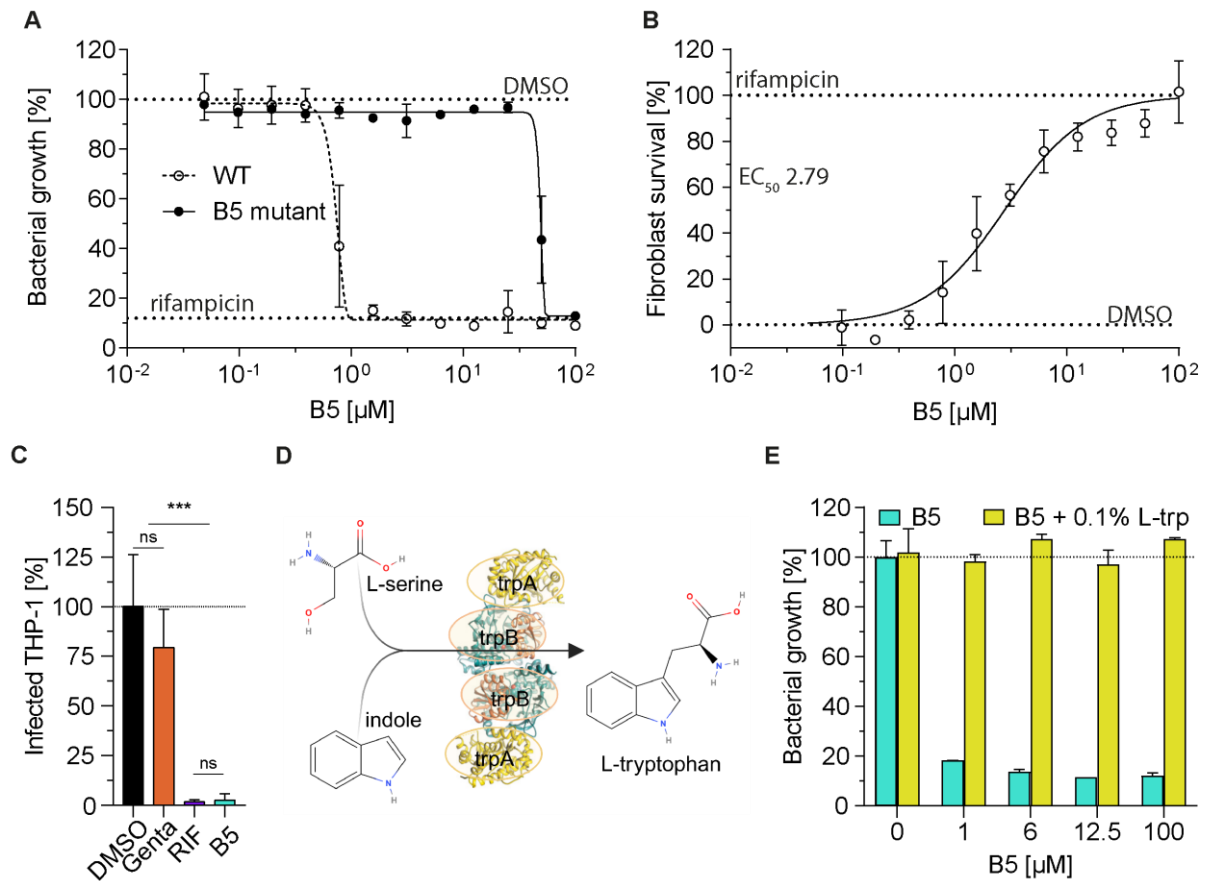


Figure 10: Compound B5 shows potential anti-mycobacterial activity by inhibiting L-tryptophan biosynthesis. (A) Bacterial growth in the presence of different concentrations of B5 tested in a resazurin microtiter assay (REMA) against the wild type (WT; white) and a B5 resistant mutant (black). (B) Fibroblast survival of MRC-5 cells infected by *Mtb* (MOI 10) in the presence of different concentrations of B5. (C) Intracellular growth of GFP-expressing *Mtb* during infection of THP-1-derived macrophages. As controls 0.1% DMSO, 10 µM gentamicin (Genta) and 10 µM rifampicin (RIF) were used. Statistical significances are based on a one-way ANOVA combined with Bonferroni post-hoc test (ns = not significant; ***= $p < 0.001$). (D) Schematic overview of the last step of trpA/B facilitated L-tryptophan biosynthesis. Molecular structures of trpA/B of *Streptococcus pneumoniae* are based on WWPDB entry 5KIN^{168,169} (D) Rescue experiment of *Mtb* exposed to different concentrations of B5 in combination with or without 0.1% L-tryptophan. Data shown as mean and standard deviation of the mean of at least three independent experiments.

5.2.2 Characterization of Two Novel Inhibitors of the *Mycobacterium tuberculosis* Cytochrome bc₁ Complex

Resistance conveying spontaneous mutants against B6 indicated a putative target in the respiratory chain of *Mtb*. In order to confirm this activity and to further characterize the anti-mycobacterial properties of this compound, several experiments have been performed. This includes REMA, intracellular growth assays utilizing dsred2-expressing *Mtb* and eGFP-expressing THP-1 cells, cytoprotection in THP-1-derived macrophages, investigation of the mycobacterial intracellular ATP levels, relative transcription studies of the potential protein (*cydB*) and cross-resistance studies using mutation strains harboring the most common SNPs found in clinical isolates resistant to inhibitors of the cytochrome *bc₁* complex. This functional investigation of the compound B6 is described in more detail in the following publication. In addition, this publication also includes similar experiments and data about the compound MJ-22. Initial identification of this compound was performed during the bachelor thesis of Jason Chhen who is listed as shared first author of the publication. The whole-genome sequencing data were created by Dr. Viola Dreyer and Dr. Stefan Niemann from the Leibniz Research Center in Borstel. The Biological relevance was then analyzed by me and Dr. Michael Dal Molin.

I contributed to the following publication by performing the experiments determining the effect of the compound B6 on intracellular ATP levels, cytoprotection of THP-1-derived macrophages and intracellular *Mtb* growth. This includes establishing and validating the bioanalytical correlation between dsred2 signal and mycobacterial growth. In addition, I developed and partly did the quantitative real-time PCR of *cydB*. Investigation of the effect of B6 on cytoprotection of MRC-5 human lung fibroblasts during infection and growth inhibition experiments were performed by me with the help of Jason Chhen and Edeltraud van Gumpel. Furthermore, all resistant mutants generated against the compound B6 and the control compound Q203 were created by me. With the help of Dr. Michael Dal Molin, I analyzed all of the mutation patterns of resistant mutants. The manuscript was written by me and proofread by Dr. Michael Dal Molin and PD Dr. Dr. Jan Rybniker. All illustrations of the following publication were created by me.

The following manuscript has been accepted for publication in the peer-reviewed journal Antimicrobial Agents and chemotherapy.



Characterization of Two Novel Inhibitors of the *Mycobacterium tuberculosis* Cytochrome *bc*₁ Complex

Raphael Gries,^{a,b,c} Michael Dal Molin,^{a,b} Jason Chhen,^{a,b} Edeltraud van Gumpel,^{a,b} Viola Dreyer,^{d,e} Stefan Niemann,^{d,e} Jan Rybniker^{a,b,c}

^aDepartment I of Internal Medicine, Medical Faculty and University Hospital Cologne, University of Cologne, Cologne, Germany

^bCenter for Molecular Medicine Cologne (CMMC), University of Cologne, Cologne, Germany

^cGerman Center for Infection Research (DZIF), Partner Site Bonn-Cologne, Cologne, Germany

^dMolecular and Experimental Mycobacteriology, Research Center Borstel, Borstel, Germany

^eGerman Center for Infection Research (DZIF), Partner Site Hamburg-Lübeck-Borstel-Riems, Borstel, Germany

Raphael Gries, Michael Dal Molin, and Jason Chhen contributed equally. Author order was determined according to the amount of work invested in this project.

ABSTRACT Drug-resistant tuberculosis is a global health care threat calling for novel effective treatment options. Here, we report on two novel cytochrome *bc*₁ inhibitors (MJ-22 and B6) targeting the *Mycobacterium tuberculosis* respiratory chain with excellent intracellular activities in human macrophages. Both hit compounds revealed very low mutation frequencies and distinct cross-resistance patterns with other advanced cytochrome *bc*₁ inhibitors.

KEYWORDS *Mycobacterium tuberculosis*, QcrB, antibiotic, cytochrome *bc*₁, ATP, drug screening

After a constant decline of new tuberculosis (TB) cases in the past decades, 2021 marks the first year with an increase of 0.5 million tuberculosis cases compared to the previous year. Among these 10.6 million cases there were an estimated 450,000 cases of multidrug-resistant TB (MDR-TB), which no longer respond to the standard antibiotic regimen (1). This illustrates that there is an urgent need for lead compounds with novel modes of action active against drug-resistant *Mycobacterium tuberculosis*. The past decade revealed that the *M. tuberculosis* respiratory chain is a highly susceptible target for synthetic small molecules (2–4). With bedaquiline, inhibiting the ATP synthase, and Q203, targeting the cytochrome *bc*₁ complex, two respiratory chain inhibitors have been approved by regulatory authorities or are currently being investigated in phase 2 clinical trials (5, 6). Screening of 60,000 small molecules using a phenotypic resazurin microtiter assay (REMA) (7) at single concentrations (10 μ M) identified 425 hit compounds (0.71% hit rate) with antituberculous activity (8, 9). A subsequent secondary screening based on a fibroblast-associated infection model (10) allowed for exclusion of cytotoxic compounds and indicated potential intracellular antibiotic activity. After confirmation of activity in 2-fold serial dilutions, this dual screening yielded 11 compounds (0.02% hit rate) with potential intracellular antibiotic activity. Out of these hit compounds we selected two substances, namely, B6, a quinoline-amine, and MJ-22, a thiazole, for further investigations (Fig. 1A). Both compounds showed good antituberculous activity with minimal inhibitory concentrations (MICs) of 1.12 μ M (B6) and 3.69 μ M (MJ-22) in 7H9 broth using the REMA (Fig. 1B) (7). Intracellular activity was determined using enhanced green fluorescent protein (eGFP)-expressing THP-1-derived macrophages which were infected with dsred2-expressing *M. tuberculosis*. To confirm that the red fluorescent signal obtained in this assay correlates with the intracellular mycobacterial load, we first generated a standard curve, correlating fluorescence with the number of bacteria in macrophages (see Fig. S3 and the methods section in the supplemental material). This correlation analysis

Copyright © 2023 American Society for Microbiology. All Rights Reserved.

Address correspondence to Jan Rybniker, jan.rybniker@uk-koeln.de.

The authors declare no conflict of interest.

Received 25 February 2023

Returned for modification 19 March 2023

Accepted 5 June 2023

5 Results

Inhibitors of *M. tuberculosis* Cytochrome bc₁ Complex

Antimicrobial Agents and Chemotherapy

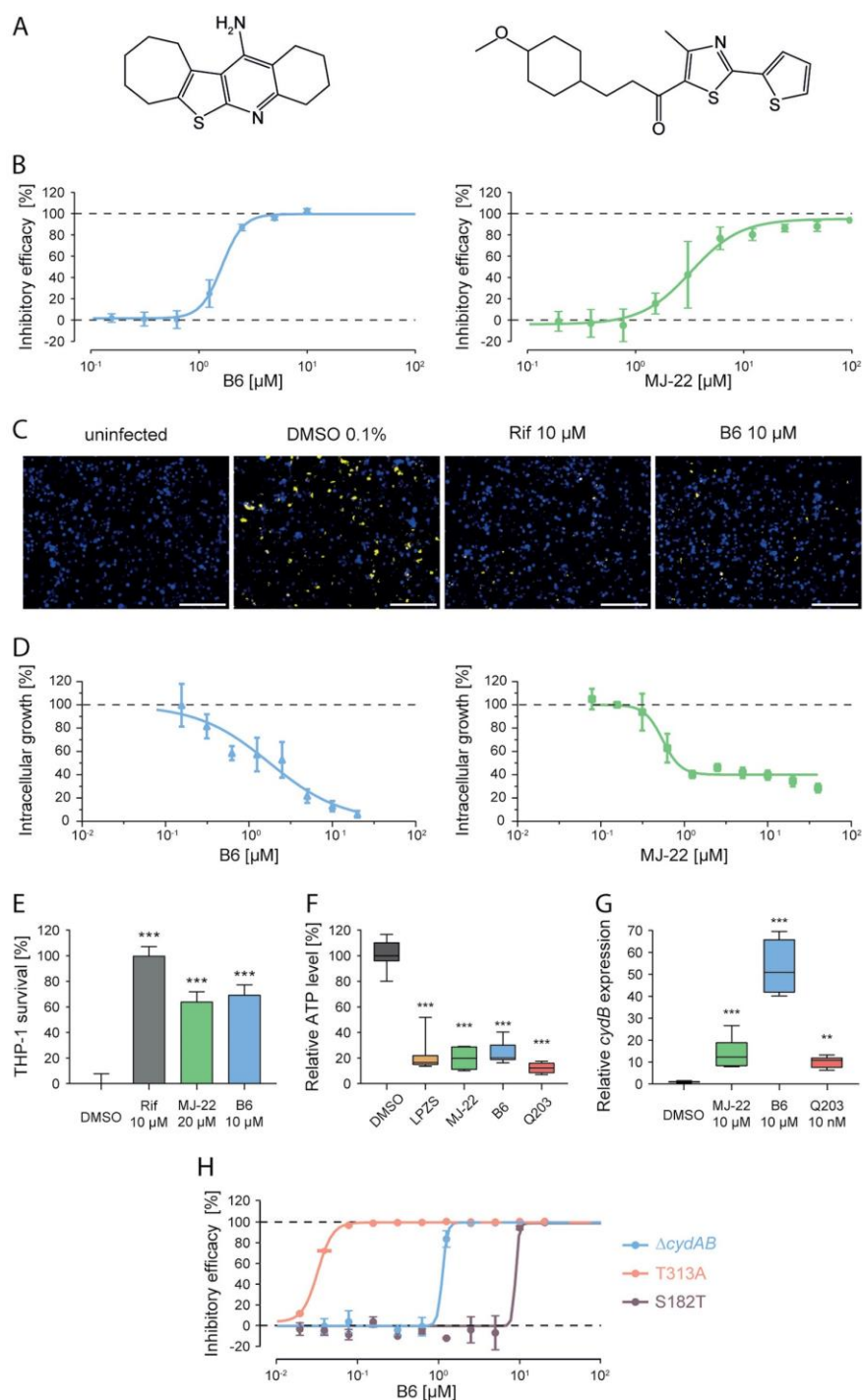


FIG 1 Small molecules show antituberculous activity, host cell protection, and inhibition of the respiratory chain of *Mycobacterium tuberculosis*. (A and B) The two compounds (A) B6 (left) and MJ22 (right) show high efficacy (B) in 7H9 broth with MIC_{50} s of 1.62 μ M and 3.69 μ M, respectively. (C) Representative microscopy pictures 48 h after infection with dsred2-expressing *M. tuberculosis* (yellow) of eGFP-expressing THP-1-derived macrophages (blue) (Rif, rifampicin; DMSO, dimethyl sulfoxide). (D) Intracellular growth of dsred2-expressing *M. tuberculosis* 48 h postinfection (multiplicity of infection of 2) after exposure to different concentrations of B6 (left) or MJ-22 (right). Data (Continued on next page)

between CFU extracted from infected macrophages and the fluorescent signal provided an R^2 value of 0.81, indicating that the measured dsred2 signal is a good surrogate for the number of intracellular bacteria. Using this assay, we treated intracellular bacteria with the two compounds, which led to a dose-dependent reduction of intracellular growth of *M. tuberculosis* with a 50% inhibitory concentration (IC_{50}) of 1.78 μ M for B6 and 0.55 μ M for MJ-22 (Fig. 1C and D). MJ-22 did not lead to a full suppression of the dsred2 signal compared to B6. The reason for this is not fully understood. Nevertheless, a clear concentration-dependent effect could be observed for both compounds. Further investigation of the infected macrophages also revealed strongly increased host cell survival following treatment, which is an additional surrogate for excellent intracellular activity of antimycobacterial drugs (Fig. 1E). Using an additional, highly sensitive assay which quantifies survival of *M. tuberculosis*-infected MRC-5 human lung fibroblasts (10), we determined 50% effective concentrations (EC_{50}) of 0.78 μ M (B6) and 1.36 μ M (MJ-22) (Fig. S1). No cytotoxic effects were observed for MJ-22 in exposed THP-1 macrophages at concentrations up to 200 μ M after 72 h, whereas B6 showed cytotoxicity only at very high concentrations (IC_{50} of 89.37 μ M), providing a selectivity index (SI) of 79.8 (Fig. S2). To elucidate the modes of action, we performed a series of secondary assays including quantification of intracellular ATP pools, which revealed that exposure to either of the compounds strongly reduced ATP levels in *M. tuberculosis*, suggesting the respiratory chain as a potential molecular target (Fig. 1F). The known cytochrome *bc₁* complex inhibitors Q203 and lansoprazole sulfide (LPZS) were used as positive controls (11, 12). Based on these findings, we focused on potential effects on components of the respiratory chain and could show that treatment of *M. tuberculosis* with either compound led to significant upregulation of *cydB* (Rv1622c) in reverse transcriptase quantitative PCR (RT-qPCR) experiments (Fig. 1G). The gene *cydB* codes for a component of the alternative terminal oxidase cytochrome *bd*. Upregulation of cytochrome *bd* represents a compensatory mechanism of *M. tuberculosis* which partly restores activity of the respiratory chain following chemical inhibition of cytochrome *bc₁*, indirectly showing that cytochrome *bc₁* is the putative target of B6 and MJ-22 (13). In contrast, deletion of cytochrome *bd* facilitates the generation and selection of spontaneous cytochrome *bc₁* mutants resistant to the respective inhibitors (13). By plating bacteria on agar containing the compounds at concentrations five times above the MIC, we were able to generate a single resistant clone for B6 and MJ-22, respectively. We were not able to raise additional clones despite several attempts. Based on the number of bacteria plated for these experiments, we calculated the frequency of resistance for both compounds (B6, 2.17×10^{-10} ; MJ-22, 3.33×10^{-9}). For Q203 we calculated a frequency of 5×10^{-9} (own data versus 6.25×10^{-9} described by Lee et al. [14]). Thus, at least for B6, the frequency is considerably lower than for Q203 and other cytochrome *bc₁* inhibitors (14–17). Whole-genome sequencing of the resistant clones confirmed mutations exclusively in the cytochrome *bc₁* complex b-subunit *qcrB* (Rv2196) at codon 182 (S182T) for B6 and at codon 342 (M342V) for MJ-22. This provides further evidence that cytochrome *bc₁* is the molecular target of B6 and MJ-22. Testing both compounds for cross-resistance to the most frequent resistance-conveying mutations in other cytochrome *bc₁* inhibitors such as T313A (12, 18) and A178V (15) resulted in a distinct pattern. While both B6 and MJ-22 showed an increase of MIC in QcrB mutants with S182T/P, A178V, and M342V amino acid changes or the QcrA (Rv2195) L356V/W amino acid change, no resistant phenotype was observed in the QcrB T313A mutant, which is a key driver of resistance for the most advanced cytochrome *bc₁* inhibitor, Q203 (Table 1 and Fig. S4) (12). Interestingly, the T313A

FIG 1 Legend (Continued)

are normalized to 0.1% DMSO (100%) and 10 μ M rifampicin (0%). (E) Cell count of eGFP-expressing THP-1-derived macrophages 48 h postinfection (multiplicity of infection of 2). Data are normalized to rifampicin (Rif; survival = 100%) or 0.1% DMSO (DMSO; host cell death = 0%). *M. tuberculosis* dsred2 signal and THP-1 cell count were determined using ImageJ. (F) Relative intracellular ATP levels after 24 h of exposure to the respective compound normalized to 0.1% DMSO. (G) Relative expression of the cytochrome *bd* subunit II *cydB* (Rv1622c) after 4 h of exposure and normalized to 0.1% DMSO. (H) Antituberculous activity of B6 against the Δ *cydAB* parental strain (blue) and Δ *cydAB* mutants containing the QcrB mutation T313A (orange) or S182T (brown). Data are shown as mean and standard error of the mean. Box plot whiskers represent minimal and maximum values. Statistical significances are compared to DMSO based on one-way analysis of variance with a *post hoc* pairwise comparison and Bonferroni correction (**, $P < 0.01$; ***, $P < 0.001$). Scale bars shown in microscopy images represent 200 μ m.

TABLE 1 Cross-resistance patterns of various resistance-facilitating mutations^a

Compound	<i>M. tuberculosis</i> H37Rv Δ <i>cydAB</i> (MIC ₅₀)							
	Parental	QcrB					QcrA	
		S182T	S182P	A178V	T313A	M342V	L356V	L356W
Q203 (nM)	1.27 (0.98–1.47)	1.57 (1.04–2.37)	5.84 (4.55–6.19)	0.86 (0.75–1.01)	>100 (NA)	13.01 (12.17–16.72)	13.05 (11.68–16.58)	>100 (NA)
MJ-22 (μ M)	4.89 (4.48–5.28)	>50 (NA)	>50 (NA)	>50 (NA)	7.43 (6.57–9.74)	>50 (NA)	>50 (NA)	>50 (NA)
B6 (μ M)	1.12 (0.86–1.22)	8.43 (6.66–9.51)	8.90 (7.00–9.84)	5.38 (3.76–8.09)	0.03 (0.03–0.03)	8.43 (6.90–9.49)	7.94 (6.66–9.40)	6.14 (5.34–8.46)

^aThe MIC₅₀s of Q203, B6, and MJ-22 against the *M. tuberculosis* Δ *cydAB* parental strain and mutants harboring mutations in the QcrB (Rv2196) (S182T, S182P, A178V, T313A, and M342V) and QcrA (Rv2195) (L356V and L356W) loci were tested in resazurin microtiter assays. The lower and upper confidence levels of the MIC₅₀ are indicated in parentheses. Dose-response curves of each compound to the respective mutant are displayed in Fig. S4 in the supplemental material. NA, not applicable. Boldface highlights most common mutation in Q203 resistant mutants.

mutant strain showed antibiotic hypersensitivity to B6, with a 36-fold increase in susceptibility and an MIC in the low nanomolar range (Fig. 1H). The mechanism for this interesting phenotype requires further investigations.

To conclude, with B6 and MJ-22 we identified two promising antituberculous hit compounds targeting the *M. tuberculosis* respiratory chain. Both substances showed good intracellular activity and selectivity indices regarding cytotoxicity. Although compound B6 was previously described in an independent screening focusing on ATP homeostasis inhibitors (19), with cytochrome *bc₁*, we were now able to fully elucidate the target of this hit compound. Lack of cross-resistance or even hypersensitivity in *M. tuberculosis* strains with reduced efficacy of the frontrunner drug Q203 or other cytochrome *bc₁* inhibitors may allow for extended clinical application of B6 and MJ-22 derivatives in pretreated individuals. Combining two cytochrome *bc₁* inhibitors with well-defined and distinct resistance mechanisms could be another possibility to combat the emerging problem of multidrug resistance.

SUPPLEMENTAL MATERIAL

Supplemental material is available online only.

SUPPLEMENTAL FILE 1, PDF file, 0.9 MB.

ACKNOWLEDGMENTS

We thank Kevin Pethe from Nanyang Technological University in Singapore for providing us with the *cydAB* deletion mutant (H37Rv Δ *cydAB*).

J.R. is supported by the German Research Foundation (DFG) grant SFB 1403, the German Center for Infection Research (DZIF; TTU-TB grants 02.806, 02.814, and 02.913), the German Federal Ministry of Education and Research (BMBF, grant IdEpiCo), a research grant of the CMMC (B10), and the European Union Innovative Medicines Initiative 2 Joint Undertaking program grant no. 853989 (ERA4TB).

Conceptualization, R.G., M.D.M., and J.R.; methodology, R.G., M.D.M., J.C., E.V.G., V.D., and J.R.; validation, R.G., M.D.M., J.C., E.V.G., V.D., S.N., and J.R.; formal analysis, R.G., M.D.M., J.C., E.V.G., V.D., S.N., and J.R.; investigation, R.G., M.D.M., J.C., E.V.G., V.D., S.N., and J.R.; resources, J.R.; data curation, R.G., M.D.M., J.C., E.V.G., V.D., and J.R.; writing – original draft, R.G., M.D.M., J.C., and J.R.; writing – review & editing, R.G., M.D.M., J.C., E.V.G., V.D., S.N., and J.R.; visualization, R.G., M.D.M., and J.R.; supervision, J.R.; project administration, J.R.; funding acquisition, J.R.

All authors declare no competing interests.

REFERENCES

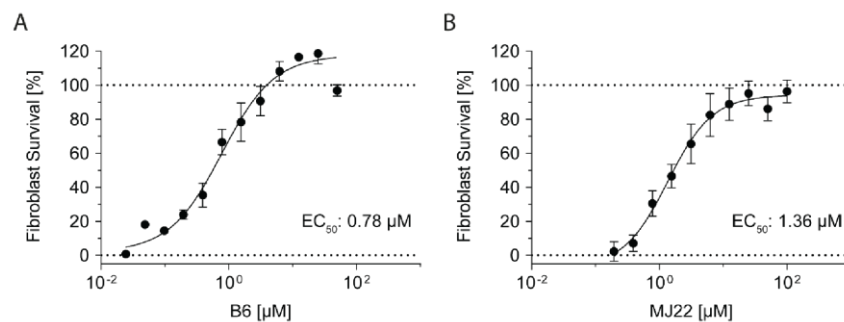
- WHO. 2022. Global tuberculosis report. WHO, Geneva, Switzerland.
- Foo CS-Y, Pethe K, Lupien A. 2020. Oxidative phosphorylation—an update on a new, essential target space for drug discovery in *Mycobacterium tuberculosis*. *Appl Sci* 10:2339. <https://doi.org/10.3390/app10072339>.
- Bajeli S, Baid N, Kaur M, Pawar GP, Chaudhari VD, Kumar A. 2020. Terminal respiratory oxidases: a targetable vulnerability of mycobacterial bioenergetics? *Front Cell Infect Microbiol* 10:589318. <https://doi.org/10.3389/fcimb.2020.589318>.
- Bahuguna A, Rawat S, Rawat DS. 2021. QcrB in *Mycobacterium tuberculosis*: The new drug target of antitubercular agents. *Med Res Rev* 41:2565–2581. <https://doi.org/10.1002/med.21779>.
- Mahajan R. 2013. Bedaquiline: first FDA-approved tuberculosis drug in 40 years. *Int J Appl Basic Med Res* 3:1–2. <https://doi.org/10.4103/2229-516X.112228>.
- de Jager VR, Dawson R, van Niekerk C, Hutchings J, Kim J, Vanker N, van der Merwe L, Choi J, Nam K, Diacon AH. 2020. Telacebec (Q203), a new antituberculosis agent. *N Engl J Med* 382:1280–1281. <https://doi.org/10.1056/NEJMc1913327>.
- Palomino JC, Martin A, Camacho M, Guerra H, Swings J, Portaels F. 2002. Resazurin microtiter assay plate: simple and inexpensive method for detection of drug resistance in *Mycobacterium tuberculosis*. *Antimicrob Agents Chemother* 46:2720–2722. <https://doi.org/10.1128/AAC.46.8.2720-2722.2002>.

8. Malin JJ, Winter S, van Gumpel E, Plum G, Rybniker J. 2019. Extremely low hit rate in a diverse chemical drug screen targeting *Mycobacterium abscessus*. *Antimicrob Agents Chemother* 63:e01008-19. <https://doi.org/10.1128/AAC.01008-19>.
9. von Amburen J, Schreiber F, Fischer J, Winter S, van Gumpel E, Simonis A, Rybniker J. 2020. Comprehensive host cell-based screening assays for identification of anti-virulence drugs targeting *Pseudomonas aeruginosa* and *Salmonella Typhimurium*. *Microorganisms* 8:1096. <https://doi.org/10.3390/microorganisms8081096>.
10. Rybniker J, Chen JM, Sala C, Hartkoorn RC, Vocat A, Benjak A, Boy-Rottger S, Zhang M, Szekeley R, Greff Z, Orfi L, Szabadkai I, Pato J, Keri G, Cole ST. 2014. Anticytolytic screen identifies inhibitors of mycobacterial virulence protein secretion. *Cell Host Microbe* 16:538–548. <https://doi.org/10.1016/j.chom.2014.09.008>.
11. Rybniker J, Vocat A, Sala C, Busso P, Pojer F, Benjak A, Cole ST. 2015. Lansoprazole is an antituberculous prodrug targeting cytochrome *bc₁*. *Nat Commun* 6:7659. <https://doi.org/10.1038/ncomms8659>.
12. Pethe K, Bifani P, Jang J, Kang S, Park S, Ahn S, Jiricek J, Jung J, Jeon HK, Cechetto J, Christophe T, Lee H, Kempf M, Jackson M, Lenaerts AJ, Pham H, Jones V, Seo MJ, Kim YM, Seo M, Seo JJ, Park D, Ko Y, Choi I, Kim R, Kim SY, Lim S, Yim SA, Nam J, Kang H, Kwon H, Oh CT, Cho Y, Jang Y, Kim J, Chua A, Tan BH, Nanjundappa MB, Rao SP, Barnes WS, Wintjens R, Walker JR, Alonso S, Lee S, Kim J, Oh S, Oh T, Nehrbass U, Han SJ, No Z, Lee J, Brodin P, Cho SN, Nam K, Kim J. 2013. Discovery of Q203, a potent clinical candidate for the treatment of tuberculosis. *Nat Med* 19:1157–1160. <https://doi.org/10.1038/nm.3262>.
13. Kalia NP, Hasenoehrl EJ, Ab Rahman NB, Koh VH, Ang MLT, Sajorda DR, Hards K, Gruber G, Alonso S, Cook GM, Berney M, Pethe K. 2017. Exploiting the synthetic lethality between terminal respiratory oxidases to kill *Mycobacterium tuberculosis* and clear host infection. *Proc Natl Acad Sci U S A* 114:7426–7431. <https://doi.org/10.1073/pnas.1706139114>.
14. Lee BS, Hards K, Engelhart CA, Hasenoehrl EJ, Kalia NP, Mackenzie JS, Sviriaeva E, Chong SMS, Manimekalai MSS, Koh VH, Chan J, Xu J, Alonso S, Miller MJ, Steyn AJC, Gruber G, Schnappinger D, Berney M, Cook GM, Moraski GC, Pethe K. 2021. Dual inhibition of the terminal oxidases eradicates antibiotic-tolerant *Mycobacterium tuberculosis*. *EMBO Mol Med* 13:e13207. <https://doi.org/10.15252/emmm.202013207>.
15. Harrison GA, Mayer Bridwell AE, Singh M, Jayaraman K, Weiss LA, Kinsella RL, Aneke JS, Flentie K, Schene ME, Gaggioli M, Solomon SD, Wildman SA, Meyers MJ, Stallings CL. 2019. Identification of 4-amino-thieno[2,3-*d*]pyrimidines as QcrB inhibitors in *Mycobacterium tuberculosis*. *mSphere* 4:e00606-19. <https://doi.org/10.1128/mSphere.00606-19>.
16. Abrahams KA, Cox JA, Spivey VL, Loman NJ, Pallen MJ, Constantinidou C, Fernandez R, Alemparte C, Remuinan MJ, Barros D, Ballell L, Besra GS. 2012. Identification of novel imidazo[1,2-*a*]pyridine inhibitors targeting *M. tuberculosis* QcrB. *PLoS One* 7:e52951. <https://doi.org/10.1371/journal.pone.0052951>.
17. Lu X, Williams Z, Hards K, Tang J, Cheung CY, Aung HL, Wang B, Liu Z, Hu X, Lenaerts A, Woolhiser L, Hastings C, Zhang X, Wang Z, Rhee K, Ding K, Zhang T, Cook GM. 2019. Pyrazolo[1,5-*a*]pyridine inhibitor of the respiratory cytochrome *bcc* complex for the treatment of drug-resistant tuberculosis. *ACS Infect Dis* 5:239–249. <https://doi.org/10.1021/acsinfecdis.8b00225>.
18. Rybniker J, Kohl TA, Barilar I, Niemann S. 2019. No evidence for acquired mutations associated with cytochrome *bc₁* inhibitor resistance in 13,559 clinical *Mycobacterium tuberculosis* complex isolates. *Antimicrob Agents Chemother* 63:e01317-18. <https://doi.org/10.1128/AAC.01317-18>.
19. Mak PA, Rao SP, Ping Tan M, Lin X, Chyba J, Tay J, Ng SH, Tan BH, Cherian J, Duraiswamy J, Bifani P, Lim V, Lee BH, Ling Ma N, Beer D, Thayalan P, Kuhen K, Chatterjee A, Supek F, Glynne R, Zheng J, Boshoff HI, Barry CE, III, Dick T, Pethe K, Camacho LR. 2012. A high-throughput screen to identify inhibitors of ATP homeostasis in non-replicating *Mycobacterium tuberculosis*. *ACS Chem Biol* 7:1190–1197. <https://doi.org/10.1021/cb2004884>.

Supplementary information for:

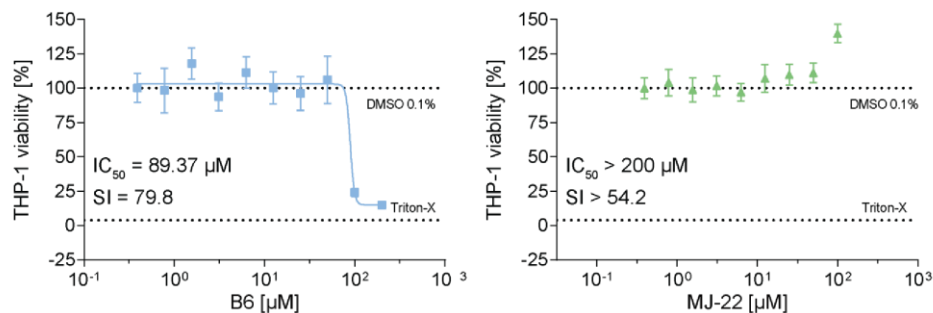
Characterization of two novel inhibitors of the *Mycobacterium tuberculosis* cytochrome *bc₁* complex

Raphael Gries^{1,2,3,+}, Michael Dal Molin^{1,2,+}, Jason Chhen^{1,2,+}, Edeltraud van Gumpel^{1,2}, Viola Dreyer^{4,5}, Stefan Niemann^{4,5}, Jan Rybniker^{1,2,3#}



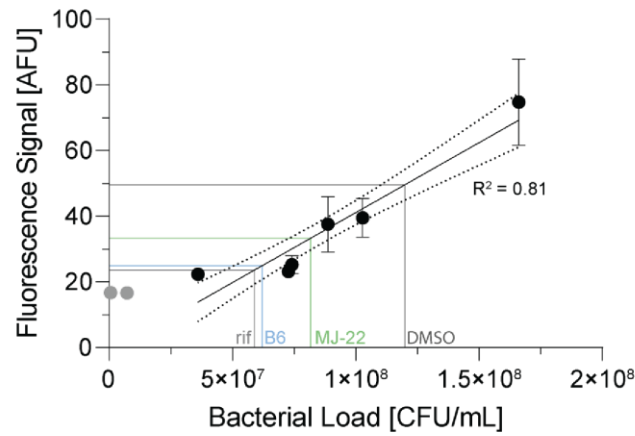
Supplementary Figure 1: Compound facilitated host cell survival.

MRC-5 human lung fibroblasts were treated with different concentrations of B6 (A) or MJ-22 (B) and infected with *Mycobacterium tuberculosis* (MOI 10). Fibroblast survival was measured three days post infection using the cell viability kit CellTiter-Glo. Survival was calculated relative to 10 µM rifampicin (100%) and the solvent control 0.1% DMSO (0%).



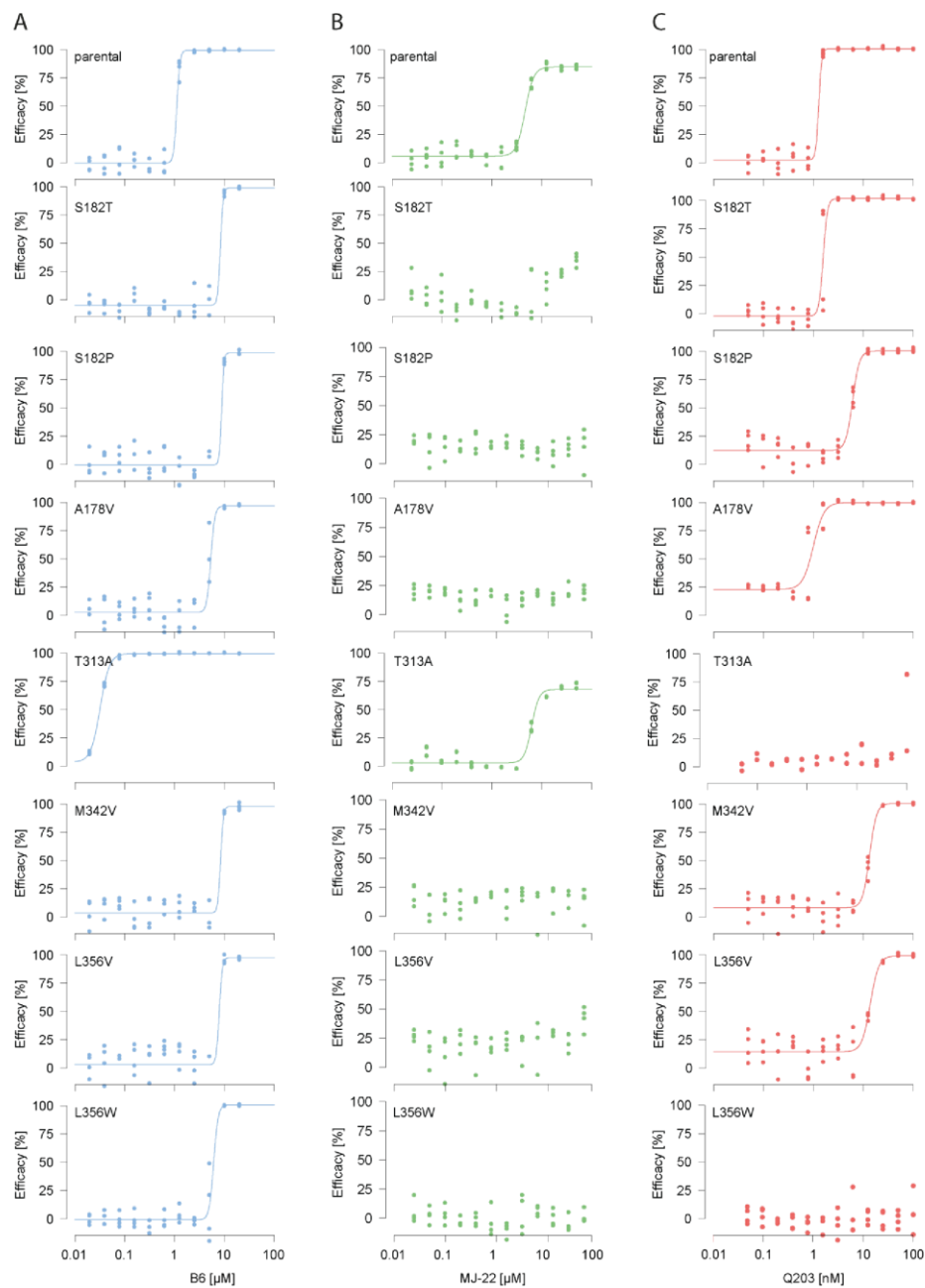
Supplementary Figure 2: Cytotoxicity Assay.

THP-1 derived macrophages were exposed to different concentrations of B6 (left) and MJ-22 (right) for three days. Cell viability was measured using Resazurin. Viability was calculated in correlation to cells treated with 0.1% DMSO (100%) or 1 % Triton-X (0%). IC₅₀ (50% inhibitory concentration) was calculated using GraphPad Prism based on the fit shown in the respective graph. Selectivity indices (SI) were calculated based on the anti-tuberculous MIC₅₀ activity (IC₅₀/MIC₅₀).



Supplementary Figure 3: Correlation dsred2 signal and intracellular bacterial load.

THP-1 derived macrophages were infected with different MOI of *Mtb* expressing dsred2. After 48 h host-cells were lysed and intracellular bacteria were plated on 7H10 agar. Colony forming units (CFU) were then counted two weeks post plating. The calibration curve was calculated using GraphPad Prism assuming linear progression of dsred2 signal (grey points with very low numbers of input bacteria were excluded). Additional lines represent mean values detected during experiments for different test compounds and controls (rif = 5 μ M rifampicin, B6 = 10 μ M B6, MJ-22 = 20 μ M MJ-22 and DMSO = 0.1% DMSO).



Supplementary Figure 4: MIC determination for resistant mutants.

Panels show growth inhibition curves based on REMA of the parental strain (*Mtb* H37Rv Δ *cydAB*) and mutants harboring the respective point mutations. Bacteria were exposed to (A) B6, (B) MJ-22 and (C) Q203 in 2-fold serial dilutions. Mycobacterial growth was measured after eight days and inhibitory efficacy was calculated based on growth inhibition with 0.1% DMSO representing 0% efficacy and 10 μ M rifampicin representing 100% efficacy.

Experimental setup

Screening of small molecule libraries

The tested small molecules were sourced from two libraries. 10,000 molecules of the SPECS World Diversity set 3 library (SPECS, Netherlands) and 50,000 molecules from the FMP Berlin (Leibniz-Forschungsinstitut für Molekulare Pharmakologie).

Generation of resistant Mutants

Mycobacterium tuberculosis were cultivated under aerobic conditions in 7H9c medium at 37 °C. In order to select for spontaneous resistant mutants 3×10^7 to 3×10^9 bacteria were plated on 7H10 agar plates containing 5x or 10x the MIC₉₀ of the respective test compound. Plates were incubated for 14 to 28 days. Colonies were picked and subcultivated on 7H10 agar plates with and without compound to validated potential resistance. Mutants were inoculated in 7H9c and cultivated under aerobic conditions. Resistance against the compound was analysed in Resazurin Microtiter Assays.

Targeted Sanger Sequencing

Liquid cultures of mutants were inactivated at 85 °C for 60 minutes and then lysed using 150-212 µm glass beads (Sigma-Aldrich, St. Louis, USA) in a cell disruptor (Disruptor Genie; Scientific Industry, Bohemia, USA). The bacteria were beaten five times at max speed and cooled at 4 °C in between each run. Samples were then centrifuged for 10 min at $14,000 \times$ rcf and the supernatant was separated for Sanger sequencing. Targeted Sanger sequencing the *qcrB* locus was first amplified (5'-GTTCGACGCATTGCATTTCG-3' and 5'-ATTGGCATTGCGTTGATTGC-3') and then sequenced using forward (5'-ACGGGTATCTGGTCGCCA-3'; 5'-CGCCCTGCACATTTTACTGT-3') and backward (5'-CGAAAACCAGGCCCATGATC-3'; 5'-TCTTGATCAGCTACGGGTT-3') sequencing primer.

Resazurin Microtiter Assay (REMA)

A frozen *Mtb* stock was diluted to an OD₅₆₀ of 0.0003. Subsequently 90 µL of this suspension was added to the testing plates containing 10 µL test compound in serial dilutions (1:2). The plates were incubated for 7 days at 37°C. 10 µL Resazurin was added and the plates were incubated for another 24 h at 37°C. Measurement was performed using a plate reader (Cytation5

Cell Imaging Multi-Mode Reader; Agilent BioTek) with excitation of 570 nm and an emission of 590 nm.

ATP measurement

Mtb cultivated at 37°C in a shaking incubator up to midlog phase were harvested and resuspended at an OD₅₆₀ of 0.1 in 7H9c containing the respective test substance. 100 µL were then dispensed into 96-well plates and incubated for 24 h at 37°C at 100 rpm. Mycobacteria were then harvested and 50 µL culture was transferred into a white, opaque 96-well assay plate with clear bottom (Costar™). 50 µL of freshly prepared BacTiter-Glo™ (Promega, Fitchburg, USA) was added and the plate were incubated for 10 min at room temperature and shaking conditions. Chemiluminescence were measured at OD₆₀₀ using a Cytation5 Cell Imaging Multi-Mode Reader (Agilent BioTek). ATP levels were normalized to samples treated with 0.1 % DMSO.

Infection of THP-1-derived macrophages

In 96-well plates (Corning Costar™) 50,000 eGFP expressing THP-1 cells were plated and differentiated to macrophages in the presence of 200 nM PMA in RPMIc for 24 h. Afterwards the medium was replaced with RPMIc. Infection was performed 24 h later by replacing the medium with RPMI containing red fluorescent *Mtb* grown to midlogphase at an MOI of 2. After 4 h of co-cultivation the medium was removed, the cells washed 2x with PBS and medium containing the test compounds was added and the cells were incubated for 48 h. In order to determine macrophage survival and *Mtb* growth supernatant was replaced with PBS and fluorescence microscopy was performed. For quantification of bacteria using microscopy, at least four images were taken of the center of the well at 10x magnification. After background subtraction, intracellular growth was determined by measuring the total fluorescence signal in each well. Visualization and counting of macrophage numbers and fluorescence intensities was done using ImageJ. Data were normalized to the respective controls 0.1% DMSO and 10 µM rifampicin.

Correlating bacterial load and dsred2 signal

THP-1 derived macrophages were infected with different MOI with *Mtb* expressing dsred2 (see above). After four hours of incubation, extracellular bacteria were removed by washing with PBS and cells were incubated for additional 48 h in culture medium. Dsred2 signal was then quantified using fluorescence microscopy images at 10 times magnification using ImageJ. After microscopy, macrophages were lysed using 0.1% SDS. The cell lysates were subsequently

diluted in a 1:10 serial dilution and plated on 7H10 agar plates in order to determine intracellular bacterial loads. Colony forming units were counted after 14 days.

CFU determination

Infected THP-1 macrophages were lysed using 0.1% SDS. The cell lysates were subsequently diluted in a 1:10 dilution series and plated on 7H10 agar plates in order to determine intracellular bacterial loads. Colony forming units (CFU) were counted two weeks post plating.

RNA extraction

RNA extraction of *Mtb* liquid cultures was done by cell lysis using 150 - 212 μm glass beads in a cell disruptor (Disruptor Genie; Scientific Industry, Bohemia, USA). Lysates were centrifuged at $14,000 \times \text{rcf}$ and the supernatant was mixed with RLT lysis buffer containing 1% β -mercaptoethanol and ethanol (3:2). This mixture was then purified using the RNeasy kit (Qiagen, Venlo, Netherlands) according to its protocol.

cDNA synthesis

SuperScriptTM III First-Strand Synthesis SuperMix for qRT-PCR (Invitrogen, Waltham, USA) was used to synthesis the cDNA according to its protocol.

Quantitative realtime PCR (qPCR)

Light Cycler Fast Start DNA Master^{Plus} SYBR[®] Green I kit (Roche, Basel, Switzerland) was used according to its protocol to perform qPCR. The house-keeping gene *sigA* (fwd: 5'-CGCGACATGATGTGGA-3'; rev: 5'-GGAGAACTTGATCCCCT-3') was analyzed as reference for *cydB* expression (fwd: 5'-ACGGTCTTAGTGTGGC-3', rev: 5'-ATACGTCCATGTCTGGT-3')

Whole Genome Sequencing

Mutants have been heat killed and suspended in TE buffer. The samples were shipped to the Research Center Borstel. Chromosomal DNA (gDNA) was extracted using the cetyltrimethylammonium bromide (CTAB) method as described previously (1). Libraries for next generation sequencing (NGS) were prepared from gDNA using a modified Nextera protocol (2) Briefly, input DNA was fragmented by tagmentation and indexed adapters were added by reduced cycle amplification. DNA libraries were sequenced with 2×150 bp paired-end reads on an Illumina NextSeq 500 platform as instructed by the manufacturer (Illumina, San Diego, CA). For sequencing analysis raw read data (fastq files) were analyzed with

MTBseq v1.0.3, a semi-automated bioinformatics pipeline for the analysis of MTBC isolates (3). Briefly, raw reads were mapped to the *M. tuberculosis* H37Rv reference genome (GenBank accession number NC_000962.3) using BWA-MEM, and mapping was refined with the GATK software package. All data sets had a minimum mean genome-wide coverage of the H37Rv reference genome of at least 50-fold. Variants (single nucleotide polymorphisms [SNPs] and insertions and deletions [indels]) were detected based on the SAMtools pileup file, and variants with a minimum coverage of 4 reads in both the forward and reverse orientations, 4 reads calling the allele with a Phred score of at least 20, and an allele frequency of 75% were considered confident variant calls. Multiple consecutive SNP calls (in a 12-bp window), which could reflect artificial variant calls around indels, drug resistance-associated genes, and repetitive regions (e.g., PPE/PGRS genes), were excluded.

Fibroblast survival assay (FSA)

MRC-5 human lung fibroblasts were seeded in opaque, white 384-well plates at 4,000 cells per well and pre-incubated for 3 hours in the presence of the test compound. Afterwards, *Mtb* at a MOI of 10 were added to the fibroblasts and co-incubated for 72 h. Fibroblast viability was then measured using CellTiter-Glo (Promega, Fitchburg, USA) according to its protocol. Survival of fibroblasts was normalized to the solvent control (0% survival) and 10 μ M rifampicin (100% survival) using GraphPad Prism.

THP-1 cytotoxicity assay

THP-1 derived macrophages were seeded with a density of 50,000 (THP-1) cells per well and incubated at 37°C and 5% CO₂ in the presence of the test compound (1:2 dilution series). After 72 h, viability of macrophages was determined using resazurin and measuring in a plate reader (570/590 nm). As survival control 0.1% DMSO and as cytotoxic control 1% Triton-X were used.

References

1. van Embden JD, Cave MD, Crawford JT, Dale JW, Eisenach KD, Gicquel B, Hermans P, Martin C, McAdam R, Shinnick TM, et al. 1993. Strain identification of *Mycobacterium tuberculosis* by DNA fingerprinting: recommendations for a standardized methodology. *J Clin Microbiol* 31:406-9.
2. Baym M, Kryazhimskiy S, Lieberman TD, Chung H, Desai MM, Kishony R. 2015. Inexpensive multiplexed library preparation for megabase-sized genomes. *PLoS One* 10:e0128036.
3. Kohl TA, Utpatel C, Schleusener V, De Filippo MR, Beckert P, Cirillo DM, Niemann S. 2018. MTBseq: a comprehensive pipeline for whole genome sequence analysis of *Mycobacterium tuberculosis* complex isolates. *PeerJ* 6:e5895.

5.3 Hit Compounds with Potential Anti-virulence Activity against *Mtb*

In addition to the compounds of interest with direct growth inhibitory activity, as described above, the initial cross-screening regarding cytoprotection (fibroblast survival; FSA) also revealed interesting compounds with anti-virulence activity (Figure 11).

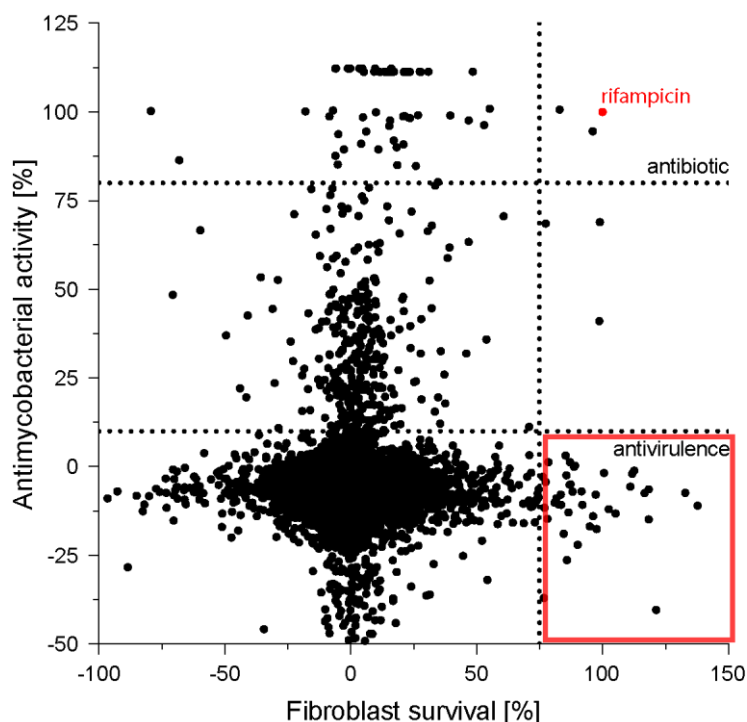


Figure 11: Screening for anti-virulence compounds. 10,000 compounds of the SPECS biodiversity set 3 molecule library were tested for their respective antimycobacterial activity (REMA) and cytoprotection (fibroblast survival, FSA). Compounds were tested at 10 μ M in two independent replicates and normalized to 5 μ M rifampicin or 0.1% DMSO. The highlighted rectangle includes potential anti-virulence compounds.

Extensive literature review and consideration of commercial availability reduced the initial 43 hits to eleven compounds that were further investigated (Table 3). Despite not directly leading to death or growth inhibition of exposed *Mtb* in broth, these molecules potentially inhibit *Mtb* during infection, either by modulation of the host cell or by abrogating the ability of *Mtb* to successfully infect its host^{105,170}. One major, and potentially the best-described, virulence factor of *Mtb* is the type VII secretion system ESX-1. Deletion of ESX-1 leads to a phenotype with strongly abrogated infection efficacy. As described in the literature, ESX-1 inhibitors also exhibit a distinct phenotype that aligns with the outcomes of the initial screening process, including the absence of bacterial growth inhibition in broth, cytoprotection during infection, and, to some extent, even a co-cultivation of host cell and pathogen during experiments, which is observable through microscopy¹³². All of the selected hits already fit this phenotype leading to the assumption that some of these compounds might be able to inhibit

ESX-1. To validate this hypothesis, the effect of the test compounds on the ESX-1 secretion system was analyzed. In the used standardized experimental setup, *Mtb* is cultivated in relatively large volumes (30 mL) in protein free Sauton's medium, while being exposed to the test compounds^{132,150,151,155,156,171}. The supernatant is then collected, 100 times concentrated and analyzed by SDS-PAGE followed by Western Blot detection. Here, the strictly ESX-1-mediated substrate EsxA is probed by a specific, monoclonal antibody and a secondary polyclonal antibody conjugated to a horseradish peroxidase to detect the abundance of the substrate in the supernatant. A decrease of extracellular EsxA directly correlates with abrogation of ESX-1 activity. To exclude potential expression changes of the probed ESX-1 substrate, the respective cell lysates were also investigated. Further controls include the intracellular heat shock protein HSP65 to exclude potential cell lysis and the TAT substrate Ag85 to exclude abrogation of general secretion. As this experimental setup requires a great amount of substance and pathogenic biomass, an optimal range of concentration needed to be evaluated before testing. For the individual testing of the anti-virulence test compounds, the efficacy in the host cell associated infection model FSA was used to determine the potential concentration to test for ESX-1 inhibition. Here, five times the concentration of the EC₅₀ was tested (Figure 12) with 0.02% DMSO being used as control and reference for native protein levels.

Of the eleven tested compounds only three reduced EsxA level in the supernatant (cell filtrate) but not in the cell lysate, namely S1, S3 and S10. These three molecules also did not induce cell lysis, which in contrast is clearly visible for compound S5, as the HSP65 signal is distinctly detectable in the supernatant sample (Figure 12). Neither S1, S3 nor S10 led to a reduction in the intracellular protein levels, nor did exposure to these compounds visibly impact the secretion of Ag85. The intracellular levels of EsxA after exposure to S3 or S10 potentially even increases slightly. This indicates that S1, S3 and S10 might not impact the protein biosynthesis, nor at least one alternative secretion system (TAT).

5 Results

Table 3: Overview of hit compounds with anti-virulence activity. Shown is the concentration at which 50% effective cytoprotection was still measurable in a fibroblast survival assay (EC_{50}) and if the compound tested positive for inhibition of ESX-1 in Western Blot analysis of secreted EsxA (EsxA inhibitor).

ID	EC_{50}	EsxA inhibitor
S1	9.2	Yes
S3	7.2	Yes
S4	5.0	No
S5	8.9	No
S8	2.5	No
S9	1.3	No
S10	8.8	Yes
S11	0.7	No
S13	2.9	No
S14	1.8	No
S25	2.76	No

Interestingly, two of the three ESX-1 inhibitors are structurally similar. S3 and S10 both contain a 1,3,4-oxadiazol scaffold extended by a sulfanyl-ethanone. Based on this, the following research focused on S3 as the slightly more promising candidate molecule. Extensive investigation and characterization of S3 as an anti-virulence compound are described in chapter 5.3.1.

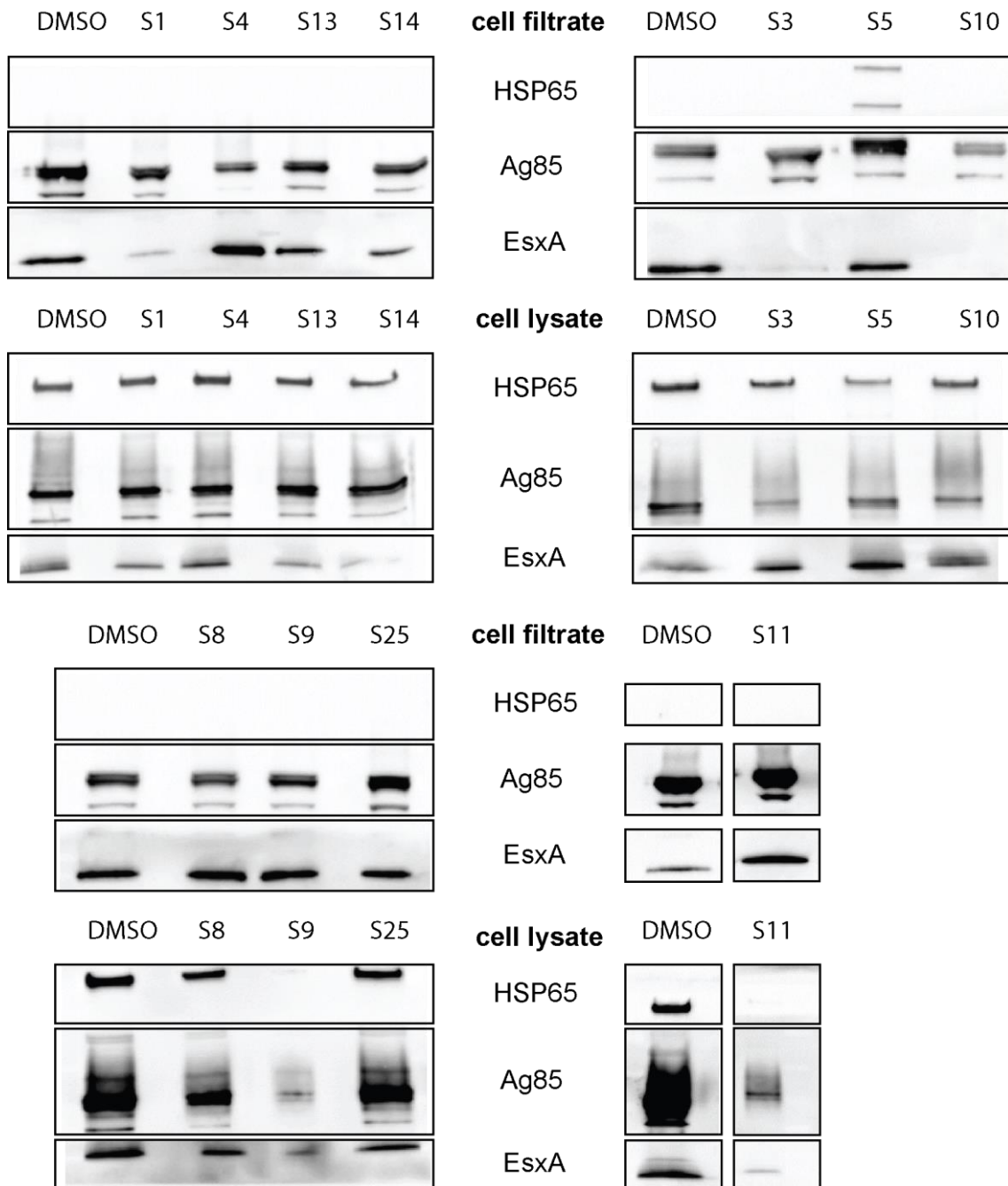


Figure 12: Representative Western blots of samples taken from *Mtb* cultures after exposure to anti-virulence compounds. Representative Western Blots of two replicates of supernatant samples (cell filtrate) and cell lysate samples of *Mtb* cultures exposed to five times the EC_{50} of the respective compound are depicted. EsxA was probed as indicator for ESX-1 activity. DMSO was used as a solvent control, the intracellular heat shock protein HSP65 as a lysis control and the TAT substrate Ag85 as a control for general abrogation of secretion.

5.3.1 Discovery of dual-active ethionamide boosters inhibiting the *Mycobacterium tuberculosis* ESX-1 secretion system

The 1,3,4-oxadiazol compound S3 was identified as potential ESX-1 inhibitor during initial anti-virulence screening. This small molecule was further investigated regarding its effect on *Mtb* and its interaction with *Mtb* in a host cell context. The respective results culminated in the following manuscript, which is currently under peer-review. The initial investigation included dose-dependent testing of ESX-1 inhibition, cross-testing of cytoprotection in peripheral blood mononuclear cell (PBMCs)-derived macrophages, investigation of cytokine (IL-1 β) release during infection and impact on intracellular *Mtb* growth during infection. In addition, in-depth analyzes of translational changes using RNA sequencing (RNA-Seq) of *Mtb* exposed to S3 revealed a highly favorable secondary effect. This experimental setup indicated the presence of S3 leads to up-regulation of the gene *ethA* (Rv3854c), which encodes the prodrug-activating enzyme EthA. The reprocessing of RNA-Seq data was greatly assisted by Dr. Lindsay Sonnenkalb and Dr. Christian Utpatel from the Leibniz Research Center in Borstel, as well as Dr. Michael Dal Molin. The secondary effect was then validated by growth inhibition studies that combined S3 with the prodrug ethionamide, an EthA substrate. This phenomenon was labeled as the ‘ethionamide booster effect’. Protein-small molecule interaction studies revealed that S3 binds to the repressor protein EthR, which is responsible for inhibition of *ethA* expression. This experiment was done with the help of Dr. Kamel Djaout and Dr. Alain Baulard from the Pasteur Institute in Lille. In an attempt to identify a 1,3,4-oxadiazol derivative with improved activity, a structure-activity relationship study was performed, testing 112 analogues of S3. To streamline the Western blot-based screening setup for ESX-1 inhibition, an ELISA-based method was developed. This method appears to have an increased specificity as it avoids the 100x concentration step, and it significantly increases testing throughput. Utilizing this novel testing platform, two promising S3 analogues were identified, namely S3_100 and S3_106. All three analogues (S3, S3_100 and S3_106) inhibit the ESX-1 secretion system but differ in their described booster effect. While S3_106 did not show any booster effect on ethionamide efficacy, S3_100 confirmed this effect. Interestingly, S3_100 does not bind to the repressor protein EthR but upregulates an alternative prodrug-activating enzyme, MymA. This was confirmed by targeted quantitative real-time PCR. Furthermore, the following manuscript attempts to identify the molecular interaction of S3 with ESX-1 to explain the mode of action of inhibition. Firstly, the secondary effect on EthA expressing could be uncoupled of the ESX-1 inhibition. Neither overexpression by chemical induction (BDM41906) nor biological means,

using an *ethA* overexpressing plasmid, lead to inhibition of ESX-1. Furthermore, the direct interaction partner of S3 with the ESX-1 secretion system remains elusive.

The initial screening was conducted by myself with substantial help from Edeltraud van Gumpel for the REMA. Western blot-based secretome assays were developed by myself and were performed with great help from Edeltraud van Gumpel and Jason Chhen. All host cell-associated experiments were performed by myself. Dr. Sebastian Theobald conducted the cytokine quantification ELISA. Investigation of intracellular growth of *Mtb*, development of the ELISA-based testing platform for ESX-1 inhibition and subsequent testing of compounds and biologically modified *Mtb* were carried out by myself. RNA extraction for qRT-PCR and RNA-Seq were established by myself and were performed together with Edeltraud van Gumpel and Jason Chhen. The *ethA* overexpressing plasmid was designed and created by myself support help from Edeltraud van Gumpel. Evaluation of ethionamide booster effects was executed by myself with help from Jason Chhen. RNA-Seq data were evaluated by myself with the supervision of Dr. Michael Dal Molin and PD Dr. Dr. Jan Rybniker. Gene ontology investigation of these data was performed by myself. In addition, the EthA-deficient mutant was also generated by myself.

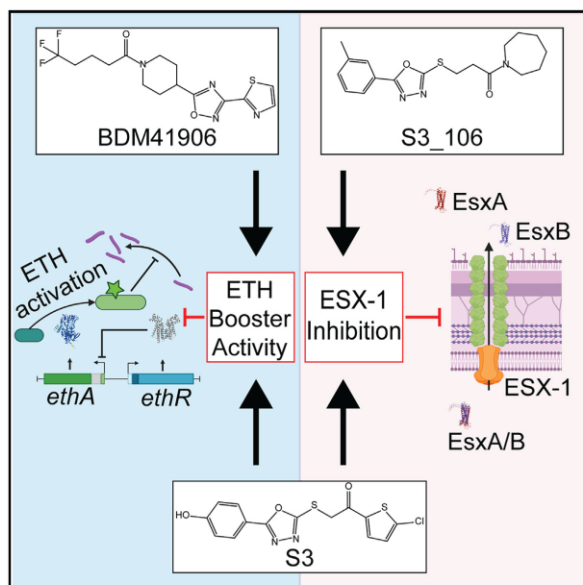
The manuscript was written by myself and prof-read by PD Dr. Dr. Jan Rybniker. All illustrations were created by myself. With the exception of the RNA-Seq associated statistics, all statistical analyses and interpretation in the following publication were performed by myself.

Preliminary Data of this manuscript have been presented as a poster at the internal Retreat of the Clinic I at the University Hospital Cologne in 2021 and 2023 in Cologne, Germany, as well as at the DGI-DZIF Joint Annual Meeting 2022 in Stuttgart, Germany. The following manuscript has been published in the peer-reviewed journal Cell Chemical Biology.

Cell Chemical Biology

Discovery of dual-active ethionamide boosters inhibiting the *Mycobacterium tuberculosis* ESX-1 secretion system

Graphical abstract



Authors

Raphael Gries, Jason Chhen, Edeltraud van Gumpel, ..., Alain Baulard, Michael Dal Molin, Jan Rybniker

Correspondence

jan.rybniker@uk-koeln.de

In brief

Gries et al. identified oxadiazole derivatives that block pathogenicity of *Mycobacterium tuberculosis* by inhibiting the ESX-1 secretion system. Mode of action studies revealed two analogs which potently upregulate monooxygenases leading to increased efficacy of the prodrug ethionamide. These dual-active compounds allow for the development of new treatment options against tuberculosis.

Highlights

- 1,3,4-oxadiazoles limit intracellular growth of *Mycobacterium tuberculosis*
- These compounds inhibit the mycobacterial ESX-1 secretion system
- Some analogs have a dual mechanism and strongly improve ethionamide activity

Please cite this article in press as: Gries et al., Discovery of dual-active ethionamide boosters inhibiting the *Mycobacterium tuberculosis* ESX-1 secretion system, Cell Chemical Biology (2023), <https://doi.org/10.1016/j.chembiol.2023.12.007>

Article

Discovery of dual-active ethionamide boosters inhibiting the *Mycobacterium tuberculosis* ESX-1 secretion system

Raphael Gries,^{1,2,3} Jason Chhen,^{1,2} Edeltraud van Gumpel,^{1,2} Sebastian J. Theobald,^{1,2} Lindsay Sonnenkalb,^{4,5} Christian Utpatel,^{4,5} Fabian Metzger,⁶ Manuel Koch,⁶ Tobias Dallenga,^{4,7} Kamel Djaout,⁸ Alain Baulard,^{8,9} Michael Dal Molin,^{1,2} and Jan Rybniker^{1,2,3,9,10,*}

¹Department I of Internal Medicine, Faculty of Medicine and University Hospital Cologne, University of Cologne, 50937 Cologne, Germany

²Center for Molecular Medicine Cologne (CMMC), University of Cologne, 50931 Cologne, Germany

³German Center for Infection Research (DZIF), Partner Site Bonn-Cologne, 50931 Cologne, Germany

⁴German Center for Infection Research (DZIF), Partner Site Hamburg-Lübeck-Borstel-Riems, 23845 Borstel, Germany

⁵Molecular and Experimental Mycobacteriology, Research Center Borstel, Leibniz Lung Center, 23845 Borstel, Germany

⁶Institute for Dental Research and Oral Musculoskeletal Biology, Center for Biochemistry, Faculty of Medicine and University Hospital Cologne, University of Cologne, 50931 Cologne, Germany

⁷Cellular Microbiology, Research Center Borstel, Leibniz Lung Center, 23845 Borstel, Germany

⁸University of Lille, CNRS, Inserm, CHU Lille, Institut Pasteur de Lille, Center for Infection and Immunity of Lille, 59000 Lille, France

⁹These authors contributed equally

¹⁰Lead contact

*Correspondence: jan.rybniker@uk-koeln.de

<https://doi.org/10.1016/j.chembiol.2023.12.007>

SUMMARY

Drug-resistant *Mycobacterium tuberculosis* (*Mtb*) remains a major public health concern requiring complementary approaches to standard anti-tuberculous regimens. Anti-virulence molecules or compounds that enhance the activity of antimicrobial prodrugs are promising alternatives to conventional antibiotics. Exploiting host cell-based drug discovery, we identified an oxadiazole compound (S3) that blocks the ESX-1 secretion system, a major virulence factor of *Mtb*. S3-treated mycobacteria showed impaired intracellular growth and a reduced ability to lyse macrophages. RNA sequencing experiments of drug-exposed bacteria revealed strong upregulation of a distinct set of genes including *ethA*, encoding a monooxygenase activating the anti-tuberculous prodrug ethionamide. Accordingly, we found a strong ethionamide boosting effect in S3-treated *Mtb*. Extensive structure-activity relationship experiments revealed that anti-virulence and ethionamide-boosting activity can be uncoupled by chemical modification of the primary hit molecule. To conclude, this series of dual-active oxadiazole compounds targets *Mtb* via two distinct mechanisms of action.

INTRODUCTION

Despite global efforts to better control tuberculosis, the disease remains a leading cause of mortality worldwide.¹ Drug-resistant strains of the causative agent *Mycobacterium tuberculosis* (*Mtb*) further exacerbate and complicate the epidemic situation in various regions of the world.¹ In order to tackle the problem of drug resistance, bioactive substances with alternative antibacterial mechanisms are required. Although a concerted effort of academic and company-driven research generated a reasonable amount of lead compounds active against resistant *Mtb*, it remains increasingly difficult to find substances with novel modes of action. Structural limitations coupled with a lack of diversity in screening libraries ask for alternative approaches such as anti-virulence or host-directed drugs.^{2–6}

Prominent targets for anti-virulence drugs are the mycobacterial type VII secretion systems such as ESX-1. ESX-1 is essential

for successful host cell infection, bacterial spread, and macrophage escape but not for bacterial growth in axenic cultures. Secreted substrates such as the membranolytic protein EsxA mediate phagosomal escape and necrotic cell death of infected host cells.^{7,8} ESX-1 is also required for release of pro-inflammatory cytokines such as type I interferon via the cyclic GMP-AMP synthase and interleukin-1 β via activation of the NLRP3 inflammasome. ESX-1 deletion mutants show strongly attenuated phenotypes *ex vivo* and *in vivo* making chemical inhibition of this system a highly attractive therapeutic approach.⁹

An additional mechanism to overcome the problem of anti-tuberculous drug resistance is the concept of so-called “booster” substances that enhance prodrug activation by upregulation of the respective activating enzyme.¹⁰ Several of the clinically used anti-mycobacterial drugs are prodrugs (e.g., isoniazid, ethionamide, and delamanid), which are inactive in the administered form but are converted into the active molecule

Please cite this article in press as: Gries et al., Discovery of dual-active ethionamide boosters inhibiting the *Mycobacterium tuberculosis* ESX-1 secretion system, *Cell Chemical Biology* (2023), <https://doi.org/10.1016/j.chembiol.2023.12.007>



CellPress

Cell Chemical Biology
Article

by mycobacterial enzymes.¹¹ For ethionamide, this enzymatic activation is catalyzed by the Baeyer-Villiger flavin adenine dinucleotide-containing monooxygenase EthA (Rv3854c), which generates an ethionamide-derived NAD adduct that blocks mycobacterial cell wall synthesis. Compounds that inhibit the regulatory protein EthR (Rv3855), a repressor of *ethA*, lead to strong upregulation of *ethA* and thus boost the activity of ethionamide without showing growth inhibitory activity by themselves.¹² This principle, which also includes targeting other ethionamide-converting monooxygenases such as MymA and EthA2, is currently being exploited in several advanced drug discovery projects.^{10,13,14}

Here, we describe the identification of oxadiazole compounds with a dual effect on *Mtb*. These inhibitors block the mycobacterial ESX-1 secretion system leading to impaired intracellular mycobacterial growth and abrogation of necrotic host cell death. In addition, these substances also lead to upregulation of *ethA* or *mymA*, improving the activity of ethionamide thus providing the possibility to target *Mtb* via two separate mechanisms. This approach has the potential to improve efficacy of standard antibiotic regimen while greatly reducing the development of antibiotic resistance.

RESULTS

Host cell-based screening identifies a cytoprotective 1,3,4-oxadiazole compound

Host cell-based drug screening detects antimicrobial agents in the context of an infected phagocyte. In contrast to conventional phenotypic drug screening performed in broth, host cell-based approaches largely extend the target spectrum toward anti-virulence and host-directed targets.⁴ We are exploiting a high-throughput screening platform selecting for compounds that abrogate *Mtb*-induced host cell death in infected human lung fibroblasts (fibroblast survival assay).^{9,15,16} In this assay, MRC-5 lung fibroblasts are seeded in 384-well plates in the presence of library compounds followed by infection with *Mtb* at a multiplicity of infection of 10 (MOI 10; Figure S1). After 72 h of incubation, the number of viable fibroblasts is quantified by measuring cellular ATP with a luminescent probe. Library compounds are tested in parallel for anti-tuberculous activity in broth using conventional resazurin microtiter assays. Using this comprehensive dual-screening platform, we tested 10,000 synthetic small molecules at a concentration of 10 μ M (SPECS world diversity set). In order to exclude false negative hits with anti-mycobacterial activity, a cutoff of 80% for potential antibiotics and a cutoff of 75% for potential anti-virulence compounds was selected. This allowed us to proceed with a feasible number of hit compounds in secondary assays. We identified only two (hit rate of 0.02%) compounds that were active in both assays and most likely represent antibiotic agents with intracellular activity, similar to rifampicin which was used as a control (Figure 1A). A total of 43 compounds (hit rate of 0.43%) were exclusively active in the fibroblast survival assay showing a cytoprotective effect in *Mtb*-infected cells without direct inhibition of mycobacterial growth in broth and were thus labeled as potential anti-virulence or host-directed compounds. After exclusion of known chemical entities and moieties associated with potential side effects (e.g.,

thiourea¹⁷), exclusion of cytotoxic compounds, and evaluation of commercial availability, we focused on an oxadiazole compound (1,3,4-oxadiazole-2-ylsulfanylanthone) for further evaluation (Figure 1B). This compound, which was named S3, protected human lung fibroblast in a dose-dependent manner with an IC₅₀ of 8.6 μ M and did not show any cytotoxic effects on HepG2 cells at concentrations up to 100 μ M (Figures 1C and S2). S3 completely failed to inhibit mycobacterial growth in broth even at concentrations above 50 μ M further confirming that this substance functions through a mechanism that is distinct from classical antibiotics (Figure 1D).

S3 inhibits the mycobacterial ESX-1 secretion system

To better understand the mechanism of action by which S3 protects infected fibroblasts, we performed a series of secondary assays. First, we speculated that S3 might inhibit the ESX-1 secretion system, which is the key virulence factor mediating mycobacteria-induced necrotic cell death. *Mtb* mutants lacking a functional ESX-1 secretion system also fail to induce cell death in the fibroblast-based screening assay indicating that small molecules with activity in this assay may target ESX-1.⁹ Consequently, we tested for potential inhibition of ESX-1 by growing *Mtb* exposed to S3 in protein-free medium for 72 h. Culture filtrates were harvested, concentrated, and tested for the presence of the ESX-1 substrates EsxA and EsxB by western blot. EsxA and EsxB are strictly co-secreted and exclusive substrates of ESX-1 and are therefore used as reporters for ESX-1 function.^{18,19} In order to exclude EsxA/B leakage caused by cell lysis, we monitored the non-secreted heat shock protein 65 (HSP65). The twin arginine protein transporter (TAT)-secreted protein complex Ag85 was used as an indicator for non-specific disruption of mycobacterial protein secretion.²⁰ We found that S3 treatment fully blocked the secretion of EsxA and EsxB without showing inhibitory effects on the TAT substrate Ag85 or the induction of cell lysis (Figures 2A, 2B, and S3). We also quantified intracellular EsxA in *Mtb* lysates and revealed a significant intracellular accumulation of EsxA, indicating that S3 blocks the transfer of this protein across the mycobacterial cell wall rather than downregulating *esxA* (Rv3875) or *esxB* (Rv3874) expression (Figure 2C).

S3 impairs intracellular mycobacterial growth and blocks necrotic cell death of human macrophages

Secreted effector proteins of ESX-1 have multiple immunological effects on the major target cell of *Mtb*, the human macrophage. Thus, we further investigated the impact of S3 treatment on macrophages infected with *Mtb*. Similar to observations made in lung fibroblasts, we determined a dose-dependent cytoprotective effect of S3 in macrophages derived from human peripheral blood mononuclear cells at 48 h post infection (Figures 2D and 2E). S3 remained cytoprotective at low micromolar concentration (Figure 2E). We have recently shown that *Mtb*-infected macrophages undergo pyroptotic cell death, a highly pro-inflammatory type of necrosis which leads to release of the pro-inflammatory cytokine interleukin-1 β (IL-1 β).⁷ Secreted levels of the pro-inflammatory cytokine IL-1 β were reduced by S3 treatment of infected macrophages at submicromolar concentrations (Figure 2F). ESX-1 is also required for successful intracellular replication of *Mtb*. Accordingly, we were able to show that S3 treatment

Please cite this article in press as: Gries et al., Discovery of dual-active ethionamide boosters inhibiting the *Mycobacterium tuberculosis* ESX-1 secretion system, Cell Chemical Biology (2023), <https://doi.org/10.1016/j.chembiol.2023.12.007>

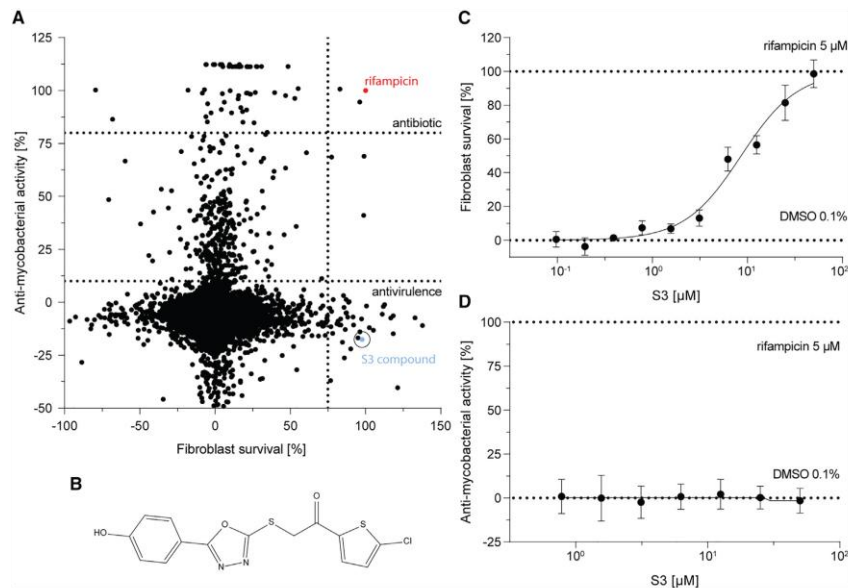


Figure 1. Dual-screening reveals oxadiazole compound S3 with anti-virulence activity

(A) Screening results of 10,000 compounds (at 10 μ M) regarding anti-mycobacterial activity in broth (REMA) and cytoprotection (fibroblast survival, see also Figure S1) during mycobacterial infection. S3 is marked in blue and rifampicin in red. For potential antibiotic compounds, a minimal of 80% antimycobacterial activity and 75% fibroblast survival were selected, whereas for potential anti-virulence compounds cutoffs of maximal 10% antimycobacterial and a minimal of 75% fibroblast survival were selected. Data are shown as mean of two independent experiments.

(B) Chemical structure of selected lead compound S3.

(C) Dose-dependent survival of human lung fibroblasts (MRC-5) exposed to compound S3 during infection with *Mycobacterium tuberculosis* (Mtb).

(D) S3 shows no growth inhibitory activity on *Mtb* in 7H9c broth. If not stated differently, data are shown as mean and standard error of the mean of at least 3 independent experiments. For cytotoxicity data see Figure S2.

significantly reduced intracellular bacterial growth by monitoring growth of eGFP-expressing *Mtb* for 7 days post infection (Figures 2G, 2H, and S4). Taken together, our data show that S3 treatment of intracellular *Mtb* impacts the fate of both host cell and bacteria despite the fact that S3 lacks anti-tuberculous activity in broth.

Transcriptomic analyses reveal a dual mechanism of S3

In order to better define the mechanism of S3-mediated cytoprotection, we performed transcriptomic analyses using RNA sequencing (RNA-Seq) of *Mtb* grown in the presence of S3 in broth for 4 h (Figure 3). Bioinformatic data analyses revealed that S3 treatment induces differential regulation of 65 genes (50 upregulated and 15 downregulated) compared to the DMSO-treated control (Tables S1 and S2). A gene ontology analysis showed upregulation of either oxidoreductases (e.g., Rv3177, Rv3174), hydrolases (e.g., Rv3175, Rv3176c), or efflux pumps which are associated with detoxification of metabolites or xenobiotics. Of note, none of the genes coding for known ESX-1 regulators or putative structural components of this secretion system were differentially regulated in compound-treated cells. Surprisingly, we found that both *ethA*

(Rv3854c) and *ethR* (Rv3855) were strongly upregulated upon exposure to S3 (Figures 3A–3C). EthA is the monooxygenase required for activation of several anti-tuberculous products such as ethionamide and thiacetazone,²¹ while EthR is the regulatory repressor of *ethA* transcription. S3-mediated differential regulation of *ethA* was confirmed by quantitative reverse-transcription PCR (qRT-PCR) experiments which showed dose-dependent upregulation of *ethA* (Figure 4A). Strong upregulation of *ethA* leads to an increased availability of intracellular EthA which implies that S3 represents an ethionamide-boosting agent (Figure 4B). To test this hypothesis, we performed growth assays with ethionamide-treated *Mtb* in presence or absence of S3 (Figure 4C). Addition of S3 to subinhibitory concentrations of ethionamide improved growth inhibitory activity of ethionamide comparable to the control substance rifampicin used at concentrations above the minimal inhibitory concentration (MIC). In a serial dilution assay, addition of 10 μ M S3 led to a shift of ethionamide activity and improved the 90% minimal inhibitory concentration (MIC₉₀) from 16.25 to 2.38 μ M (Figure 4D). Low micromolar concentrations of S3 combined with subinhibitory amounts of ethionamide led to pronounced growth inhibition of *Mtb*

Please cite this article in press as: Gries et al., Discovery of dual-active ethionamide boosters inhibiting the *Mycobacterium tuberculosis* ESX-1 secretion system, *Cell Chemical Biology* (2023), <https://doi.org/10.1016/j.chembiol.2023.12.007>



CellPress

Cell Chemical Biology
Article

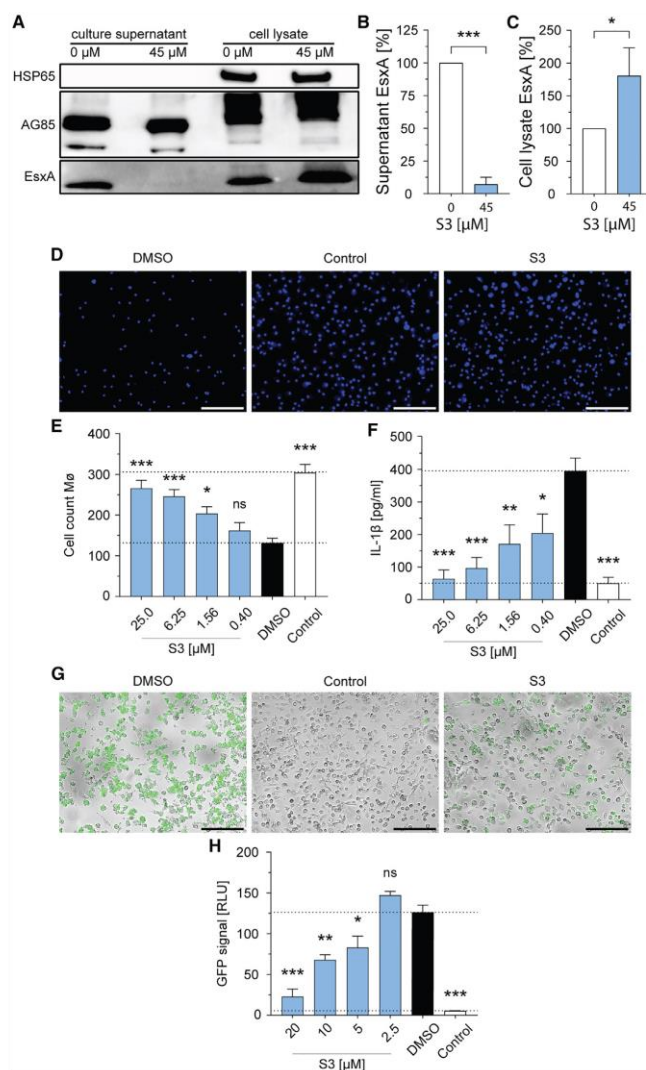


Figure 2. S3 is an ESX-1 inhibitor with intracellular activity

(A) Representative immunoblot of culture supernatant and cell lysate samples of *Mycobacterium tuberculosis* (*Mtb*) after 72 h of exposure to S3 in protein-free medium. Ag85 was detected as an ESX-1-independent secreted control protein; HSP65 was used as a lysis control (see Figure S3). Quantification of band intensities of EsxA in (B) culture supernatant and (C) cell lysate (two-tailed unpaired t test with 95% confidence level). (D) Representative microscopy images of DAPI-stained primary human macrophages 48 h post infection with *Mtb* (MOI 2) (DMSO = 0.05% DMSO; Control = 5 μM rifampicin, S3 = 10 μM S3). (E) Cell counts of DAPI-stained primary human macrophages (Mo) of images taken at the center of the well at 10× magnification of at least three different wells per replicate of five independent experiments, 48 h post infection with *Mtb* (MOI 2) (DMSO = 0.05% DMSO; Control = 5 μM rifampicin). (F) Extracellular levels of IL-1β 48 h post infection (Control = 5 μM rifampicin, DMSO = 0.05% DMSO). (G) Representative microscopy images of primary human macrophages infected with eGFP-expressing *Mtb* (MOI 1) 7 days post infection (ctrl = 10 μM isoniazid, DMSO = 0.05% DMSO). See Figure S4 for data on colony forming units. (H) Quantification of eGFP signal as a surrogate for intracellular growth of eGFP-expressing *Mtb* 7 days post infection in primary human macrophages (Control = 10 μM isoniazid, DMSO = 0.05% DMSO). If not stated differently, data are shown as mean and standard error of the mean of at least 3 independent experiments and statistical significances are shown compared to DMSO based on one-way ANOVA combined with Bonferroni post hoc test (ns = not significant; * = $p < 0.05$; ** = $p < 0.01$; *** = $p < 0.001$). Scale bars shown in microscopy images represent 200 μm.

Structure-activity relation studies delineate ESX-1-inhibiting activity from transcriptional upregulation of *ethA*

Strong upregulation of the gene coding for the monooxygenase EthA observed here may have multiple downstream effects on *Mtb* biology and intracellular behavior of this pathogen. Although the exact function of EthA has not yet been fully understood, there is evidence that alterations in the *ethA/ethR* operon in *Mycobacterium bovis* BCG affect the mycolic acid composition of the mycobacterial cell wall,²⁵ which potentially affects ESX-1 functionality. To elucidate a possible link between S3-induced upregulation of *ethA* and inhibition of ESX-1, we decided to exploit a chemical biology approach using a library of S3-analogs. This library consists of 112 molecules with a 1,3,4-oxadiazole core structure connected to a sulfanyl-ethanone and variable chains on both sides (Figure 5A; Table S3). Following the screening pipeline described previously, we first

(MIC₉₀ 1.6 μM) (Figure 4E). These data confirm that S3 is an ethionamide-boosting agent which functions via upregulation of *ethA*. Recently, small molecules have been described which show similar activity by binding to the EthA regulatory protein EthR.^{22–24} By performing thermal shift assays, we were able to show that S3 represents an EthR-binding molecule (Figure 4F). Thus, it is highly conceivable that S3 is a direct EthR inhibitor inducing dysregulation of *ethA*, subsequently leading to augmented ethionamide activity.

Please cite this article in press as: Gries et al., Discovery of dual-active ethionamide boosters inhibiting the *Mycobacterium tuberculosis* ESX-1 secretion system, Cell Chemical Biology (2023), <https://doi.org/10.1016/j.chembiol.2023.12.007>

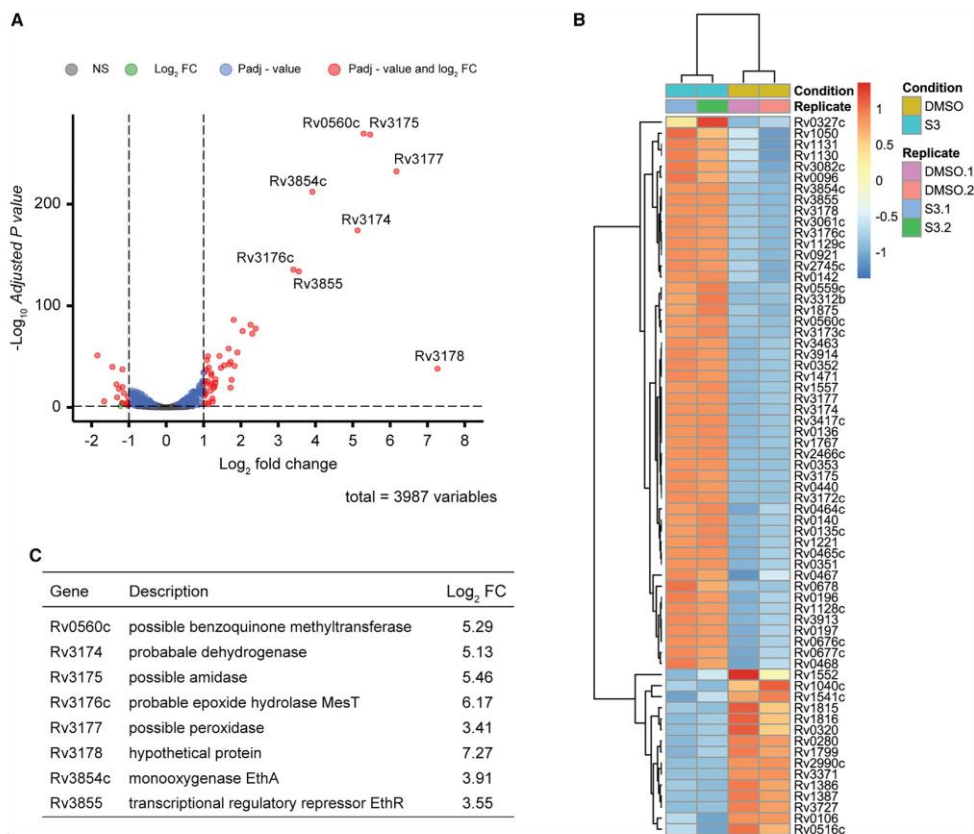


Figure 3. Upregulation of EthA/R in presence of S3

(A) Volcano plot of expression levels of genes of *Mycobacterium tuberculosis* identified by RNA sequencing in the presence of 20 μ M S3. (B) Heatmap of the 50 most upregulated genes after exposure to 20 μ M S3 compared to DMSO control (padj < 0.05). (C) List of genes of interest with a significantly increased expression level. Data shown represent the mean of two biological replicates.

tested these analogs for cytoprotective activity in the fibroblast survival assays (Figure 5A). A total of 25 cytoprotective molecules were then tested for their respective inhibition of EsxA secretion. To increase assay throughput and to allow for quantitative measurement of EsxA released from drug-exposed *Mtb*, we developed an ELISA-based ESX-1 activity screening assay. For this, we harvested *Mtb* supernatants after exposure to the respective compounds and indirectly detected EsxA using a monoclonal anti-EsxA primary antibody and a secondary antibody conjugated with a horseradish peroxidase (See STAR Methods, Figure S5 for more details). Testing the 1,3,4-oxadiazole core structure library in this ELISA-based assay revealed 13 additional analogs which were cytoprotective and inhibited EsxA secretion by at least 50% (Figure 5B). We then focused on two analogs (S3_100 and S3_106) which also showed no

cytotoxic effects on HepG2 cells (Figure S2) and slightly superior inhibition of EsxA secretion compared to the original hit molecule S3 at 20 μ M. For both substances, we could confirm a dose-dependent ESX-1-inhibiting activity (EC₅₀ of 1.52 and 2.36 μ M, respectively) (Figures 5C–5E). Compared to S3, which showed an EC₅₀ of 3.00 μ M, the chemical structures of these ESX-1 inhibitors differ mainly by an exchange of the para-phenol in R₁ into a benzene (S3_100) or into a meta-toluol (S3_106) ring. Regarding R₂, S3_100 and S3_106 have the chlorothiophene ring replaced by a piperidine or an azepane ring, respectively. S3_106 is additionally characterized by its sulfanyl spacer region being elongated by a single carbon atom (Figures 5C–5E).

In a further step, we tested for upregulation of *ethA* by qRT-PCR in *Mtb* exposed to S3_100 or S3_106 at concentrations of 10 μ M, which is well above the IC₅₀ of these substances.

Please cite this article in press as: Gries et al., Discovery of dual-active ethionamide boosters inhibiting the *Mycobacterium tuberculosis* ESX-1 secretion system, *Cell Chemical Biology* (2023), <https://doi.org/10.1016/j.chembiol.2023.12.007>

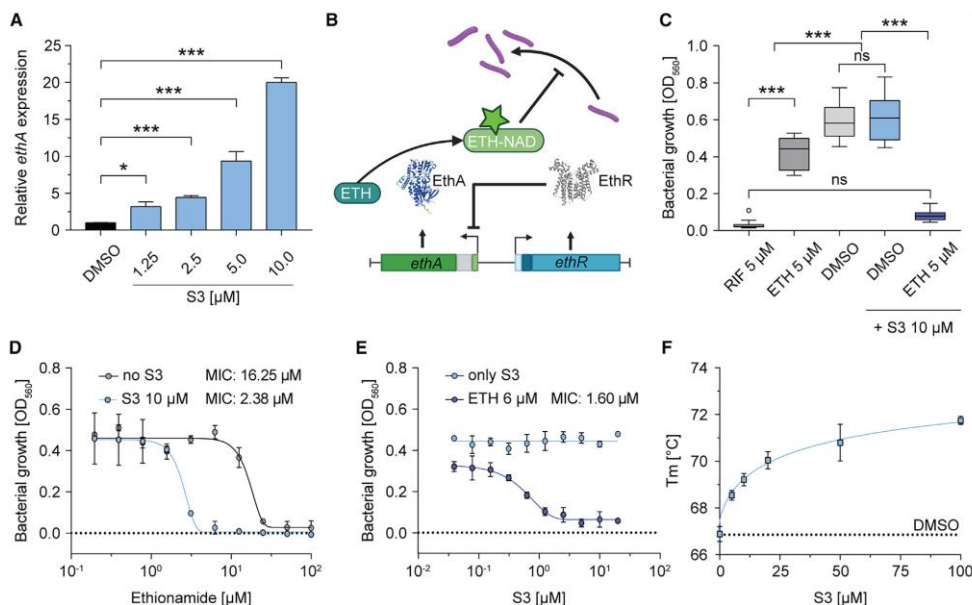


Figure 4. Ethionamide-booster effect in combination experiments

(A) Relative *ethA* expression at different S3 concentrations (DMSO = 0.05% DMSO). RNA was isolated during exponential growth after 4 h of exposure to the respective compound.

(B) Schematic overview of *ethA*-dependent activation of ethionamide (ETH).

(C) Growth of *Mycobacterium tuberculosis* after exposure to 5 μM rifampicin (RIF), 5 μM ethionamide (ETH), DMSO (=0.05% DMSO), and in combinations with 10 μM S3.

(D) Dose-dependent growth inhibition of ETH in the presence or absence of 10 μM S3.

(E) Dose-dependent growth inhibition of S3 in the presence or absence of 6 μM ETH. Bacterial growth was measured after 10 days of incubation with a starting OD_{600} of 0.01.

(F) Shift of the melting temperature (T_m) of EthR binding to different concentrations of S3 compared to 1% DMSO. Data are shown as mean and standard error of the mean of at least two independent experiments and statistical significances are shown compared to DMSO based on one-way ANOVA combined with Bonferroni post hoc test (ns = not significant; * = $p < 0.05$; ** = $p < 0.01$; *** = $p < 0.001$). MICs are calculated as 90% minimal inhibitory concentration.

Interestingly, both analogs completely failed to increase *ethA* expression, which stands in stark contrast to observations made with S3-exposed *Mtb* (Figure 5F). In line with these findings, S3_100 and S3_106 showed a lower and non-significant thermostabilizing effect on EthR as shown in thermal shift assays indicating that these substances fail to bind EthR (Figure 5G). Here, the compound BDM41906 was used as a control. BDM41906 is a well-defined ethionamide-boosting agent which blocks activity of EthR.²⁴ Finally, we performed electrophoretic mobility shift assays of EthR bound to the 62 bp intergenic *ethA-R* region (EthR-binding region¹²). As expected, the DNA/EthR complex migrated slower through an SDS-PAGE gel which allowed us to visualize two distinct bands (complexed/bound DNA and free/unbound DNA) after ethidium bromide staining. Importantly, the amount of bound DNA could be reduced when S3 or BDM41906 was added to the assay. This was not the case for S3_100 or S3_106 (Figures 5H, S6A and S6B). These findings are in line with the transcriptional data and the assumption that S3, but not S3_100 or S3_106, inhibits EthR.

Overexpression of EthA does not translate into impaired virulence of *Mtb*

The concept of augmenting ethionamide activity via upregulation of *ethA* represents an important and advanced anti-tuberculous approach.¹⁰ To fully confirm that this mechanism lacks additional and intrinsic effects on virulence of *Mtb*, we generated an *Mtb* strain which constitutively overexpressed *ethA* under control of the potent mycobacterial *hsp60* promoter (pMV361: *ethA*). qRT-PCR revealed 70-fold upregulation of *ethA* (Figure 6A). As expected, ethionamide activity was improved in bacteria carrying pMV361:*ethA* in comparison to bacteria that had been transformed with the pMV361 backbone as control (Figure S7A). We did not observe impaired virulence of this *ethA*-overexpressing strain in the fibroblast survival assay whereas a control strain lacking the ESX-1 operon failed to kill infected cells (Figure 6B). Addition of the S3 compound to *ethA*-overexpressing *Mtb* rendered these bacteria avirulent to levels comparable to the ESX-1 mutant strain again indicating that S3 functions via an EthA-independent mechanism. S3 also significantly

Please cite this article in press as: Gries et al., Discovery of dual-active ethionamide boosters inhibiting the *Mycobacterium tuberculosis* ESX-1 secretion system, *Cell Chemical Biology* (2023), <https://doi.org/10.1016/j.cchembiol.2023.12.007>

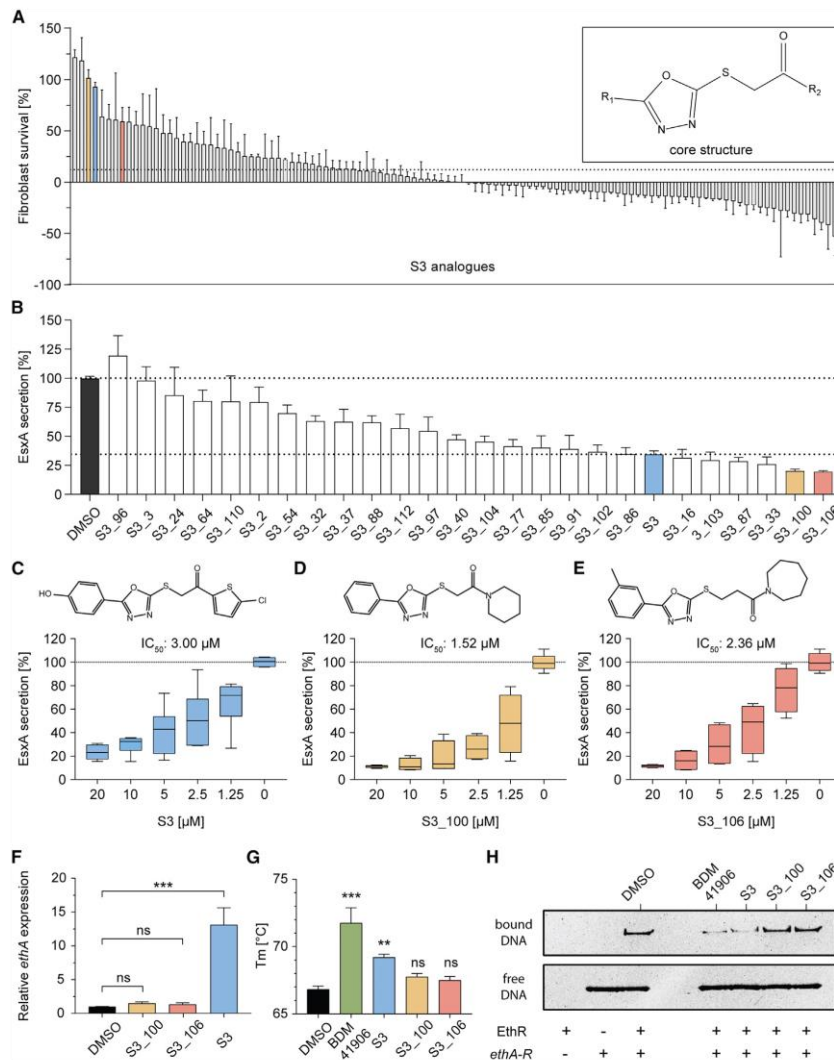


Figure 5. Screening of analogs yields additional inhibitors of the ESX-1 secretion system

(A) Core structure of S3 analogs which differ mainly in R₁ and R₂ (see Table S3) and phenotypic screening of analogous (20 μM, n = 2) for cytoprotection of human lung fibroblasts (MRC-5) during *Mycobacterium tuberculosis* infection.

(B) Evaluation of hit compounds (20 μM, n = 2) in regard to inhibition of ESX-1 activity by probing EsxA in the culture supernatants. Dose-dependent inhibitory effect of compounds (C) S3, (D) S3_100, and (E) S3_106 on EsxA secretion in the supernatant after exposure for 72 h. EsxA levels were detected using an ELISA-based assay. See Figure S5 for further information on ELISA. For cytotoxicity data see Figure S2.

(C) Dose-dependent inhibition of EsxA secretion by S3 (IC₅₀: 3.00 μM).

(D) Dose-dependent inhibition of EsxA secretion by S3_100 (IC₅₀: 1.52 μM).

(E) Dose-dependent inhibition of EsxA secretion by S3_106 (IC₅₀: 2.36 μM).

(F) Relative *ethA* expression after 4 h of exposure to DMSO 0.05%, S3, S3_100, and S3_106 at 10 μM.

(G) Shift of the melting temperature (T_m) of EthR binding to 1% DMSO or 10 μM of either BDM41906, S3, S3_100, or S3_106.

(H) Electrophoretic mobility shift assay performed with 0.6 μM EthR and 0.15 μM of the *ethA-R* intergenic DNA fragment (62 bp) in the presence of 5% DMSO or 50 μM of either BDM41906, S3, S_100, or S3_106. Lane 1 was loaded with EthR only which provides no visible band; lane 2 was loaded with DNA only. Lanes 4

(legend continued on next page)

Cell Chemical Biology 31, 1–13, March 21, 2024 7

Please cite this article in press as: Gries et al., Discovery of dual-active ethionamide boosters inhibiting the *Mycobacterium tuberculosis* ESX-1 secretion system, *Cell Chemical Biology* (2023), <https://doi.org/10.1016/j.chembiol.2023.12.007>



CellPress

Cell Chemical Biology
Article

increased survival of fibroblasts infected with an EthA-deficient strain (EthA^{C131X}) (Figure 6B). This strain harbors a premature stop-codon in *ethA* which results in the production of non-functional EthA (Figure S7B). Together, this indicates that S3 does not require EthA for ESX-1-blocking activity. Next, we performed similar experiments with the well-defined and chemically distinct ethionamide-boosting agent BDM41906.²⁴ We first determined the boosting EC₅₀ (0.10 μM) of BDM41906 in combination with ethionamide. At concentrations ten times above the EC₅₀ (1 μM), BDM41906-treated *Mtb* did not show impaired ESX-1-mediated virulence or EsxA secretion (Figure 6C, 6D, and S7C).

S3_100 but not S3_106 leads to upregulation of *mymA* and improves ethionamide activity

Finally, in a confirmatory experiment, we intended to show that the two ESX-1 inhibitors S3_100 and S3_106 fail to lower the MIC of ethionamide as suggested by our qRT-PCR experiments targeting *ethA* transcription. We could verify this for S3_106, which had no impact on ethionamide activity in combination assays (Figure 7A). Surprisingly, we found that S3_100 treatment led to significant boosting of ethionamide comparable to findings made with the initial hit compound S3 (Figure 7A). Consequently, compound-exposed bacteria were tested for upregulation of EthA2 (Rv0077c) and *MymA* (Rv3083), two alternative monooxygenases involved in ethionamide activation.^{26,27} Interestingly, transcriptional analyses using qRT-PCR revealed increased expression of *mymA* in *Mtb* exposed to S3_100, but not in bacteria treated with S3 or S3_106 (Figure 7B). Differential expression of *ethA2* was not detectable in bacteria exposed to either compound. Thus, S3_100 co-treatment leads to significantly improved activity of ethionamide, most likely by upregulating *mymA*, a mechanism that has also been described for other ethionamide-boosting compounds.¹⁰ Small molecules boosting ethionamide activity in a *MymA*-dependent mechanism are capable of overcoming ethionamide resistance linked to mutations in EthA. We could confirm this for S3_100 which reversed ethionamide resistance in the EthA^{C131X} mutant (Figure 7C). As expected, this was not the case for S3 which depends on a fully functional EthA protein for its boosting activity (Figure 7C and D). Therefore, each of the three ESX-1 inhibitors exerts a distinct impact on the mechanisms involved in the activation of ethionamide.

Considering our comprehensive analysis of transcriptional and phenotypic data obtained from S3_106-exposed bacteria, we can conclude that the upregulation of *ethA* or *mymA* is dispensable for inhibiting EsxA secretion. Moreover, our research highlights that the inhibitors S3 and S3_100 exhibit distinct and dual mechanisms of action, which can be uncoupled through subtle chemical modifications.

DISCUSSION

In this study, we describe a series of 1,3,4-oxadiazole compounds which target the ESX-1 secretion system, a key virulence

factor of *Mtb*. Our data confirm that this system is druggable and that phenotypic screening exploiting ESX-1-mediated host cell death is a potent tool for the identification of molecules with intracellular activity against *Mtb*. By showing that ESX-1 inhibition not only leads to abrogation of host cell death but also to impaired intracellular growth in macrophages, we provide evidence that ESX-1 inhibitors function as an alternative approach to conventional antibiotics.

Despite abrogation of EsxA and EsxB secretion in S3-treated cells, we detected no differential expression of ESX-1-related regulatory or structural genes in the mycobacterial transcriptome. This is a remarkable observation in light of the strong EsxA accumulation in these cells. Thus, our data show that there is no ESX-1 autoregulatory feedback mechanism sensing the amount of intracellular substrates subsequently leading to differential regulation of the secretion machinery. This stands in contrast to the intrinsic regulatory mechanism known for the type 3 secretion (T3SS) system of gram-negative bacteria in which secretion of substrates or regulator proteins is coupled to differential transcription of T3SS components.^{28,29} In addition, our transcriptomic data distinguish S3 from two other inhibitors of the ESX-1 secretion system, which impact regulatory proteins and metal ion homeostasis indicating that 1,3,4-oxadiazoles represent a distinct class of ESX-1-blocking agents.⁹

Unexpectedly, we found strong transcriptional upregulation of the monooxygenase *ethA* and the associated transcriptional regulator *ethR* following S3 treatment of *Mtb*. While the pro-drug-activating mechanisms of EthA are well described, the biological function of EthA in *Mtb* is unknown. EthA/EthR deficiency alters mycolic acid composition indicating involvement in cell wall processes.²⁵ We thus speculated that dysregulation of EthA may directly or indirectly impact ESX-1 secretion via an unknown, cell wall-related mechanism. However, we were able to provide several lines of evidence showing that EthA dysregulation and blockage of ESX-1 secretion are independent events induced by a dual mechanism of the compound S3.

Further investigation of the close analogs S3_100 and S3_106 revealed divergent effects on ethionamide-boosting activity. S3_106, which retains inhibitory capacity of *Mtb*-induced cell death and EsxA secretion, failed to upregulate EthA or other relevant monooxygenases at concentrations well above the EC₅₀. This analog lacks the thiophene ring attached to the S3 oxadiazole core which is replaced by an azepane, indicating that the thiophene or at least a 5-membered ring is required for upregulation of EthA, but not for ESX-1 blockage. Of note, some of the well-described ethionamide booster compounds, which function by upregulating *ethA*, also carry thiophenes and oxadiazoles.³⁰ These thiophen-2-yl-1,2,4-oxadiazoles bind to the regulatory protein EthR and block transcriptional repression of *ethA*.³⁰ Since we were able to show that S3 also interacts with EthR, it is highly conceivable that this compound has a similar mechanism of action with regard to its ethionamide-boosting activity. The RNA-Seq signature we obtained in S3-exposed cells also revealed dysregulation of multiple oxidoreductases other

and 5 were left empty. The upper band represents the EthR-DNA complex and the lower band represents unbound DNA which migrates faster through the SDS gel. After SDS-PAGE, the gel was stained with ethidium bromide. Representative gel of three independent experiments. See Figure S6 for unprocessed gel and quantification of bands. If not stated differently, data are shown as mean with standard error of the mean of at least three biological replicates and statistical significances are shown compared to DMSO based on one-way ANOVA combined with Bonferroni post hoc test (ns = not significant; ** = $p < 0.01$; *** = $p < 0.001$).

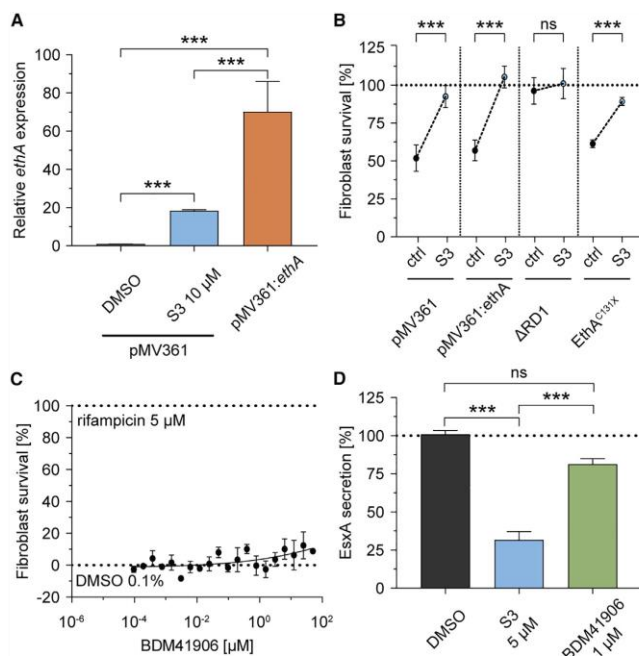


Figure 6. Overexpression of EthA does not translate into impaired virulence of *Mycobacterium tuberculosis*

(A) Relative *ethA* expression of *Mtb* strains harboring the empty plasmid pMV361, in combination with either 0.05% DMSO or 10 μ M S3, or the *ethA* overexpression plasmid pMV361:*ethA* treated with 0.05% DMSO.

(B) Fibroblast survival of MRC-5 cells infected with *Mycobacterium tuberculosis* (*Mtb*) strains harboring the empty pMV361 plasmid, the *ethA*-overexpressing pMV361:*ethA* plasmid, the Δ RD1 deletion or the *ethA*-deficient mutation EthA^{C151X}, either in the presence or absence of S3 (ctrl = 0.01% DMSO, S3 = 10 μ M S3).

(C) Survival of human lung fibroblast (MRC-5) exposed to different concentrations of the EthR inhibitor BDM41906 during infection with *Mtb*.

(D) ELISA-based detection of EsxA in the culture supernatant of *Mtb* exposed for 3 days, in protein-free medium, to concentrations ten times the EC₅₀ for ethionamide booster activity of S3 and BDM41906 (DMSO = 0.01% DMSO) normalized to DMSO. Data are shown as mean with standard error of the mean of at least three biological replicates and statistical significances are shown compared to DMSO based on one-way ANOVA combined with Bonferroni post hoc test (ns = not significant; *** = $p < 0.001$). See Figure S7 for more biological data in combination with ethionamide.

than EthA. This could represent a general stress response of drug-exposed bacteria or differential regulation due to binding of S3 to other regulatory proteins. Furthermore, the signature we observed also mirrors a general response seen in bacteria exposed to antibiotics or xenobiotics, including upregulation of the MmpL5/MmpS5 and MmpL6 efflux pumps, the sigma factor SigE, the TrcX/TrxB1 thioredoxin system, and several chaperones.^{31–34} Again, none of these genes are linked to regulatory processes of the ESX-1 secretion system. Thus, the exact molecular target of S3 with regard to inhibition of the ESX-1 secretion system remains to be determined.

Interestingly, our investigations into the S3 analog S3_100 revealed an EthR-independent ethionamide-boosting activity, most likely through upregulation of the monooxygenase MymA, which has been described as an alternative mechanism for ethionamide activation.²⁷ Structural differences between the close analogs S3_100 and S3_106 appear to be responsible for the differential regulation of *mymA* and thus the dual activity of S3_100. In S3_100, the R₂-located ring consists of a piperidine instead of an azepane. S3_100 also contains the S3-originated, shorter sulfanyl spacer region, which is elongated by one carbon atom in S3_106. It is highly likely that these differences in the R₂ region are responsible for MymA dysregulation and ethionamide-boosting activity of S3_100. Piperidine rings also seem to be essential components of recently described MymA-dependent ethionamide booster drugs which act via modulation of the MymA regulatory protein VirS.¹⁰ As the most common mutation

conveying resistance to ethionamide is located in *ethA*,^{10,11} targeting these alternative pathways for ethionamide activation enables reversion of ethionamide resistance.^{10,14} We were able to confirm this for S3_100 which was able to overcome inactivity of ethionamide in an EthA mutant strain.

Taken together, we describe a series of inhibitors of the mycobacterial ESX-1 secretion system. Chemical modification of these compounds revealed a dual mechanism which improves ethionamide activity in co-treated *Mtb*. This characteristic may help to improve treatment outcome in drug-resistant *Mtb*. It is believed that anti-virulence approaches produce a milder evolutionary pressure toward the development of resistance compared to conventional antibiotics.³⁵ Moreover, antibiotic-boosting agents are considered as resistance-converting agents for their respective prodrug.¹⁰ Thus, a dual-active single agent covering both aspects has potential as an adjunct therapy in future tuberculosis regimens. This will, however, require the generation of dual-active compounds with pharmacokinetic attributes that allow for oral administration of these drugs. Finally, our data also extend our knowledge on the diverse anti-mycobacterial effects of oxadiazole compounds, which can function as conventional antibiotics, anti-virulence drugs, as well as prodrug-boosting agents.^{27,30}

Limitations of the study

This study has some limitations regarding the elucidation of the molecular targets of the small molecules described here. The

Please cite this article in press as: Gries et al., Discovery of dual-active ethionamide boosters inhibiting the *Mycobacterium tuberculosis* ESX-1 secretion system, Cell Chemical Biology (2023), <https://doi.org/10.1016/j.cchembiol.2023.12.007>

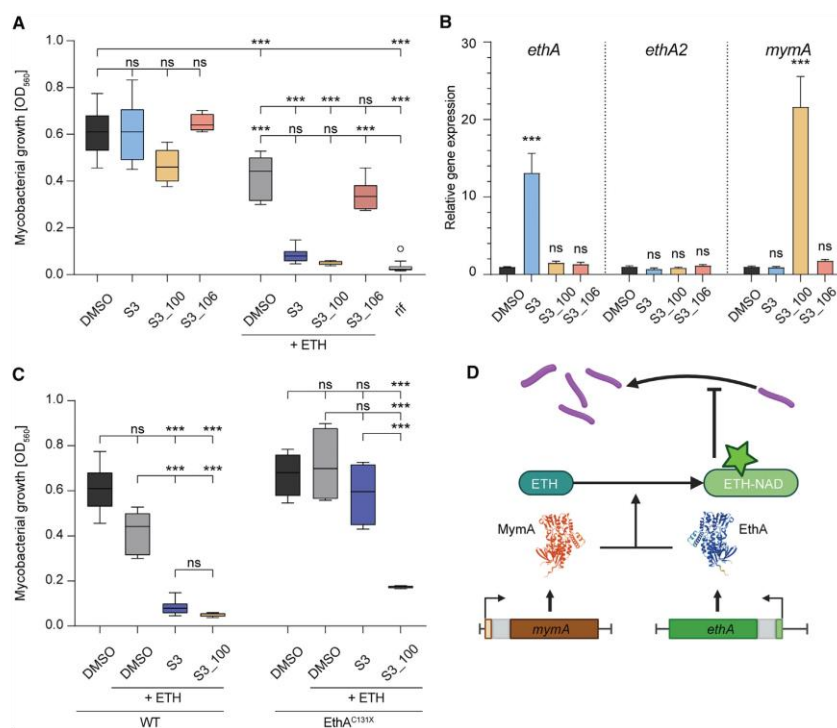


Figure 7. ETH-booster activity of S3 analogs

(A) Growth of *Mycobacterium tuberculosis* (*Mtb*) treated with S3, S3_100, and S3_106 (all at 10 μ M) with (right panel) or without (left panel) addition of 5 μ M ETH. Controls: 5 μ M rifampicin (RIF), DMSO (0.05% DMSO).

(B) Relative expression of *ethA* (left), *ethA2* (middle), and *mymA* (right) after exposure to 10 μ M S3, S3_100, or S3_106 (DMSO control = 0.05% DMSO). RNA was isolated during exponential growth after 4 h of exposure to the respective compound.

(C) Growth of either wild-type (left; WT) or EthA-deficient (right; EthA^{C131X}) *Mtb* strains after exposure to 0.05% DMSO or to combinations of 6 μ M ethionamide (ETH) with 10 μ M S3, S3_100, or 0.05% DMSO.

(D) Schematic overview of EthA and MymA-dependent activation of ethionamide (ETH). If not stated differently, data are shown as mean with standard error of the mean of at least three biological replicates and statistical significances are shown compared to DMSO based on one-way ANOVA combined with Bonferroni post hoc test (ns = not significant; *** = $p < 0.001$).

three compounds S3, S3_100, and S3_106 inhibit EsxA secretion and thus abrogate ESX-1 activity; however, the specific mode of action on the secretion system requires further investigation. The transcriptomic analysis of *Mtb* exposed to S3 did not reveal differentially expressed genes coding for ESX-1 substrates or components, which may rule out altered transcriptional regulation of ESX-1 as the primary mechanism. A more detailed analysis of transcriptional changes induced by the two analogs, S3_100 and S3_106, may provide greater clarity on this matter. Of particular interest for this approach is S3_106, which lacked ethionamide-boosting activity and may show a more distinct transcriptional footprint. In addition, this work provides only indirect insight on the mechanism by which S3_100 improves activity of ethionamide. While we could demonstrate that S3_100 leads to significant upregulation of the monoxyge-

nase *mymA*, we have not yet deciphered the regulatory aspects behind this effect. Further investigations should primarily focus on the regulator protein VirS, which has been described as the molecular target of other MymA-dependent boosting agents. Finally, *in vivo* pharmacokinetic and activity data would validate the potential use of oxadiazole derivatives as anti-*Mtb* compounds.

SIGNIFICANCE

The increasing abundance of multidrug-resistant *Mtb* clinical isolates, coupled with the challenges faced in discovering antibiotics against mycobacteria, poses an emerging global health threat. Using phenotypic drug screening performed with *Mtb*-infected host cells, we identified the

Please cite this article in press as: Gries et al., Discovery of dual-active ethionamide boosters inhibiting the *Mycobacterium tuberculosis* ESX-1 secretion system, *Cell Chemical Biology* (2023), <https://doi.org/10.1016/j.chembiol.2023.12.007>

Cell Chemical Biology Article



compound S3, a 1,3,4-oxadiazole, which inhibits intracellular replication of *Mtb* by targeting the ESX-1 secretion system. ESX-1 is a highly relevant virulence factor required for induction of host cell death, tissue damage, and bacterial spread *in vivo*. Further mechanistic investigations of S3 revealed an independent secondary effect on *Mtb* – the strong upregulation of the monooxygenase EthA most likely through inhibition of the regulatory protein EthR which was found to interact with S3. This mycobacterial enzyme is essential for the prodrug activation of the clinically approved antibiotic ethionamide. Drug-induced upregulation of EthA can be exploited as a “booster” mechanism to increase the efficacy of ethionamide. Using a library of S3-like compounds which retain the central 1,3,4-oxadiazole led to the identification of two additional compounds, S3_100 and S3_106, with anti-virulence activity via inhibition of ESX-1. Cross validation studies revealed that S3_106 fails to impact *ethA* transcriptional levels and ethionamide-boosting activity. This observation allowed us to delineate ESX-1-dependent anti-virulence activity from upregulation of the monooxygenase EthA. Interestingly, S3_100 significantly improved ethionamide activity but failed to upregulate EthA. Transcriptional analyses targeting alternative monooxygenases revealed that S3_100 upregulates *MymA*. Chemical modulation of this monooxygenase has recently been identified as a highly attractive approach to target drug-resistant *Mtb*. Thus, our data provide an interesting example of pharmacological pleiotropy by showing that subtle chemical modifications of synthetic small molecules have major impact on antimicrobial mechanisms. Combining the potential to overcome existing resistance to approved antibiotics with anti-virulence properties represents an unexplored avenue in the fight against mycobacterial infections.

STAR★METHODS

Detailed methods are provided in the online version of this paper and include the following:

- KEY RESOURCES TABLE
- RESOURCE AVAILABILITY
 - Lead contact
 - Materials availability
 - Data and code availability
- EXPERIMENTAL MODEL AND STUDY PARTICIPANT DETAILS
 - Culture conditions of mycobacteria
 - Culture conditions of eukaryotic cell lines
- METHOD DETAILS
 - Small molecules used in this study
 - Fibroblast survival assay (FSA)
 - Resazurin microtiter assay (REMA)
 - Hit selection after primary screening
 - Macrophage survival assays
 - Determining intracellular growth
 - HepG2 cytotoxicity assays
 - Ethionamide booster assay
 - Determining intracellular colony forming units

- Immunoblot analysis and secretion assay
- Enzyme-linked immunosorbent assay (ELISA)
- Cultivation conditions for RNA studies
- RNA extraction
- RNA sequencing
- cDNA synthesis
- Quantitative real-time RT-PCR
- Thermal shift assay
- Electrophoretic mobility shift assay (EMSA)
- Cloning
- Generation of the ethionamide resistant strain EthA^{C131X}

● QUANTIFICATION AND STATISTICAL ANALYSIS

SUPPLEMENTAL INFORMATION

Supplemental information can be found online at <https://doi.org/10.1016/j.chembiol.2023.12.007>.

ACKNOWLEDGMENTS

We thank Jesús Gonzalo-Asensio from the Grupo de Genética de Micobacterias of the University of Zaragoza for the methodological support regarding potential target elucidation. We also thank Dr. Jeffrey Chen (University of Saskatchewan, VIDO-InterVac) for support with ESX-1 *in vitro* assays. The following reagent was obtained through BEI Resources, NIAID, NIH: Polyclonal Anti-*Mycobacterium tuberculosis* Antigen 85 Complex (FbpA/FbpB/FbpC; Genes Rv3804c, Rv1886c, Rv0129c) (antiserum, Rabbit), NR-13800. Schemes were created with [BioRender.com](https://biorender.com).

J.R. is supported by the German Research Foundation (DFG) grant SFB 1403, the German Center for Infection Research (DZIF; TTU-TB grants 02.806, 02.814 and 02.913), the German Federal Ministry of Education and Research (BMBF, grant IdEpiCo) and by the European Union Innovative Medicines Initiative 2 Joint Undertaking program grant no. 853989 (ERA4TB). S.J.T. and J.R. are supported by a research grant of the CMMC (B10), and S.J.T. by stipends from the Imhoff-Stiftung and the Köln Fortune Program. A.B. is supported by the French Agence Nationale de la Recherche (ANR) Programme d'Investissement d'Avenir (Mustart ANR-20-PAMR-0005). L.S. is supported by the Research Training Group 2501 TransEvo.

AUTHOR CONTRIBUTIONS

Conceptualization, R.G., M.D.M., and J.R.; methodology, R.G., J.C., E.v.G., S.J.T., T.D., F.M., M.K., K.D., A.B., M.D.M., and J.R.; software, L.S., C.U., and M.D.M.; validation, R.G., J.C., E.v.G., S.J.T., F.M., M.K., K.D., A.B., M.D.M., and J.R.; formal analysis, R.G., J.C., E.v.G., S.J.T., L.S., C.U., F.M., M.K., K.D., A.B., M.D.M., and J.R.; investigation, R.G., J.C., E.v.G., S.J.T., T.B., F.M., M.K., K.D., A.B., M.D.M., and J.R.; resources, J.R.; data curation, R.G., J.C., E.v.G., L.S., C.U., M.D.M., and J.R.; writing – original draft, R.G. and J.R.; writing – review and editing, R.G., S.J.T., T.D., K.D., A.B., M.D.M., and J.R.; visualization, R.G., L.S., F.M., M.K., K.D., A.B., M.D.M., and J.R.; supervision, M.D.M. and J.R.; project administration, J.R.; funding acquisition; J.R.

DECLARATION OF INTERESTS

R.G., J.C., and J.R. have a patent pending related to this work.

INCLUSION AND DIVERSITY

We support inclusive, diverse, and equitable conduct of research.

Received: January 17, 2023

Revised: August 22, 2023

Accepted: December 8, 2023

Published: January 4, 2024

Please cite this article in press as: Gries et al., Discovery of dual-active ethionamide boosters inhibiting the *Mycobacterium tuberculosis* ESX-1 secretion system, *Cell Chemical Biology* (2023), <https://doi.org/10.1016/j.cchembiol.2023.12.007>



REFERENCES

- WHO, W.H.O. (2022). Global Tuberculosis Report.
- Kaufmann, S.H.E., Lange, C., Rao, M., Balaji, K.N., Lotze, M., Schito, M., Zumla, A.I., and Maeurer, M. (2014). Progress in tuberculosis vaccine development and host-directed therapies—a state of the art review. *Lancet Respir. Med.* 2, 301–320.
- Wallis, R.S., and Hafner, R. (2015). Advancing host-directed therapy for tuberculosis. *Nat. Rev. Immunol.* 15, 255–263.
- Gries, R., Sala, C., and Rybniker, J. (2020). Host-Directed Therapies and Anti-Virulence Compounds to Address Anti-Microbial Resistant Tuberculosis Infection. *Applied Sciences-Basel* 10, ARTN 2688.
- Torfs, E., Piller, T., Cos, P., and Cappoen, D. (2019). Opportunities for Overcoming Mycobacterium tuberculosis Drug Resistance: Emerging Mycobacterial Targets and Host-Directed Therapy. *Int. J. Mol. Sci.* 20, 2868.
- Cole, S.T. (2016). Inhibiting Mycobacterium tuberculosis within and without. *Philos. Trans. R. Soc. Lond. B Biol. Sci.* 371, 20150506.
- Theobald, S.J., Gräß, J., Fritsch, M., Suárez, I., Eisefeld, H.S., Winter, S., Koch, M., Hölscher, C., Pasparakis, M., Kashkar, H., and Rybniker, J. (2021). Gasdermin D mediates host cell death but not interleukin-1 β secretion in Mycobacterium tuberculosis-infected macrophages. *Cell Death Discov.* 7, 327.
- Madacki, J., Mas Fiol, G., and Brosch, R. (2019). Update on the virulence factors of the obligate pathogen Mycobacterium tuberculosis and related tuberculosis-causing mycobacteria. *Infect. Genet. Evol.* 72, 67–77.
- Rybniker, J., Chen, J.M., Sala, C., Hartkoon, R.C., Vocat, A., Benjak, A., Boy-Röttger, S., Zhang, M., Székely, R., Greff, Z., et al. (2014). Anticytolytic screen identifies inhibitors of mycobacterial virulence protein secretion. *Cell Host Microbe* 16, 538–548.
- Filpo, M., Frita, R., Bourotte, M., Martínez-Martínez, M.S., Boesche, M., Boyle, G.W., Derimanov, G., Drewes, G., Gamallo, P., Ghidelli-Disse, S., et al. (2022). The small-molecule SMART751 reverses Mycobacterium tuberculosis resistance to ethionamide in acute and chronic mouse models of tuberculosis. *Sci. Transl. Med.* 14, eaaz6280.
- Laborde, J., Deraeve, C., and Bernardes-Génissin, V. (2017). Update of Antitubercular Prodrugs from a Molecular Perspective: Mechanisms of Action, Bioactivation Pathways, and Associated Resistance. *ChemMedChem* 12, 1657–1676.
- Engohang-Ndong, J., Baillat, D., Aumercier, M., Bellefontaine, F., Besra, G.S., Locht, C., and Baulard, A.R. (2004). EthR, a repressor of the TetR/CamR family implicated in ethionamide resistance in mycobacteria, octamerizes cooperatively on its operator. *Mol. Microbiol.* 51, 175–188.
- Willand, N., Diré, B., Carette, X., Bifani, P., Singhal, A., Desroses, M., Leroux, F., Willery, E., Mathys, V., Déprez-Poulain, R., et al. (2009). Synthetic EthR inhibitors boost antituberculous activity of ethionamide. *Nat. Med.* 15, 537–544.
- Blondiaux, N., Moune, M., Desroses, M., Frita, R., Filpo, M., Mathys, V., Soetaert, K., Kiass, M., Delorme, V., Djaout, K., et al. (2017). Reversion of antibiotic resistance in Mycobacterium tuberculosis by spiroisoxazoline SMART-420. *Science* 355, 1206–1211.
- Gräß, J., Suárez, I., van Gumpel, E., Winter, S., Schreiber, F., Esser, A., Hölscher, C., Fritsch, M., Herb, M., Schramm, M., et al. (2019). Corticosteroids inhibit Mycobacterium tuberculosis-induced necrotic host cell death by abrogating mitochondrial membrane permeability transition. *Nat. Commun.* 10, 688.
- Rybniker, J., Vocat, A., Sala, C., Busso, P., Pojer, F., Benjak, A., and Cole, S.T. (2015). Lansoprazole is an antituberculous prodrug targeting cytochrome bc1. *Nat. Commun.* 6, 7659.
- Ronchetti, R., Moroni, G., Carotti, A., Gioiello, A., and Camaioni, E. (2021). Recent advances in urea- and thiourea-containing compounds: focus on innovative approaches in medicinal chemistry and organic synthesis. *RSC Med. Chem.* 12, 1046–1064.
- Renshaw, P.S., Panagiotidou, P., Whelan, A., Gordon, S.V., Hewinson, R.G., Williamson, R.A., and Carr, M.D. (2002). Conclusive evidence that the major T-cell antigens of the Mycobacterium tuberculosis complex ESAT-6 and CFP-10 form a tight, 1:1 complex and characterization of the structural properties of ESAT-6, CFP-10, and the ESAT-6*CFP-10 complex. Implications for pathogenesis and virulence. *J. Biol. Chem.* 277, 21598–21603.
- Guinn, K.M., Hickey, M.J., Mathur, S.K., Zakel, K.L., Grotzke, J.E., Lewinson, D.M., Smith, S., and Sherman, D.R. (2004). Individual RD1-region genes are required for export of ESAT-6/CFP-10 and for virulence of Mycobacterium tuberculosis. *Mol. Microbiol.* 51, 359–370.
- Solans, L., Gonzalo-Asensio, J., Sala, C., Benjak, A., Uplekar, S., Rougemont, J., Guilhot, C., Malaga, W., Martín, C., and Cole, S.T. (2014). The PhoP-dependent ncRNA Mcr7 modulates the TAT secretion system in Mycobacterium tuberculosis. *PLoS Pathog.* 10, e1004183.
- Dover, L.G., Alahari, A., Gratraud, P., Gomes, J.M., Bhowruth, V., Reynolds, R.C., Besra, G.S., and Kremer, L. (2007). EthA, a common activator of thiocarbamide-containing drugs acting on different mycobacterial targets. *Antimicrob. Agents Chemother.* 51, 1055–1063.
- Villemagne, B., Machelart, A., Tran, N.C., Filpo, M., Moune, M., Leroux, F., Piveteau, C., Wohlkönig, A., Wintjens, R., Li, X., et al. (2020). Fragment-Based Optimized EthR Inhibitors with in Vivo Ethionamide Boosting Activity. *ACS Infect. Dis.* 6, 366–378.
- Nikiforov, P.O., Blaszczyk, M., Surade, S., Boshoff, H.I., Sajid, A., Delorme, V., Deboosere, N., Brodin, P., Baulard, A.R., Barry, C.E., 3rd, et al. (2017). Fragment-Sized EthR Inhibitors Exhibit Exceptionally Strong Ethionamide Boosting Effect in Whole-Cell Mycobacterium tuberculosis Assays. *ACS Chem. Biol.* 12, 1390–1396.
- Filpo, M., Desroses, M., Lecat-Guillet, N., Villemagne, B., Blondiaux, N., Leroux, F., Piveteau, C., Mathys, V., Flament, M.P., Slepmann, J., et al. (2012). Ethionamide boosters. 2. Combining bioisosteric replacement and structure-based drug design to solve pharmacokinetic issues in a series of potent 1,2,4-oxadiazole EthR inhibitors. *J. Med. Chem.* 55, 68–83.
- Ang, M.L.T., Zainul Rahim, S.Z., Shui, G., Dianiskova, P., Madacki, J., Lin, W., Koh, V.H.Q., Martínez Gomez, J.M., Sudarkodi, S., Bendt, A., et al. (2014). An ethA-ethR-deficient Mycobacterium bovis BCG mutant displays increased adherence to mammalian cells and greater persistence in vivo, which correlate with altered mycolic acid composition. *Infect. Immun.* 82, 1850–1859.
- Ang, M.L.T., Zainul Rahim, S.Z., de Sessions, P.F., Lin, W., Koh, V., Pethe, K., Hibberd, M.L., and Alonso, S. (2017). EthA/R-Independent Killing of Mycobacterium tuberculosis by Ethionamide. *Front. Microbiol.* 8, 710.
- Grant, S.S., Wellington, S., Kawate, T., Desjardins, C.A., Silvis, M.R., Wivagg, C., Thompson, M., Gordon, K., Kazanskaya, E., Nietupski, R., et al. (2016). Baeyer-Villiger Monooxygenases EthA and MymA Are Required for Activation of Replicating and Non-replicating Mycobacterium tuberculosis Inhibitors. *Cell Chem. Biol.* 23, 666–677.
- Urbanowski, M.L., Lykken, G.L., and Yahr, T.L. (2005). A secreted regulatory protein couples transcription to the secretory activity of the Pseudomonas aeruginosa type III secretion system. *Proc. Natl. Acad. Sci. USA* 102, 9930–9935.
- Diaz, M.R., King, J.M., and Yahr, T.L. (2011). Intrinsic and Extrinsic Regulation of Type III Secretion Gene Expression in Pseudomonas Aeruginosa. *Front. Microbiol.* 2, 89.
- Filpo, M., Desroses, M., Lecat-Guillet, N., Diré, B., Carette, X., Leroux, F., Piveteau, C., Demirkaya, F., Lens, Z., Rucktooa, P., et al. (2011). Ethionamide boosters: synthesis, biological activity, and structure-activity relationships of a series of 1,2,4-oxadiazole EthR inhibitors. *J. Med. Chem.* 54, 2994–3010.
- Attarian, R., Bennie, C., Bach, H., and Av-Gay, Y. (2009). Glutathione disulfide and S-nitrosoglutathione detoxification by Mycobacterium tuberculosis thioredoxin system. *FEBS Lett.* 583, 3215–3220.
- Arumugam, P., Shankaran, D., Bothra, A., Gandotra, S., and Rao, V. (2019). The MmpS6-MmpL6 Operon Is an Oxidative Stress Response

Please cite this article in press as: Gries et al., Discovery of dual-active ethionamide boosters inhibiting the *Mycobacterium tuberculosis* ESX-1 secretion system, *Cell Chemical Biology* (2023), <https://doi.org/10.1016/j.chembiol.2023.12.007>

Cell Chemical Biology Article

CellPress

- System Providing Selective Advantage to *Mycobacterium tuberculosis* in Stress. *J. Infect. Dis.* *219*, 459–469.
33. Briffotiaux, J., Huang, W., Wang, X., and Gicquel, B. (2017). MmpS5/MmpL5 as an efflux pump in *Mycobacterium* species. *Tuberculosis* *107*, 13–19.
 34. Pisu, D., Provvedi, R., Espinosa, D.M., Payan, J.B., Boldrin, F., Palù, G., Hernandez-Pando, R., and Manganelli, R. (2017). The Alternative Sigma Factors SigE and SigB Are Involved in Tolerance and Persistence to Antitubercular Drugs. *Antimicrob. Agents Chemother.* *61*, e01596-17.
 35. Dickey, S.W., Cheung, G.Y.C., and Otto, M. (2017). Different drugs for bad bugs: antivirulence strategies in the age of antibiotic resistance. *Nat. Rev. Drug Discov.* *16*, 457–471.
 36. Schneider, C.A., Rasband, W.S., and Eliceiri, K.W. (2012). NIH Image to ImageJ: 25 years of image analysis. *Nat. Methods* *9*, 671–675.
 37. Langmead, B., and Salzberg, S.L. (2012). Fast gapped-read alignment with Bowtie 2. *Nat. Methods* *9*, 357–359.
 38. Liao, Y., Smyth, G.K., and Shi, W. (2014). featureCounts: an efficient general purpose program for assigning sequence reads to genomic features. *Bioinformatics* *30*, 923–930.
 39. Love, M.J., Huber, W., and Anders, S. (2014). Moderated estimation of fold change and dispersion for RNA-seq data with DESeq2. *Genome Biol.* *15*, 550.
 40. Kevin Blighe, S.R., and Lewis, M. (2022). EnhancedVolcano: Publication-Ready Volcano Plots with Enhanced Colouring and Labeling. <https://bioconductor.org/packages/devel/bioc/vignettes/EnhancedVolcano/inst/doc/EnhancedVolcano.html>.
 41. Theobald, S.J., Simonis, A., Mudler, J.M., Göbel, U., Acton, R., Kohlhas, V., Albert, M.C., Hellmann, A.M., Main, J.J., Winter, S., et al. (2022). Spleen tyrosine kinase mediates innate and adaptive immune crosstalk in SARS-CoV-2 mRNA vaccination. *EMBO Mol. Med.* *14*, e15888.
 42. Stover, C.K., de la Cruz, V.F., Fuerst, T.R., Burlein, J.E., Benson, L.A., Bennett, L.T., Bansal, G.P., Young, J.F., Lee, M.H., Hatfull, G.F., et al. (1991). New use of BCG for recombinant vaccines. *Nature* *351*, 456–460.

Please cite this article in press as: Gries et al., Discovery of dual-active ethionamide boosters inhibiting the *Mycobacterium tuberculosis* ESX-1 secretion system, *Cell Chemical Biology* (2023), <https://doi.org/10.1016/j.cchembiol.2023.12.007>



STAR★METHODS

KEY RESOURCES TABLE

REAGENT or RESOURCE	SOURCE	IDENTIFIER
Antibodies		
Mouse monoclonal anti Esat-6 HYB 076-08	Santa Cruz	Cat# sc-57730; RRID: AB_629451
Polyclonal Anti-Mycobacterium tuberculosis CFP10	BEI Resources	NR-13801
Polyclonal Anti-Mycobacterium tuberculosis Antigen 85 Complex	BEI Resources	NR-13800
Mouse Monoclonal anti Hsp65	Invitrogen	Cat# MA1-7422; RRID: AB_1017679
Anti-mouse IgG, HRP-linked Antibody	Cell Signaling Technology	Cat# 7076; RRID: AB_330924
Anti-rabbit IgG, HRP-linked Antibody	Cell Signaling Technology	Cat# 7074; RRID: AB_2099233
Bacterial and virus strains		
Mtb Erdman	ST Cole, Rybniker et al. ⁹	ATCC 35801
Mtb Erdman GFP	ST Cole Rybniker et al. ⁹	N/A
Mtb Erdman pMV361::ethA	This paper	N/A
Mtb Erdman EthA ^{C131X}	This paper	N/A
Chemicals, peptides, and recombinant proteins		
SPECS world diversity set 3	SPECS	N/A
S3 analogues (Table S3)	SPECS	N/A
S3	SPECS / Vitas-M	AP-853/43445427 / STK514215
S3_100	SPECS / Vitas-M	AP-853/41822759 / STK267384
S3_106	SPECS / Vitas-M	AP-853/42160069 / STK205403
Rifampicin	Sigma-Aldrich	Cat# R3501
Isoniazid	Sigma-Aldrich	Cat# I3377
Dimethyl sulfoxide (DMSO)	Sigma-Aldrich	Cat# D8418
BDM41906	Institut Pasteur de Lille ²⁴	N/A
Human M-CSF	Miltenyi Biotec	Cat# 130-096-491
Phorbol 12-myristate 13-acetate (PMA)	Sigma-Aldrich	Cat# P8139
Resazurin	Sigma-Aldrich	Cat# R12204
Ficoll-PlaqueTM plus	Sigma-Aldrich	Cat# GE17-1440-03
Critical commercial assays		
IL-1 beta Human Uncoated ELISA Kit	Thermo Fisher Scientific	Cat# 88-7261-88
Micro BCA™ Protein-Assay-Kit	Thermo Fisher Scientific	Cat# 23235
CellTiter-Glo® Luminescent Cell Viability Assay	Promega	Cat# G7572
Resazurin	Sigma-Aldrich	Cat# R7017
1Step™ Ultra TMB ELISA	Thermo Fisher Scientific	Cat# 34029
NEBNext® rRNA Depletion Kit	New England Biolabs	Cat# E7850
NEBNext® Ultra™ II Directional RNA Library Prep Kit for Illumina	New England Biolabs	Cat# E7760
SuperScript™ III First-Strand Synthesis SuperMix	Invitrogen	Cat# 18080400
Light Cycler Fast Start DNA Master ^{Plus}	Roche	Cat# 03515885001
SYBR® Green I kit		
SYPRO® Orange	Sigma-Aldrich	Cat# S5692
Deposited data		
RNA-Seq data	This paper	GEO: GSE226474
Experimental models: Cell lines		
THP-1	LGC Standards GmbH, Germany	ATCC-TIB202; RRID: CVCL_0006
MRC-5	Coriell Institute for Medical Research	RRID: CVCL_0440

(Continued on next page)

Please cite this article in press as: Gries et al., Discovery of dual-active ethionamide boosters inhibiting the *Mycobacterium tuberculosis* ESX-1 secretion system, *Cell Chemical Biology* (2023), <https://doi.org/10.1016/j.chembiol.2023.12.007>

Continued

REAGENT or RESOURCE	SOURCE	IDENTIFIER
HepG2	ATCC	RRID: CVCL_0027; Cat# HB-8065
Oligonucleotides		
qPCR_ethA_fwd TCATTACCGCAACGGG	This paper	N/A
qPCR_ethA_rev CGACAGACAAACTCCGA	This paper	N/A
qPCR_ethA2_fwd: CGGGTACATGATGGGC	This paper	N/A
qPCR_ethA2_rev: CGTTCGGGATAGTGGAC	This paper	N/A
qPCR_mymA_fwd: GACCTATAAGGGTGTGCT	This paper	N/A
qPCR_mymA_rev: CCTCCACGGATGCTTG	This paper	N/A
qPCR_sigA_fwd CGCGACATGATGGA	This paper	N/A
qPCR_sigA_rev GGAGAACTGTACCCT	This paper	N/A
pMV361:ethA_fwd ATGCCAAGACAATTATGACCGACACCTCGACG	This paper	N/A
pMV361:ethA_rev GCTGGATCCGCAATTCTAAACCCACCGGGG	This paper	N/A
ethA-ethR IG fwd: CTGACTGGCCGCGGAGGTGGT	This paper	N/A
ethA-ethR IG rev: CGGTCATGGATCCACGCTATCAAC	This paper	N/A
Recombinant DNA		
Plasmid: pMV361	This paper	N/A
Plasmid: pMV361:ethA	This paper	N/A
Software and algorithms		
GraphPad Prism Version 8	GraphPad Software, San Diego, CA, USA	www.graphpad.com
ImageJ	Schneider et al. ³⁶	https://imagej.nih.gov/ij/
R	R Core Team (2021). R: A language and environment for statistical computing	https://cran.r-project.org/
Bowtie2 version 2.3.4.1	Langmead et al., 2012, <i>Nat Methods</i> ³⁷	https://github.com/BenLangmead/bowtie2/releases
featureCounts 1.5	Liao et al., 2014, <i>Bioinformatics</i> ³⁸	http://www.bioconductor.org/packages/release/bioc/html/Rsubread.html
DESeq2 version 1.34	Love et al., 2014, <i>Genome Biol</i> ³⁹	https://bioconductor.org/packages/release/bioc/html/DESeq2.html
EnhancedVolcano version 1.12	Blighe et al. ⁴⁰	https://bioconductor.org/packages/devel/bioc/vignettes/EnhancedVolcano/inst/doc/EnhancedVolcano.html
pheatmap version 1.0.12	Cran.r-project	https://CRAN.R-project.org/package=pheatmap
LightCycler® Thermal Shift Analysis software	Roche	https://diagnostics.roche.com/us/en/home.html

RESOURCE AVAILABILITY

Lead contact

Further information and requests for resources and reagents should be directed to and will be fulfilled by the lead contact, Jan Rybniker (jan.rybniker@uk-koeln.de) upon reasonable request.

Materials availability

All unique/stable and non-commercially available reagents generated in this study can be requested from the lead contact in reasonable amounts with a completed Materials Transfer Agreement.

Data and code availability

- RNA-Seq data have been deposited at GEO and are publicly available as of the date of publication. Accession numbers are listed in the [key resources table](#).

Please cite this article in press as: Gries et al., Discovery of dual-active ethionamide boosters inhibiting the *Mycobacterium tuberculosis* ESX-1 secretion system, *Cell Chemical Biology* (2023), <https://doi.org/10.1016/j.chembiol.2023.12.007>



CellPress

Cell Chemical Biology
Article

- This paper does not report original code.
- Any additional information required to re-analyze the data reported in this paper is available from the [lead contact](#) upon request.

EXPERIMENTAL MODEL AND STUDY PARTICIPANT DETAILS

Culture conditions of mycobacteria

Mycobacterium tuberculosis Erdman strains (wild type and eGFP-expressing strains were provided by S.T. Cole, Institute Pasteur Paris³) were cultivated in BD Difco™ Middlebrook 7H9 broth (Becton Dickinson, Franklin Lakes, USA) supplemented with 0.2% glycerol (Th. Geyer GmbH & Co. KG, Renningen, Germany), 10% albumin dextrose catalase (ADC Middlebrook; Becton Dickinson, Franklin Lakes, USA) and 0.05% Tween80 (Carl Roth GmbH + Co. KG, Karlsruhe, Germany) (7H9c), if not stated differently. For selected experiments protein-free Sauton's medium containing the following components per 1 liter was used: 0.5 g of monopotassium phosphate (Carl Roth GmbH + Co. KG, Karlsruhe, Germany), 0.5 g of magnesium sulfate (Thermo Fisher Scientific, Waltham, USA), 4 g of L-asparagine (Sigma-Aldrich, St. Louis, USA), 0.05 g of ammonium iron (III) citrate (Thermo Fisher Scientific, Waltham, USA), 2 g of citric acid (Th. Geyer GmbH & Co. KG, Renningen, Germany), 100 μ L of 1% zinc sulfate (Sigma-Aldrich, St. Louis, USA) and 60 mL of glycerol.

Culture conditions of eukaryotic cell lines

MRC-5 human lung fibroblasts (Coriell Institute for Medical Research, Camden, USA) were grown in gibco minimum essential medium (Thermo Fisher Scientific, Waltham, USA) supplemented with 10% heat-inactivated fetal bovine serum (FBS; Thermo Fisher Scientific, Waltham, USA), 1% gibco nonessential amino acids (Thermo Fisher Scientific, Waltham, USA) and 1 mM gibco sodium pyruvate (Thermo Fisher Scientific, Waltham, USA) (MEMc). PBMC derived macrophages, THP-1 and THP-1-derived macrophages were grown in gibco RPMI 1640 medium (Thermo Fisher Scientific, Waltham, USA) supplemented with 10% FBS (Pan-Biotech, Aidenbach, Germany) (RPMI). HepG2 were grown in gibco Dulbecco's minimum essential medium (Thermo Fisher Scientific, Waltham, USA) supplemented with 10% heat-inactivated fetal bovine serum (FBS; Thermo Fisher Scientific, Waltham, USA) (MEM).

All cell lines were cultivated at 37°C and 5% CO₂.

METHOD DETAILS

Small molecules used in this study

Initial screening compounds were all part of the World Diversity Set 3 provided by Specs (Zoetermeer, Netherlands). Compounds for hit validation and consequent experimentation were either sourced from Specs (Zoetermeer, Netherlands), Vitas-M (Hong Kong, Hong Kong) or Sigma-Aldrich (St. Louis, USA). The S3 analogue library was provided by Specs (Zoetermeer, Netherlands) (see [Table S3](#) for full list of structures).

The compound S3 (1-(5-Chlorothiophen-2-yl)-2-([5-(4-hydroxyphenyl)-1,3,4-oxadiazol-2-yl]sulfanyl)ethanone; molecular weight: 352.82 g/mol) was provided by Specs (Zoetermeer, Netherlands; AP-853/43445427) and by Vitas-M (Hong Kong, Hong Kong; STK514215).

The compound S3_100 (2-(5-Phenyl-[1,3,4]oxadiazol-2-ylsulfanyl)-1-piperidin-1-yl-ethanone; molecular weight: 303.38 g/mol) was provided by Specs (Zoetermeer, Netherlands; AP-853/41822759) and by Vitas-M (Hong Kong, Hong Kong; STK267384).

The compound S3_106 (1-(Azepan-1-yl)-3-[[5-(3-methylphenyl)-1,3,4-oxadiazol-2-yl]sulfanyl]propan-1-one; 345.46 g/mol) was provided by Specs (Zoetermeer, Netherlands; AP-853/42160069) and by Vitas-M (Hong Kong, Hong Kong; STK205403).

The following control compounds were provided by Sigma-Aldrich (St. Louis, USA): rifampicin (Cat# R3501), isoniazid (Cat# I3377) and dimethyl sulfoxide (DMSO; Cat# D8418). The compound BDM41906 was kindly provided by Alain Baulard (Institut Pasteur de Lille, Lille, France).²⁴

Fibroblast survival assay (FSA)

Fibroblast survival assays were performed using MRC-5 fibroblasts grown in MEMc. Adherent cells were trypsinated (Sigma-Aldrich, St. Louis, USA) and detached from tissue flasks, centrifuged for 5 min at 300 rcf, washed with Dulbecco's Phosphate Buffered Saline (PBS; Thermo Fisher Scientific, Waltham, USA), centrifuged again, resuspended in fresh medium and filtered using a 0.40 μ m Falcon® cell strainer (Corning, Corning, USA). Cell concentrations of trypan blue stained cells were counted using a Neubauer counting chamber (Corning, Corning, USA). 4,000 cells were seeded in 35 μ L per well in 384-well plates containing 5 μ L of the respective test compound. After a resting period of 3 h the fibroblasts were then infected with 10 μ L *Mtb* resuspended in MEMc at a MOI of 10 and incubated for 72 h. Fibroblast survival was determined by using the luminescent cell viability assay CellTiter-Glo according to the protocol provided by the manufacturer (Promega, Fitchburg, USA). In brief, 35 μ L of pre-mixed CellTiter-Glo solution were added to the wells followed by an incubation period of 10 min at 37°C. Finally, luminescence was quantified in a plate reader (Cytation™ 3, BioTek Instruments, Inc, Winooski, USA).

Resazurin microtiter assay (REMA)

Frozen *Mtb* stocks were thawed and diluted in 7H9c medium to an optical density (OD₅₆₀) of 0.0003. Then, 90 μ L of this suspension were combined with 10 μ L of the test substance, which had been serially diluted (1:2), in the test plate. The plates were then incubated

Please cite this article in press as: Gries et al., Discovery of dual-active ethionamide boosters inhibiting the *Mycobacterium tuberculosis* ESX-1 secretion system, Cell Chemical Biology (2023), <https://doi.org/10.1016/j.chembiol.2023.12.007>

at 37°C for 7 days. Following this, 10 μ L of resazurin (Sigma-Aldrich, St. Louis, USA) were added to each plate and they were incubated for an additional 24 h. Mycobacterial growth was measured using a plate reader (560 nm/590 nm; Cytation™ 3, BioTek Instruments, Inc, Winooski, USA).

Hit selection after primary screening

Initial screening of the World Diversity Set 3 molecule library was conducted at 10 μ M by testing all compounds in the FSA and the REMA. Fibroblast survival in the FSA was calculated based on luminescence signals of MRC-5 cells exposed to the control antibiotic rifampicin (100%) and the solvent control DMSO (0%). Anti-mycobacterial activity in the REMA was calculated accordingly based on fluorescence of *Mtb* exposed to the control antibiotic rifampicin (100%) and the solvent control DMSO (0%). The respective cut-offs for potential anti-virulence compounds were set to maximal 10% anti-mycobacterial activity and minimal 75% fibroblast survival. For potential antibiotics, the thresholds were set to a minimum of 80% anti-mycobacterial activity (REMA) and 75% fibroblast survival.

Macrophage survival assays

Human peripheral blood mononuclear cells (PBMCs) were isolated from buffy coats by using Ficoll density gradient separation. Briefly, blood was mixed with PBS (1:1) and transferred to Leucosep-Falcons (Sigma-Aldrich, St. Louis, USA) containing Ficoll solution (Ficoll-Plaque™ plus; GE Healthcare, Chicago, USA) (2:1). After centrifugation the interphase was extracted, washed with PBS and mixed with MACS Buffer (Miltenyi Biotec, Bergisch Gladbach, Germany). CD14 positive macrophages were then isolated using CD14 magnetic beads (MACS MicroBeads, Miltenyi Biotec, Bergisch Gladbach, Germany) in MS or LS columns. Trypan blue stained cells were then counted using a Neubauer counting chamber and 50,000 cells were seeded in 100 μ L RPMI medium in 96 well plates (Corning, Corning, USA). Monocytes were then differentiated into primary macrophages by exposure to 50 ng/mL human macrophage colony stimulating factor (M-CSF) for four days (Miltenyi Biotec, Bergisch Gladbach, Germany). To perform the survival assay, macrophages were pre-incubated for 2 h with the respective test compound, then infected with 10 μ L *Mtb* resuspended in RPMI (MOI 2) and incubated for 48 h. Survival of PBMC-derived macrophages was determined after fixation with 4% paraformaldehyde by counting nucleus-stained cells using 4',6-diamidino-2-phenylindole (DAPI; Thermo Fisher Scientific, Waltham, USA). For this, representative microscopy images were captured at the center of the well and cells were counted using ImageJ.³⁶

Determining intracellular growth

50,000 PBMC-derived macrophages were seeded in 96-well plates, according to the protocol described for macrophage survival assays above. After seeding and differentiation, the macrophages were infected with 10 μ L eGFP expressing *Mtb* resuspended in RPMI (MOI 2). After 4 h the infected cells were washed three times with PBS and exposed to the respective test substance. After 48 h extracellular mycobacteria were removed by washing once with PBS and representative fluorescence images were taken of the center of the well. Fluorescence signals were then analyzed using ImageJ.³⁶

HepG2 cytotoxicity assays

20,000 HepG2 cells were seeded in 90 μ L MEM in 96-well plates and exposed to 10 μ L of the respective test compound. After three days of incubation at 37°C and 5% CO₂ 10 μ L Resazurin (Sigma-Aldrich, St. Louis, USA) were added and the plates were incubated for 1 h at room temperature. Afterwards, the plates were measured in a plate reader (560 nm/590 nm).

Ethionamide booster assay

Mtb was cultivated in 7H9c to midlogarithmic phase and then seeded at OD₅₆₀ of 0.01 (in 1 mL) in a 24 well plate containing 500 μ L of the respective test compound with 500 μ L of either 6 μ M ethionamide (Sigma-Aldrich, St. Louis, USA) or 0.05 % DMSO. The plates were then incubated at 37°C for 10 days, after which growth inhibition was determined by measurement of the optical density.

Determining intracellular colony forming units

50,000 THP-1 cells were seeded in 100 μ L RPMI in 96-well plates and differentiated into macrophages using 200 nM PMA (phorbol 12-myristate 13-acetate, Sigma-Aldrich, St. Louis, USA) for 24 h. The medium was then replaced with 100 μ L RPMI. After a 24 h resting period without PMA, the medium was replaced with 90 μ L RPMI and the THP-1-derived macrophages were infected with 10 μ L *Mtb* resuspended in RPMI (MOI 2). Extracellular *Mtb* were removed by washing three times with PBS 4 h post infection and 100 μ L RPMI containing the respective test compound was added. After 72 h, infected macrophages were lysed using 50 μ L 0.1% SDS. The cell lysates were subsequently diluted in a 1:10 dilution series of which 10 μ L were plated on 7H10 agar plates to determine intracellular bacterial loads. Colony forming units (CFU) were counted two weeks post plating.

Immunoblot analysis and secretion assay

Mycobacteria were cultivated as pre-culture to midlogarithmic phase (OD₅₆₀ 0.8) in Sauton's medium supplemented with 0.05% Tween80 and then transferred to a 30 mL main culture in Sauton's medium without Tween80 starting at OD₅₆₀ 0.4. After 72 h supernatant and cell pellet were harvested. For analysis of intracellular proteins the remaining pellet was resuspended in PBS containing protease inhibitor (cOmplete mini EDTA-free; Roche, Basel, Switzerland) and lysed by beating with glass beads (150-212 μ m; Sigma-Aldrich, St. Louis, USA) in a cell disruptor (Disruptor Genie; Scientific Industry, Bohemia, USA) five times for 1 min at max speed, with

Please cite this article in press as: Gries et al., Discovery of dual-active ethionamide boosters inhibiting the *Mycobacterium tuberculosis* ESX-1 secretion system, *Cell Chemical Biology* (2023), <https://doi.org/10.1016/j.chembiol.2023.12.007>



CellPress

Cell Chemical Biology
Article

1 min cooling periods in between. Following this, beads-free supernatant was then filtered through 0.22 μm filter (Carl Roth GmbH + Co. KG, Karlsruhe, Germany). For western blotting supernatant samples were filtered (0.22 μm) and 100-times concentrated using vivaspin20 centrifuges (Sartorius, Göttingen, Germany). During this concentration step bigger proteins were removed using 100 kDa cutoff centrifuges followed by concentration using 5 kDa cutoff centrifuges for the collected flow through. Concentrated samples were then separated using TruPAGE™ Precast Gels 4-12% (Sigma-Aldrich, St. Louis, USA) and semi-dry blotted using iBlot2 (Invitrogen, Waltham, USA). Immunodetection was performed using anti ESAT6 HYB 076-08 (Santa Cruz, Dallas, USA), CFP-10 NR-13801 (BEI Resources, Manassas, USA) anti-*Mycobacterium tuberculosis* HSP65 (Invitrogen, Waltham, USA) and anti AG85 NR-13800 (BEI Resources, Manassas, USA) antibodies combined with the respective secondary antibodies (anti-mouse or anti-rabbit; Cell Signaling Technology, Cambridge, UK). Quantification of band intensities was performed using ImageJ.³⁶

Enzyme-linked immunosorbent assay (ELISA)

Quantitative IL-1 β determination of supernatant samples was performed using the IL-1 beta Human uncoated ELISA kit (Thermo Fisher Scientific, Waltham, USA) according to the manufacturer's manual and as described previously.³¹ In brief, ELISA plates were coated with 100 μL per well of the capture antibody in coating buffer and incubated overnight at 4°C. The plates were then washed three times with 250 μL wash buffer and blocked for 1 h at room temperature with 200 μL ELISA diluent. Samples were diluted 1:50 in ELISA diluent and 100 μL were transferred into each well and incubated for 2 h at room temperature. The plates were then washed three times with 250 μL wash buffer, filled with 100 μL of diluted detection antibody and incubated for 1 h at room temperature. Afterwards the plates were washed again three times with 250 μL wash buffer, 100 μL of diluted Avidin-HRP was added and incubated for 30 min at room temperature. After washing the plates three times with 250 μL wash buffer, 100 μL of TMB solution was added and incubated for 15 min at room temperature. The plates were then measured in a plate reader at 450 nm and 570 nm and the difference of both wavelengths was used as signal. The Quantification of IL-1 β was done by using an eight point, two-fold dilution series of the IL-1 β standard. Data analysis was conducted in Microsoft Excel (Microsoft, Redmond, USA) and GraphPad Prism 8 (GraphPad, San Diego, USA).

Qualitative EsxA detection in supernatants of *Mtb* cultivated in Sauton's medium was done using a direct capture / indirect detection ELISA, in which 100 μL of sample were coated overnight directly on 96-well maxisorp immune plates (Thermo Fisher Scientific, Waltham, USA) and subsequently blocked for 2 h using 10% FCS in phosphate buffered saline containing 0.05% Tween20 (Carl Roth GmbH + Co. KG, Karlsruhe, Germany) (PBST). Indirect detection was carried out by incubation for 2 h with primary antibody (1:1000 diluted in 2% FCS in PBST; anti ESAT6 HYB 076-08; Santa Cruz, Dallas, USA) followed by an incubation for 1 h with a secondary antibody conjugated with horseradish peroxidase (1:5000 diluted in 2% FCS in PBST; HRP-linked anti mouse, Cell Signaling Technology, Cambridge, UK). After the addition of 1Step™ Ultra TMB ELISA (Thermo Fisher Scientific, Waltham, USA) protein amount was measured at OD₄₅₀ and normalized to controls.

Cultivation conditions for RNA studies

Mtb was pre-cultivated in 7H9c to midlogarithmic phase and then inoculated at OD₅₆₀ of 0.1. After 48 h of cultivation at 37°C and 100 rpm the cultures were then exposed for 4 h to the test compound or the respective amount of solvent control (DMSO). The *Mtb* cultures were then harvested, centrifuged for 10 min at 14,000 rcf at 4°C. The supernatant was removed and the pellet was immediately frozen at 80°C.

RNA extraction

Mtb were mechanically lysed by beating previously frozen cells (-80°C) using a cell disruptor (Disruptor Genie; Scientific Industry, Bohemia, USA) and 150 - 212 μm glass beads. Lysates were then mixed with RLT lysis buffer (QIAGEN, Venlo, Netherlands) containing 1% β -mercaptoethanol (AppliChem GmbH, Darmstadt, Germany) and ethanol (Th. Geyer GmbH & Co. KG, Renningen, Germany) (3:2) and extracted using the RNeasy kit (QIAGEN, Venlo, Netherlands) according to its protocol.

RNA sequencing

RNA samples were first depleted of ribosomal RNA using the NEBNext® rRNA Depletion Kit (Bacteria) (New England Biolabs, Ipswich, USA). The following strand specific library creation was done using 1000 ng total RNA and the NEBNext® Ultra™ II Directional RNA Library Prep Kit for Illumina (New England Biolabs, Ipswich, USA). Next generation sequencing was then performed using a NovaSeq6000 (Illumina Inc, San Diego, USA) sequencer at 10 million reads per sample. Sequenced reads were aligned to the *Mtb* reference genome (GenBank ID: NC_000962.3) using Bowtie2 version 2.3.4.1.³⁷ Known gene transcripts were quantified using featureCounts 1.5.0-p1,³⁸ i.e. the number of reads assigned to an annotated gene feature. Count data normalization and differential expression testing was performed with DESeq2 version 1.34.³⁹ Genes were defined as differentially expressed with a fold-change ≥ 2 and an adjusted p-value cutoff (FDR) of ≤ 0.5 . Results were visualized in R with the EnhancedVolcano version 1.12⁴⁰ and pheatmap version 1.0.12 packages. Gene ontology analysis was done using geneontology.org.

cDNA synthesis

For synthesis of cDNA the SuperScript™ III First-Strand Synthesis SuperMix for qRT-PCR (Invitrogen, Waltham, USA) was used according to its protocol. In brief, up to 200 ng of total RNA in 8 μL RNase/DNase-free water were incubated with 10 μL RT buffer, 2 μL RT enzyme mix and incubated at 25°C for 10 min followed by incubation at 50°C for 45 min. The reaction was then terminated at 85°C

Please cite this article in press as: Gries et al., Discovery of dual-active ethionamide boosters inhibiting the *Mycobacterium tuberculosis* ESX-1 secretion system, *Cell Chemical Biology* (2023), <https://doi.org/10.1016/j.cchembiol.2023.12.007>

for 5 min and cooled for 5 min on ice. The initial RNA was then digested by adding 1 μ L RNaseH and incubating for 20 min at 37°C (Invitrogen, Waltham, USA).

Quantitative real-time RT-PCR

Quantitative real-time RT-PCR was performed using the LightCycler® FastStart DNA Master^{Plus} SYBR® Green I kit (Roche, Basel, Switzerland) according to its protocol in a capillary light cycler system (LC 1.5; Roche, Basel, Switzerland). In brief, 2 μ L of cDNA were combined with 4 μ L SYBR Green Mix, 10 μ L RNase/DNase-free water and 2 μ L of the respective primers (10 μ M). Specific primers for *ethA* (fwd: 5'-TCATTACCGCAACGGG-3', rev: 5'-CGACAGACAACTCCGA-3'), *ethA2* (fwd: 5'-CGGGTACATGATGGGC-3', rev: 5'-CGTTCCGGGATAGTGAC-3'), *mymA* (fwd: 5'-GACCTATAAGGGTGTGCT-3', rev: 5'-CCTCCACGGATGCTT-3') and the house-keeping gene *sigA* (fwd: 5'-CGCGACATGATGTGGA-3', rev: 5'-GGAGAACTGTACCCT-3') were used.

Thermal shift assay

Recombinant His₆-tagged *M. tuberculosis* protein EthR was expressed in *E. coli* and purified by affinity chromatography. The thermal shift assay mix consisted of 10 μ M of His-EthR, 2.5x SYPRO® Orange (Sigma-Aldrich, St. Louis, USA), 1 % DMSO with and without compounds. The mix was incubated 30 min at room temperature before processing. The thermal shift was conducted in a LightCycler 480 (Roche, Basel, Switzerland). The samples were heated from 37 to 85 °C with a heating rate of 0.04 °C/s and the fluorescence intensity was measured at Ex/Em of 465/510 nm. The melting curves were analyzed in LightCycler® Thermal Shift Analysis software (Roche, Basel Switzerland). The 1D numerical derivative of melting curves was calculated and the inflection point (T_m) was extracted.

Electrophoretic mobility shift assay (EMSA)

Recombinant His₆-tagged *M. tuberculosis* protein EthR was expressed in *E. coli* and purified by affinity chromatography. The *ethA-ethR* intergenic region was generated by PCR using specific primers and H37Rv genomic DNA (5'-CTGACTGGCCGCGGAGGTGGT-3' and 5'-CGGTCATGGATCCACGCTATCAAC-3'). The binding mix contained Tris pH 7.5 50 mM, NaCl 200 mM, MgCl₂ 10 mM, 5 % DMSO as well as DNA and His₆-EthR at the specified concentration. The mix was incubated 30 min at room temperature before loading the gel. The native polyacrylamide gels consisted of a stacking gel containing 5% acrylamide: Bis-acrylamide (29:1, Tokyo Chemical Industry, Tokyo Japan) and 130 mM Tris pH 6.8 and a separating gel containing 12% acrylamide and 280 mM Tris pH 8.8. Native polyacrylamide gel electrophoresis was run in Tris 66 mM and glycine 192 mM at 25 mA per gel for 45 min. The gel was stained using ethidium bromide (Sigma-Aldrich (St. Louis, USA) and bands were quantified using ImageJ.³⁶

Cloning

In order to generate the strain *Mtb* Erdman pMV361:*ethA* the native *ethA* of *Mtb* was amplified using a forward (5'-ATGGCCAAGA CAATTATGACCGAGCACCTCGACG-3') and reverse (5'-GCTGGATCCGCAATTCTAAACCCACCGGGGC-3') primer. The gene was then cloned into the integrative mycobacteria shuttle vector pMV361 cut with BamHI (New England Biolabs, Ipswich, USA) and HindIII (New England Biolabs, Ipswich, USA) using the In-Fusion® HD cloning kit (Takara Bio, Kyoto, Japan).⁴² The resulting vector pMV361:*ethA*, which utilizes the constitutive promoter *hsp60*, was transformed into *Mtb* Erdman creating the strain *Mtb* Erdman pMV361:*ethA*.

Generation of the ethionamide resistant strain EthA^{C131X}

Mtb was cultivated in 7H9c medium at 37°C under aerobic conditions. For the generation of spontaneous mutants resistant to ethionamide 3×10^7 to 3×10^9 bacteria were plated on 7H10 agar plates containing 50 μ M ethionamide. After 14 to 28 days of incubation, colonies were picked and subcultivated on 7H10 agar plates with and without compound. Further cultivation of mutants was done in 7H9c followed by testing for resistance in microtiter plates in the presence and absence of ethionamide.

QUANTIFICATION AND STATISTICAL ANALYSIS

DESeq2 analysis were performed in R (cran.r-project.org). Other statistical analyses were performed using GraphPad Prism 8 (GraphPad, San Diego, USA). Significant differences of only two conditions were calculated using two-tailed students t-test with a 95% confidence level. Significant differences between multiple conditions were calculated using one-way ANOVA combined with Bonferroni post-hoc test (ns = not significant; * = p < 0.05; ** = p < 0.01; *** = p < 0.001).

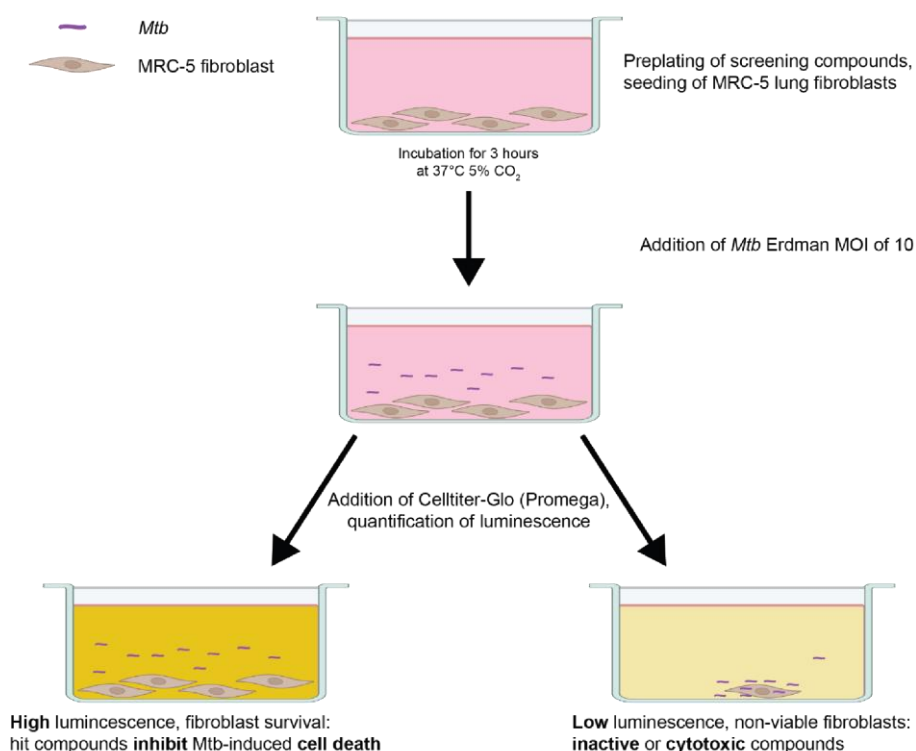


Figure S1: Schematic overview of the fibroblast survival assay (FSA), related to Figure 1. 4.000 MRC-5 fibroblasts per well were seeded and preincubated with the test-compound in a 384 well plate and incubated for 3 h at 37°C and 5% CO₂. *Mycobacterium tuberculosis* grown to midlogarithmic phase is added at a multiplicity of infection of 10 and co-cultivated for 72 h. Fibroblast survival was determined using Celltiter-Glo (Promega). After 15 min. incubation, luminescence was measured and survival was calculated based on 0.5% DMSO and 5 µM rifampicin as controls.

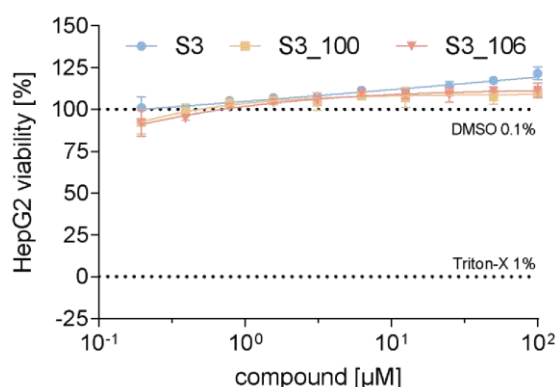


Figure S2: No cytotoxic effects on HepG2, related to text section 'host cell-based screening identifies a cytoprotective 1,3,4-oxadiazole compound' and Figure 5. HepG2 liver cancer cells were exposed to different concentrations of S3, S3_100 or S3_106 for three days. Cell viability was measured using Resazurin. Viability was calculated in correlation to cells treated with 0.1% DMSO (100%) or 1% Triton-X (0%).

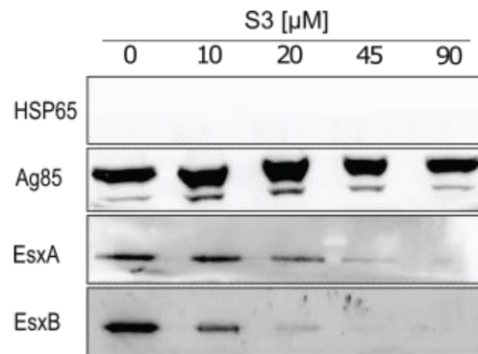


Figure S3: Representative EsxB immunoblot of culture supernatant of *Mtb* cultivated in protein-free medium in the presence of different concentrations of S3, related to Figure 2. The heat-shock protein HSP65 was used as a lysis control, whereas Ag85 acts as control for TAT-dependent secretion which is not affected by S3. EsxA and EsxB are exclusively secreted by the ESX-1 secretion system. Analysis of EsxB was done after stripping the membrane using 0.7% β -mercaptoethanol, 2% SDS in Tris HCl.

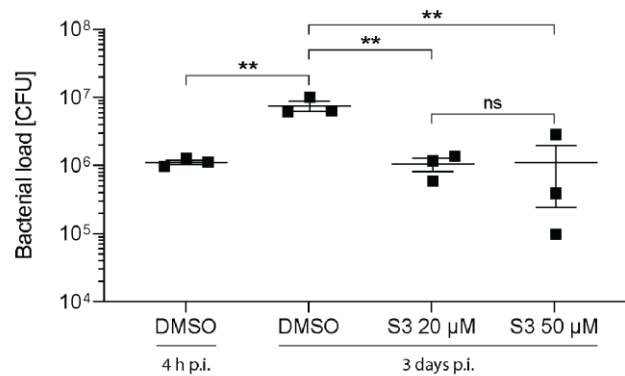


Figure S4: Intracellular reduction of *Mycobacterium tuberculosis* (*Mtb*) after three days of exposure to S3, related to Figure 2. THP-1-derived macrophages were infected with *Mtb* and exposed to either 0.1% DMSO (DMSO) or S3. Cells were lysed 4 h or 3 days post infection (p.i.) and plated on 7H10 agar. Colony forming units (CFU) were counted after 14 days.

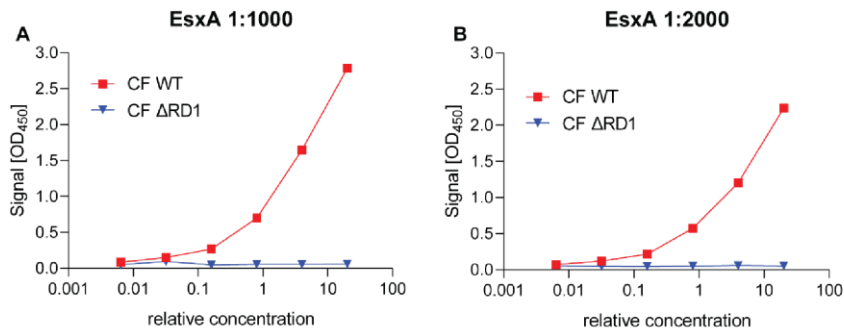


Figure S5: Sample titration in an ELISA-based assay for EsxA detection, related to Figure 5. *Mtb* wildtype (WT) and Δ RD1 strains were cultivated for three days in protein free medium. Culture supernatants were filtrated, concentrated (up to 100-fold) and serially diluted in 96 well ELISA plates. For detection of EsxA, the monoclonal anti-EsxA antibody was used at 1:1000 (A) and 1:2000 (B) dilutions. Secreted EsxA could only be detected in culture filtrates (CF) of the *Mtb* wildtype strain but not in CF of the Δ RD1 strain which fails to secrete EsxA. The detection limit was above a relative concentration of 1 which equals undiluted CF. This allowed us to monitor the activity of the ESX-1 secretion system in an ELISA based medium-throughput manner by omitting the concentration step of culture supernatants which is strictly required for Western blot dependent EsxA detection.

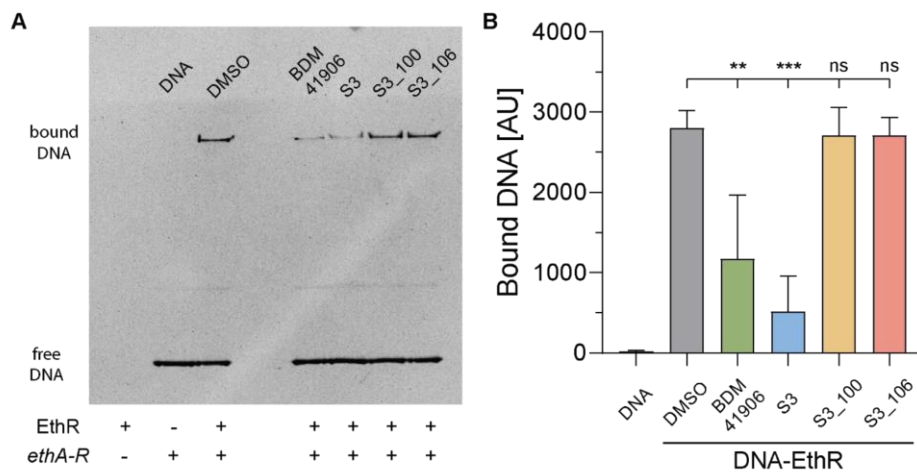


Figure S6: Electrophoretic mobility shift assay, related to Figure 5. Ethidium bromide stained SDS-PAGE gel loaded with 0.6 μ M EthR (lane 1) or with 0.15 μ M of the *ethA-R* intergenic DNA fragment (62 bp) (lane 2). The remaining lanes were loaded with both molecules in the presence of 5% DMSO or 50 μ M of either BDM41906, S3, S3_100 or S3_106. (A) Representative SDS-PAGE gel and (B) quantification of bands of three independent experiments using ImageJ. Data are shown as mean and standard deviation and statistical significances are shown compared to DMSO based on one-way ANOVA combined with Bonferroni post-hoc test (ns = not significant; **= $p < 0.01$; ***= $p < 0.001$).

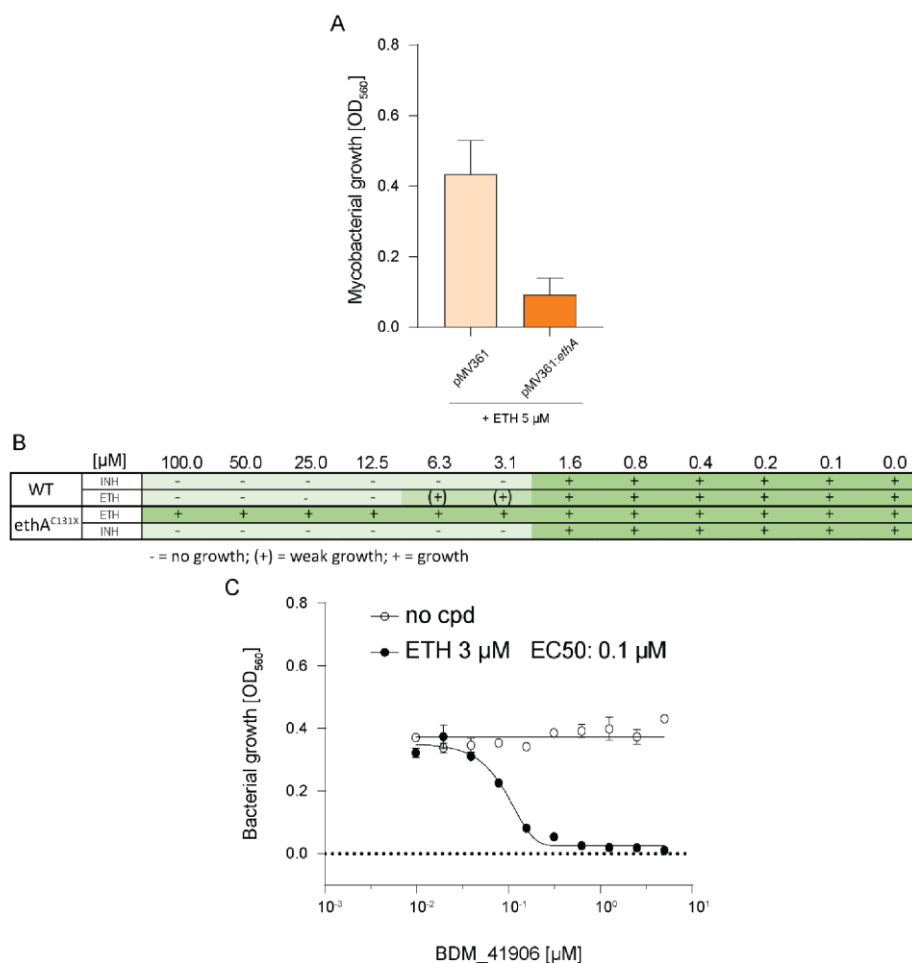


Figure S7: Characterization of *Mtb* strains expressing unregulated *ethA* or deficient *ethA*, related to Figure 6. (A) Growth of *Mtb* harbouring the pMV361 backbone or the *ethA* overexpressing plasmid pMV361:*ethA* after 10 days of treatment with 5 μM ethionamide (ETH). Data are shown as mean and standard deviation of two independent experiments. (B) Growth of *Mtb* Erdman WT and an *EthA*-deficient strain (*ethA*^{C131X}) were determined after 8 days incubation in the presence of different concentrations of isoniazid (INH) or ethionamide (ETH) by optical evaluation. Representative data of four replicates are shown. (C) Growth of *Mtb* Erdman WT at different concentrations of BDM_41906 in combination with and without 3 μM ethionamide (ETH) (no cpd = dilution of BDM_41906; ETH 3 μM = combination of 3 μM ETH and a dilution series of BDM41906; MIC = minimal inhibitory effect (90%)). Representative data of two independent experiments are shown.

5 Results

Table S1: Significantly upregulated genes after 4h exposure of *Mtb* to S3 (20 μ M). Related to Figure 3.

ID	Description	log2FC	-log(padj)
Rv0096	PPE family protein PPE1	1.13	4.98
Rv0135c	Possible transcriptional regulatory protein	1.47	39.05
Rv0136	Probable cytochrome P450 138 Cyp138	2.40	77.60
Rv0140	Conserved protein	1.72	44.91
Rv0142	Conserved hypothetical protein	1.32	24.19
Rv0196	Possible transcriptional regulatory protein	1.83	40.74
Rv0197	Possible oxidoreductase	1.91	53.99
Rv0327c	Possible cytochrome P450 135A1 Cyp135A1	1.01	4.26
Rv0351	Probable GrpE protein (HSP-70 cofactor)	1.02	34.49
Rv0352	Probable chaperone protein DnaJ1	1.09	46.41
Rv0353	Probable heat shock protein transcriptional repressor HspR (MerR family)	1.07	36.94
Rv0440	60 kDa chaperonin 2 GroEL2	1.14	39.23
Rv0464c	Conserved protein	1.21	31.74
Rv0465c	Probable transcriptional regulatory protein	2.26	81.30
Rv0467	Isocitrate lyase Icl (isocitrase) (isocitratase)	1.25	5.70
Rv0468	3-hydroxybutyryl-CoA dehydrogenase FadB2 (beta-hydroxybutyryl-CoA dehydrogenase) (BHBD)	1.02	13.89
Rv0559c	Possible conserved secreted protein	1.67	57.87
Rv0560c	Possible benzoquinone methyltransferase (methylase)	5.29	n/a
Rv0676c	Probable conserved transmembrane transport protein Mmpl5	1.20	33.60
Rv0677c	Possible conserved membrane protein MmpS5	1.32	27.64
Rv0678	Conserved protein	1.75	27.21
Rv0921	Possible resolvase	1.02	17.51
Rv1050	Probable oxidoreductase	1.24	8.70
Rv1128c	Conserved hypothetical protein	1.06	13.12
Rv1129c	Probable transcriptional regulator protein	1.55	41.33
Rv1130	Possible methylcitrate dehydratase PrpD	1.01	15.35
Rv1131	Probable methylcitrate synthase PrpC	1.21	23.60
Rv1221	Alternative RNA polymerase sigma factor SigE	1.43	50.61
Rv1471	Probable thioredoxin TrxB1	1.68	42.38
Rv1557	Probable conserved transmembrane transport protein Mmpl6	1.30	20.93
Rv1767	Conserved protein	1.01	11.31
Rv1875	Conserved protein	1.27	19.15
Rv2466c	Conserved protein	2.05	75.11
Rv2745c	Transcriptional regulatory protein ClgR	1.10	25.97
Rv3061c	Probable acyl-CoA dehydrogenase FadE22	1.03	25.70
Rv3082c	Virulence-regulating transcriptional regulator VirS (AraC/XylS family)	1.72	19.37
Rv3172c	Hypothetical protein	1.19	16.34
Rv3173c	Probable transcriptional regulatory protein (probably TetR/AcrR-family)	1.81	86.13
Rv3174	Probable short-chain dehydrogenase/reductase	5.13	174.13
Rv3175	Possible amidase (aminohydrolase)	5.46	268.38
Rv3176c	Probable epoxide hydrolase MesT	3.41	135.52
Rv3177	Possible peroxidase (non-haem peroxidase)	6.17	232.22
Rv3178	Conserved hypothetical protein	7.27	38.04
Rv3312b	Conserved hypothetical protein	1.12	3.16
Rv3417c	60 kDa chaperonin 1 GroEL1 (protein CPN60-1) (GroEL protein 1)	1.12	50.40
Rv3463	Conserved protein	2.30	72.57
Rv3854c	Monooxygenase EthA	3.91	212.09
Rv3855	Transcriptional regulatory repressor protein (TetR-family) EthR	3.55	133.83
Rv3913	Probable thioredoxin reductase TrxB2 (TRXR) (TR)	1.03	23.30
Rv3914	Thioredoxin TrxC (TRX) (MPT46)	1.17	22.04

5 Results

Table S2: Significantly downregulated genes after 4h exposure of *Mtb* to S3 (20 μ M). Related to Figure 3.

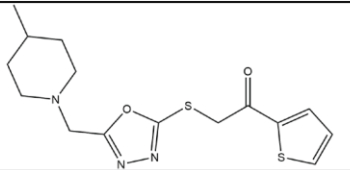
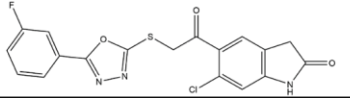
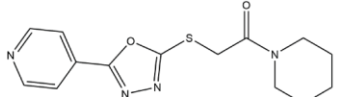
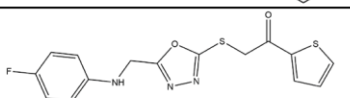
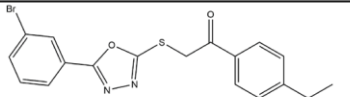
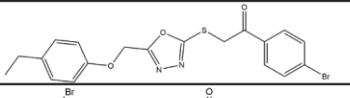
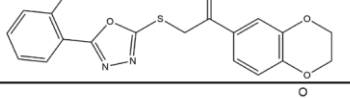
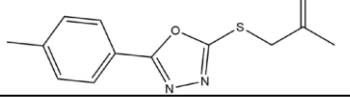
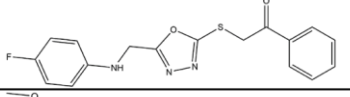
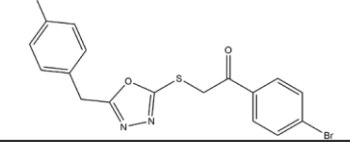
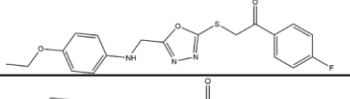
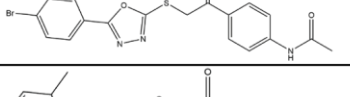
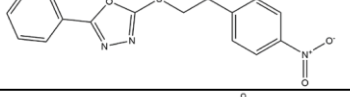
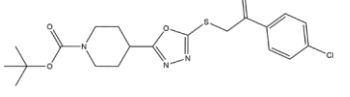
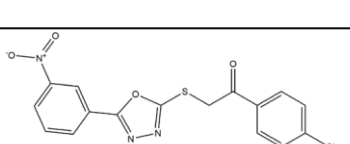
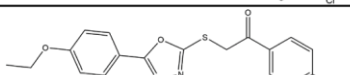
ID	Description	log2FC	-log(padj)
Rv0280	PPE family protein PPE3	-1.84	51.13
Rv2990c	Hypothetical protein	-1.44	39.82
Rv1387	PPE family protein PPE20	-1.18	37.46
Rv3371	Possible triacylglycerol synthase (diacylglycerol acyltransferase)	-1.33	22.67
Rv1386	PE family protein PE15	-1.17	20.10
Rv3727	Possible oxidoreductase	-1.27	18.18
Rv1815	Conserved protein	-1.14	14.01
Rv1816	Possible transcriptional regulatory protein	-1.03	10.39
Rv0106	Conserved hypothetical protein	-1.32	9.81
Rv0516c	Possible anti-anti-sigma factor	-1.67	6.04
Rv1799	Probable lipoprotein LppT	-1.04	4.90
Rv1040c	PE family protein PE8	-1.18	4.55
Rv0320	Possible conserved exported protein	-1.01	4.51
Rv1541c	Possible lipoprotein LprI	-1.17	3.59
Rv1552	Probable fumarate reductase [flavoprotein subunit] FrdA (fumarate dehydrogenase) (fumaric hydrogenase)	-1.04	1.74

5 Results

Supplement Table 3: S3 Analogues screening at 20 μ M. Analogues were tested for cytoprotection in fibroblast survival assays and ELISA-based testing for inhibition of ESX-1 activity (percent inhibition of EsxA secretion compared to control). Data were sorted by ESX-1 inhibitory efficacy. The most promising analogues S3_106 (orange) and S3_100 (yellow) and the reference compound S3 (blue) are highlighted.

ID	structure	Protection of MRC-5 lung fibroblasts [% survival]	ESX-1 attenuation [% inhibition]
S3_106		69	80
S3_100		115	80
S3_33		58	74
S3_87		34	71
S3_103		73	71
S3_16		20	68
S3_97		41	66
S3		102	66
S3_86		23	65
S3_102		23	63
S3_91		128	61
S3_85		21	60
S3_77		36	58
S3_104		51	55

5 Results

ID	structure	Protection of MRC-5 lung fibroblasts [% survival]	ESX-1 attenuation [% inhibition]
S3_40		30	53
S3_112		50	43
S3_88		66	38
S3_32		37	37
S3_110		23	20
S3_37		22	20
S3_54		41	19
S3_64		62	10
S3_2		22	0
S3_3		25	0
S3_24		23	0
S3_96		49	0
S3_1		-17	not tested
S3_4		15	not tested
S3_5		-3	not tested
S3_6		-4	not tested

5 Results

ID	structure	Protection of MRC-5 lung fibroblasts [% survival]	ESX-1 attenuation [% inhibition]
S3_7		-2	not tested
S3_8		-10	not tested
S3_9		8	not tested
S3_10		1	not tested
S3_11		-25	not tested
S3_12		-10	not tested
S3_13		-18	not tested
S3_14		-3	not tested
S3_15		13	not tested
S3_17		-6	not tested
S3_18		-3	not tested
S3_19		11	not tested
S3_20		30	not tested
S3_21		13	not tested
S3_22		-19	not tested

5 Results

ID	structure	Protection of MRC-5 lung fibroblasts [% survival]	ESX-1 attenuation [% inhibition]
S3_23		-13	not tested
S3_25		27	not tested
S3_26		-11	not tested
S3_27		20	not tested
S3_28		10	not tested
S3_29		-7	not tested
S3_30		5	not tested
S3_31		12	not tested
S3_34		-20	not tested
S3_35		9	not tested
S3_36		9	not tested
S3_38		-34	not tested
S3_39		-9	not tested
S3_41		-18	not tested
S3_42		-7	not tested
S3_43		48	not tested
S3_44		8	not tested

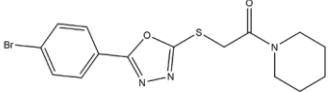
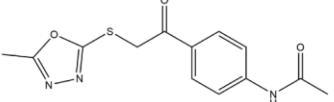
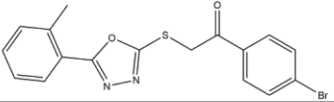
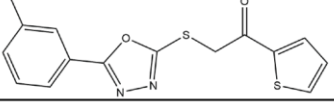
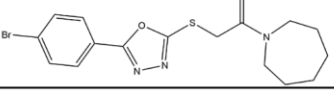
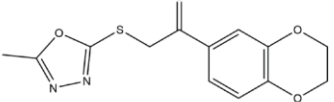
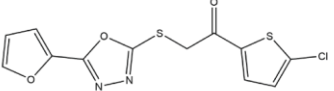
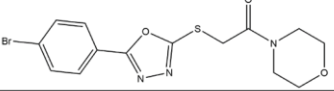
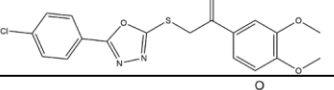
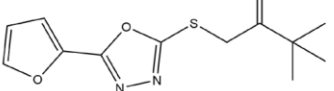
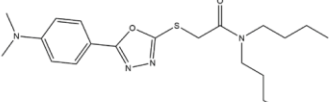
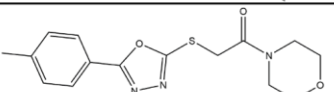
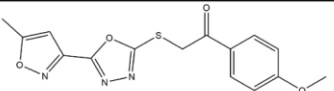
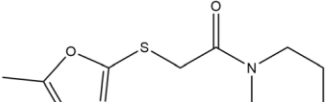
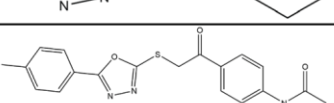
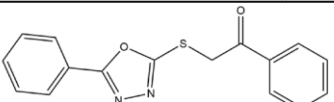
5 Results

ID	structure	Protection of MRC-5 lung fibroblasts [% survival]	ESX-1 attenuation [% inhibition]
S3_45		4	not tested
S3_46		59	not tested
S3_47		13	not tested
S3_48		18	not tested
S3_49		77	not tested
S3_50		3	not tested
S3_51		21	not tested
S3_52		-25	not tested
S3_53		5	not tested
S3_55		0	not tested
S3_56		66	not tested
S3_57		19	not tested
S3_58		9	not tested
S3_59		-7	not tested
S3_60		5	not tested
S3_61		10	not tested
S3_62		45	not tested

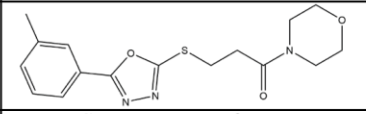
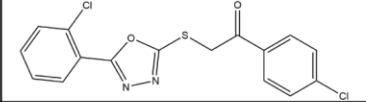
5 Results

ID	structure	Protection of MRC-5 lung fibroblasts [% survival]	ESX-1 attenuation [% inhibition]
S3_63		5	not tested
S3_65		-22	not tested
S3_66		15	not tested
S3_67		-8	not tested
S3_68		-19	not tested
S3_69		29	not tested
S3_70		-3	not tested
S3_71		117	not tested
S3_72		3	not tested
S3_73		-16	not tested
S3_74		-31	not tested
S3_75		-5	not tested
S3_76		-16	not tested
S3_78		8	not tested
S3_79		2	not tested
S3_80		0	not tested

5 Results

ID	structure	Protection of MRC-5 lung fibroblasts [% survival]	ESX-1 attenuation [% inhibition]
S3_81		14	not tested
S3_82		-7	not tested
S3_83		3	not tested
S3_84		14	not tested
S3_89		5	not tested
S3_90		-1	not tested
S3_92		3	not tested
S3_98		4	not tested
S3_99		0	not tested
S3_105		47	not tested
S3_107		40	not tested
S3_108		-5	not tested
S3_93		-14	not tested
S3_94		-14	not tested
S3_95		-3	not tested
S3_101		4	not tested

5 Results

ID	structure	Protection of MRC-5 lung fibroblasts [% survival]	ESX-1 attenuation [% inhibition]
S3_109		66	not tested
S3_111		49	not tested

6 Discussion

This cumulative work contributes to the ongoing battle between drug discovery and the emergence of drug-resistant *Mtb* by exploring traditional and novel approaches to identify potential novel lead compounds. Here, two different screening approaches, testing a total of 60,000 compounds, were described, yielding promising compounds with bioactive effects on *Mtb*. These include antibiotic compounds, targeting various potential pathways, such as a putative inhibitor of the L-tryptophan biosynthesis and also an interesting inhibitor of the respiratory chain. Additionally, compounds with promiscuous anti-virulence activity were identified, some of which have been classified as inhibitors of the ESX-1 secretion system. Furthermore, a series of compounds with a novel dual-activity were discovered, and their impact on *Mtb* host cell infection and *Mtb* functionality were further elaborated.

6.1 Screening for Small Molecules with Anti-mycobacterial Activity

Since the Nobel Prize-winning discovery of streptomycin, several other antibiotics for the treatment of *Mtb* have been discovered and combined into anti-TB regimens²⁵. Yet, the treatment regimen remains unwieldy as it consists of at least four antibiotics being administered over a long period of time. Even with the currently trialed shortened regimen, this treatment spans four months^{172,173}. Therefore, novel compounds are necessary to increase regimen compliance and patient well-being, improving treatment outcomes and avoiding the emergence of drug-resistant *Mtb*. To discover these compounds, novel, more unconventional screening approaches are required.

There are currently two primarily used screening approaches to identify antibiotics or other pharmaceutically active compounds: the bottom-up and the top-down strategy¹⁷⁴. The bottom-up, or target-directed, screening approach investigates test compounds for their activity against a specific, pre-determined, essential molecular target^{174,175}. This knowledge-driven screening can theoretically be used to identify compounds that target essential pathways that are so far unexplored. Unfortunately, up to date, this screening approach has been mostly unsuccessful for finding new compounds with activity against *Mtb*¹⁷⁶. This is attributed to the fact, that extremely promising hit compounds fail to reach their target inside of the mycobacterial cell or are metabolized inside the cell into an inactive form¹⁷⁶.

In contrast, the top-down, or drug-to-target, screening approach screens a great abundance of small molecules or natural products using scalable, phenotypic screening platforms that can

distinguish between unremarkable and bioactive, potential hit compounds. Following initial and confirmatory screenings, the next step is to identify the mode of action of these hits¹⁷⁷. One way of doing this is by evaluating resistance-conveying SNPs as it is described in this work. The advantages of this approach are the potential high-throughput, lower cost and, most importantly, the significantly higher possibilities for finding a novel mode of action^{177,178}. As shown in project II of this thesis, the experimental setup routinely used for top-down anti-tuberculous screening (REMA) can easily be adjusted to identify compounds of interest with alternative anti-*Mtb* activity. The complementary application utilizing another phenotypic whole cell-based assay (FSA) even allowed the expansion of hit compounds to identify promising anti-virulence compounds. Thus, the top-down approach in this thesis yielded interesting molecular targets that would not have been discovered by the bottom-up approach.

The screening attempts focusing on antibiotic activity of both screening projects described in this thesis resulted in roughly the same hit rate (project I: 0.022% vs project II: 0.020%). Combined, the investigation of 60,000 small molecules yielded 13 compounds that inhibited *Mtb* growth in broth, were not cytotoxic in MRC-5 human lung fibroblasts and also protected these eukaryotic cells during infection from mycobacteria-induced cell death. This hit rate is significantly lower, when compared with similar screening attempts of phenotypic screenings of small molecule libraries against *Mtb* which are reported to range between 0.1% and 1.8%¹⁷⁹⁻¹⁸². It is important to note here that the above-cited screening approaches usually report initial screening hits, describing activity against *Mtb* in broth. Unfortunately, this also includes compounds that are generally cytotoxic or even membranolytic¹⁸³. Based on the combination of complementary screening assay testing the compounds in a host cell-associated infection model, the screening approach described in this thesis is more restrictive against these unfavorable compounds¹³². Hence, we report a lower hit rate which already excludes a high number of cytotoxic substances. Interestingly, the SPECS world diversity set 3 library (screening project II) was recently also screened for antibiotic compounds against *Salmonella enterica* subsp. *enterica* ser. Typhimurium (ST) and *Mycobacterium abscessus* (*Mabs*)^{184,185}. Initial screening attempts against both organisms also report comparably low hit rates (ST: 0.01%; *Mabs*: 0.07%). In addition, the alternative approach utilized in project II also allowed the identification of more bioactive compounds. These 43 compounds proposedly could be active in a host cell-directed manner or could directly abrogate the infection capabilities of *Mtb*. Thus, this screening concept already opened up a pool of compounds which would have been immediately excluded in a common top-down screening platform focusing solely on antibiotic activity.

6.2 Hit Compounds with Growth Inhibitory Activity against *Mtb*

Despite the existence of several promising drug candidates in today's drug pipeline, the emerging drug-resistant *Mtb* strains call for the discovery of novel structures. In addition, there is a high attrition rate during clinical studies and also already rapidly emerging resistance to recently approved drugs¹⁸⁶. Optimizing the efficacy and patient tolerance of already existing drugs cannot solve all issues in the battle against *Mtb*, as prevalent resistance-conveying SNPs, e.g. mutations in *gyrA* or *gyrB* (fluoroquinolones¹⁸⁷), in *rpoB* (rifamycins¹⁸⁸) or in genes encoding prodrug activation (*katG*, *ethA*^{189,190}) still contribute to a significant loss of sensitivity against the whole respective class of drugs¹⁹¹. The current anti-*Mtb* drug pipeline for clinical phase I and II studies mostly includes compounds with a limited variety of modes of action, such as inhibitors of cell wall synthesis (DprE1, MmpL3), inhibitors of the ATP synthesis, translational or transcriptional inhibitors (Table 1). Therefore, it is important to continue and even extend existing screening attempts to find novel structures or scaffolds.

After the initial screening described in this thesis, the next step was to determine whether the investigated compounds exhibit a novel mode of action. For target identification, we employed an approach that identifies putative molecular targets by leveraging evolutionary pressure resulting from the antibiotic effect of the test compounds. The genome of *Mtb* strains which show resistance to the test compound is sequenced and is analyzed for SNPs. These SNPs then indicate potential molecular targets. While generating resistant mutants, it became evident that this method cannot be universally applied to every test compound. This approach is suitable only for molecules that exhibit reasonable stability at 37 °C for several weeks, given that the generation of *Mtb* mutants is a time-consuming process. The three compounds, B3, B4 and B10 did not meet this requirement and were excluded from this study due to thermal instability rendering them unsuitable for further drug discovery purposes¹⁹². Exposure of these compounds to 37°C for up to four weeks drastically reduced their anti-tuberculous efficacy. While stability is crucial for ensuring reproducible *in vitro* experiments and robust data, it becomes absolutely essential for *in vivo* experimentation. Therefore, the structures and potential scaffolds of B3, B4 and B10 were not further investigated in this study.

Furthermore, the potential molecular targets of compounds B1, B2 and B8 remained unidentified, as colonies of mutants carrying a resistance-conveying SNPs could not outcompete the wild type. This suggests a potentially bacteriostatic mode of action of the compounds, which was observed for LPZS, a bacteriostatic antibiotic used as a control during these experiments⁴⁷. In theory, target identification for all of the aforementioned compounds

(B1, B2, B3, B4, B8 and B10) could still be possible using this method to generate resistant mutants. This necessitates meticulous monitoring of agar plates during the initial step of generating mutants resistant to the respective test compound. It also requires the isolation and testing of numerous colonies to identify a resistant strain among a larger population of wild-type strains. To make this extended effort feasible, a significant reduction in the number of cells per agar plate is essential. However, this reduction will lead to a substantial increase in the number of required agar plates, resulting in a significant rise in the consumption of expensive and rare test compounds.

In the end, this approach to identify putative molecular targets showed promising results for the remaining compounds: B5, B6, B7, B9, S7 and S32. Exposure to these compounds revealed resistance-conveying mutations in the genes *trpA* or *trpB*, *qcrB*, *katG*, *dprE1*, *mmpL3* and *ethA*, respectively. This approach is based on the hypothesis that detectable genetic modifications provide an evolutionary advantage against the activity of the test compounds. For example, such modifications may change the conformation of an essential protein, rendering it no longer susceptible to inhibition by the antibiotic. It is important to note here that this is feasible because *Mtb* exhibits a relatively low mutation frequency in its genome and does not engage in horizontal gene transfer, as is common in other bacteria¹⁹³. This allows a direct association between SNPs and potential molecular target as long, as the SNP is located in an essential gene.

Accordingly, the proteins encoded by the putative target genes identified for B7 and S32, KatG and EthA, respectively, are unlikely to be the molecular interaction partners of these compounds. Both SNP-containing genes encode non-essential monooxygenases known to be involved in prodrug activation. It is highly unlikely that these genes are involved in the molecular mode of action and were thus not further investigated. Nevertheless, this method, based on the generation of spontaneous mutations, could still be used to identify SNPs representing the mode of action of B7 or S32. To do so, the activated derivative of the respective prodrug needs to be identified. This can be achieved by mass spectrometric analysis of the metabolome of *Mtb* exposed to sub-inhibitory concentrations of the test compound. In this manner, mycobacteria will perform the bioconversion without the active form of the compound leading to mycobacterial cell death. After identifying the active form of the compound, it must be extracted and purified *in vitro*. However, this is a time-consuming process and requires highly specialized expertise in metabolomics, bioanalytics and biochemistry. In the end, the isolation of the bioconverted molecule is only possible and feasible under the assumption that the respective activated product is suitably stable to be isolated.

For the compounds B5, B6, B9 and S7 it was possible to identify SNPs in essential genes. These SNPs indicated potential molecular modes of actions involved in either L-tryptophan biosynthesis (B5), the respiratory chain (B6), or the cell wall synthesis (B9 and S7). Both targets related to cell wall synthesis, DprE1 (B9) and MmpL3 (S7), are already known and widely recognized antimycobacterial targets⁸². DprE1 is responsible for the synthesis of the critical arabinose precursor necessary for the formation of arabinogalactans and lipoarabinomannans⁸². Although this target appears to be promising, with two BTZ-derived compounds currently under investigation in clinical trials, it has also been frequently encountered in several screening attempts. Between 2009 and 2022, more than 1500 DprE1 inhibitors have been reported in literature, representing at least 23 diverse scaffolds¹⁹⁴. Therefore, this compound was not further investigated in this study. MmpL3, the second potential target identified, which is associated with cell wall biosynthesis, presents a similar scenario. This protein complex exhibits quite promiscuous properties as an anti-tuberculous target. As an RND exporter, it is responsible for transporting trehalose monomycolates to the periplasm. On the other hand, inhibition of this transmembrane protein complex reportedly also affects the transmembrane proton motive force⁸⁵. Nonetheless, this molecular target has already been identified in various screenings, and inhibitors disrupting MmpL3 activity are widely reported as well^{82,86,195-197}. Given the wide variety of currently investigated MmpL3 inhibitors, including SQ109, which is currently being tested in clinical phase II studies, we did not further research S7 as anti-tuberculous compound.

The remaining two small molecules, B5 and B6, on the other hand were of great interest in this thesis. As a putative inhibitor of the amino acid biosynthesis of L-tryptophan, B5 represents a promising candidate molecule for a lead compound. The disruption of an essential protein complex which is not essential for mammals provides an excellent drug target as it is highly conceivable to show no adverse effect on the patient, even if administered in potentially high doses. B5 was shown to inhibit mycobacterial growth in broth, protect MRC-5 human lung fibroblasts during infection and also reduce intracellular growth of *Mtb* after infection. Furthermore, WGS of *Mtb* mutant strains resistant to B5 identified two separate SNPs, either located in TrpA (P65T) or TrpB (P321L). This target could then be validated by initial biological data. During a rescue experiment, in which L-tryptophan, the final product of the potential target, was added, a complete reversal of activity of the test compound was observable. This effect was measured even at 100 times the MIC of B5. In addition, mutations in either TrpA or TrpB are also known to confer resistance against other inhibitors of the L-tryptophan biosynthesis in *Mtb*, including sulfolanes, indoline-5-sulfonamides as well as BRD4592¹⁹⁸⁻²⁰⁰.

6 Discussion

These mutations are reported for TrpA as P65Q, G66V, Y108C, D136V and for TrpB as I184S, N185S, F188L, P208L, F293C²⁰⁰. Notably, these SNPs are not directly located in the active center of the TrpA/B holoenzyme²⁰⁰. Furthermore, the TrpA/B protein complex is known to be heavily allosterically regulated²⁰¹⁻²⁰⁴. The SNP detected in TrpA (P65T), which led to resistance against B5, is also located at amino acid position 65. In both cases, P65Q and P65T, the native non-polar proline is exchanged with a polar amino acid (glutamine or threonine), likely resulting in the same configurational changes for the $\alpha\beta\beta\alpha$ heterotetramer. On the other hand, the SNP detected in TrpB (P321L) for B5-resistant mutants has not yet been reported, making this resistance-conveying SNP unique for B5. It is important to note that the proline at position 321 is structurally closely located to the phenylalanine at position 293²⁰⁵. The locations of the resistance-conveying SNPs found in mutants resistant to B5 suggest, therefore, an allosteric inhibition of trpA/B by B5. In order to verify a potential binding of B5 to TrpA/B, crystallography or, at the very least, small molecule-protein interaction studies, such as thermal shift assays (TSA) or electrophoretic mobility shift assay (EMSA), are required.

The final compound with antibiotic activity investigated in this thesis is B6. In addition to its anti-tuberculous activity in broth and its cytoprotective effect during infection of fibroblasts, this small molecule significantly reduced the intracellular ATP levels of *Mtb*. This combined effect, along with the identification of a SNP in *qcrB* as resistance-conveying mutation against this compound, strongly suggests the respiratory chain as putative target of B6. Further investigation into the upregulation of the compensatory terminal oxidase cytochrome *bd* caused by B6 solidified this hypothesis. Interestingly, testing for cross-resistance in strains harboring SNPs that are well-described in the literature to convey resistance against alternative respiratory chain inhibitors, revealed that the T313A QcrB mutant exhibited hypersensitivity to B6^{60,206}. This increased sensitivity opens up a novel avenue for the combined application of B6 with the current frontrunner drug, Q203. This combination could potentially exploit the most commonly occurring Q203 resistance-conveying mutation (T313A), reducing the risk of developing a resistant strain. Furthermore, the creation of a resistant strain against B6 was only possible in a knock-out strain that lacks the alternative oxidase cytochrome *bd*. To fully understand this relationship, additional research on B6, especially on its interaction with QcrB, is required. It still remains unclear why the mutation frequency for resistance against B6 is so low. One way to further evaluate combinatory uses of B6 with Q203 would be to test antibiotic synergy in wild type, Q203 resistant strains and clinical isolates. Additionally, creating an interaction model of B6 and Q203 with QcrB would provide further clarity. For this, a crystal structure of QcrB combined with B6 would be indispensable.

In summary, the compounds with potential antibiotic activity identified in this thesis align with the general trend observable in the current global drug pipeline, to which researchers worldwide are contributing (Table 2). Consequently, the screening platforms utilized in this thesis have yielded similar results when compared to screening efforts around conducted worldwide. This may be attributed to the fact that most top-down screenings for anti-*Mtb* drugs employ similar strains, experimental setups and conditions. For instance, the majority of screenings attempts involve the use of *Mtb* lab strains such as H37Rv or Erdman, rather than clinical isolates. This is primarily due to the significantly higher health risk posed by clinical isolates to researchers and their suboptimal adaptation to laboratory conditions, resulting in slower and less reliable growth, which complicates hit assessment. Additionally, following the initial screening, only hits displaying high activity at low concentrations are selected for further testing. This selection is deemed necessary to narrow down the pool of hit compounds to the most ‘promising’ candidates. It can be argued that this pre-selection may favor certain same molecular targets repeatedly. Furthermore, the early testing in infection-based models described here, utilizing MRC-5 human lung fibroblasts, THP-1- or PBMC-derived macrophages, takes into account applicability in host cell-associated applications and thus allows for the early exclusion of cytotoxicity and potentially other adverse effects of test compounds. Throughout this study, two compounds with diverse modes of action, namely B5 and B6, have been identified. While B5 appears to inhibit the L-tryptophan biosynthesis, a promising and essential metabolic pathway absent in humans, B6 inhibits QcrB, the terminal oxidase of the mycobacterial respiratory chain.

6.3 Hit Compounds with Potential Anti-virulence Activity against *Mtb*

In light of the current prevalence of (multi)-drug resistant bacterial strains, it is imperative to find alternative approaches to conventional antibiotics. Therefore, investigation of compounds with potential anti-virulence activity is of crucial importance. Anti-virulence activity is loosely defined as specifically targeting the pathogenic virulence factors to hinder its ability to successfully infect the respective host cell. This indirectly benefits the infected organism by reducing the bacterial load and potentially enhancing pathogen clearance. Because anti-virulence compounds should not directly kill or inhibit the growth of the bacteria, these compounds proposedly result in less selective pressure for resistance compared to antibioticly active drugs. This approach has not only been investigated for *Mtb* but also for other bacterial pathogens such as multidrug resistant ESKAPE pathogens (*Enterococcus faecium*, *Staphylococcus aureus*, *Klebsiella pneumoniae*, *Acinetobacter baumannii*, *Pseudomonas*

6 Discussion

aeruginosa and *Enterobacter* species) ^{119,207}. Recent anti-virulence studies suggest a diverse array of leverage points to disrupt pathogenic virulence. These include targeting bacterial communication, inhibiting biofilm formation/adherence, and disrupting the secretion of virulence factors ^{119,208}. This also opens up the potential use of anti-virulence compounds as adjunctive therapy in combination with existing antibiotics to hopefully reduce the exerted pressure for resistance ¹⁰⁵. Since pathogenic bacteria depend on the secretion of various virulence factors, targeting secretion systems offers numerous targets that can be exploited by anti-virulence agents ^{82,132,170,184,209}. This is especially true for *Mtb*, as the major virulence factors are either membrane-bound or secreted, with the ESX-1-facilitated secretory proteins EsxA/B being the most important ones ^{82,120,133,134,136}.

The initial dual-screening of the SPECS world diversity set 3 molecule library (screening project II) yielded 43 potential anti-virulence compounds. All of these small molecules show cytoprotective activity during infection of MRC-5 human lung fibroblasts with *Mtb*, while simultaneously not showing any growth inhibitory effects on *Mtb* in broth. Out of these compounds, ten were selected based on the novelty of their structure and commercial availability. Further investigation of antimycobacterial activity of these molecules revealed that nearly a third (S1, S3 and S10) of the test compounds inhibited the ESX-1 secretion system. This again confirms the ability of the utilized dual-screening to identify anti-virulence compounds that inhibit the ESX-1 secretion system, as previously shown for the identification of BTP15 and BBH7 ¹³². These two inhibitors of ESX-1 were discovered in a similar screening approach resulting in distinguishable molecular targets. BTP15 shows activity as kinase inhibitor that potentially deregulates the *espACD* operon to inhibit ESX-1 activity. BBH7, on the other hand, was described to show pleiotropic activity on *Mtb* secretory systems, indicating a more general mode of action involved in cell wall biogenesis and potentially in dysregulation of the intracellular ATP pool. These examples show different possible modes of action ESX-1 inhibitors. Other anti-virulence compounds identified in this thesis, which did not inhibit EsxA secretion, might still be involved in inhibition of other virulence factors, such as MptpB, SapM or Zmp1 ^{105,129-131}. In addition, host cell-directed activity of these cytoprotective compounds cannot be completely ruled out, as these properties are not distinguishable by the FSA alone and require further experimentation ¹⁰⁶. Of the three compounds identified in this thesis that show abrogation of EsxA secretion, S1, S3 and S10, two compounds share a similar core structure. Both S3 and S10 contain a 1,3,4-oxadiazole core combined with a sulfanyl-ethanone. Since S3 showed the best overall activity, it was selected for further investigation as a representative of the above-mentioned scaffolds.

6 Discussion

After a thorough characterization of S3, it was confirmed that it provides dose-dependent cytoprotection to host cells during *Mtb* infection of MRC-5 human lung fibroblasts and PBMC-derived macrophages. Furthermore, exposure to S3 resulted in significant reduction of intracellular mycobacterial growth as well as decreased release of the pro-inflammatory cytokine IL-1 β by infected PBMC-derived macrophages. Secreted EsxA is described as being centrally involved in phagosomal escape, which is essential for *Mtb* to avoid clearance by the host and to allow mycobacterial propagation inside the host cell¹⁷. It was recently shown that macrophages infected by *Mtb* release IL-1 β while they are undergoing a highly pro-inflammatory type of necrosis, called pyroptosis²². This only occurs if the infecting pathogen is not efficiently cleared by the host cell, as it is the case for *Mtb* since it is able to escape the phagosome utilizing ESX-1. Both the reduction of intracellular growth and the reduced IL-1 β secretion therefore confirm the anti-virulence activity of S3 and its inhibition of the ESX-1 secretion system²¹⁰.

Identification of the mode of action of S3 in regard to ESX-1 inhibition was attempted by performing RNA-Seq of *Mtb* cultures exposed to S3 in comparison to untreated cultures. This transcriptomic analysis did not reveal any ESX-1 component (EccA, EccB, EccC, EccD or EccE) or ESX-1 substrate (EsxA, EsxB or Esp proteins), nor any known regulator of ESX-1 (*phoP*, *espR*, *mprA* or *lsr2*) to be significantly up or downregulated. Therefore, RNA-Seq analysis did not show any anticipated differential expression patterns and could not pinpoint the ESX-1-associated mode of action of S3. Surprisingly, the RNA-Seq data revealed a specific second activity of S3: exposure to this compound led to significant upregulation of *ethA*, which encodes a monooxygenase known for its involvement in the prodrug activation of ethionamide^{83,190}. Upregulation of *ethA* initially suggested a potential link of EthA activity to ESX-1 or a potential prodrug activation of S3^{83,211}. This thesis demonstrated that the connection between *ethA* upregulation and ESX-1 activity is uncoupled, as neither chemical nor biological upregulation of *ethA* by itself significantly affected ESX-1 activity. Moreover, *Mtb* mutant strain lacking functional EthA did not exhibit reduced S3-mediated cytoprotection during host cell infection. This also contradicts the possibility of S3 being a prodrug that needs prior activation by EthA to achieve its activity. Combinatory studies of S3 together with ethionamide revealed a booster activity of S3, increasing the efficacy of ethionamide, which was confirmed by target-specific translational experiments (qRT-PCR) showing a dose-dependent upregulation of *ethA* in the presence of S3. TSA and EMSA experiments focusing on small molecule-protein interactions revealed EthR, the regulatory protein of *ethA*, to be a molecular binding partner of S3. Inhibition of this negative regulator of *ethA* expression explains the

upregulation of *ethA*. For the next step, to verify and to describe this interaction in more detail, crystal structures are required. A molecule-protein interaction has already been shown for other small molecules by preparing EthR crystals via the vapor diffusion method, which were then exposed to the test compounds^{212,213}. The following X-ray diffraction analysis yielded the necessary structural data to model the small molecule-protein interaction to EthR^{212,213}. While the booster ability has been demonstrated for other compounds like BDM41906²¹⁴, SMART-420⁸⁴ and SMART-751²¹⁵, the combination of ethionamide boosting and ESX-1 secretion inhibition, as described here, is a novel finding. The duality of activity caused by S3 potentially opens new avenues of treatment for tuberculosis. While still providing an anti-virulent approach to combat *Mtb* by inhibiting ESX-1, the combination with the ability to booster the efficacy of an already established anti-*Mtb* drug, such as ethionamide, might provide significantly increased treatment outcome. In addition, S3 could also be utilized in ethionamide-resistant *Mtb* strains, as was recently shown *in vitro* and *in vivo* for other ethionamide boosters^{84,215}.

Hit compounds of top-down screenings often lack certain optimization to be directly used in a patient, requiring further drug development. One way of finding better suited derivatives is to perform a structure activity relationship study (SARS), in which various structural analogues of the original hit are tested. For this, 112 commercially available small molecules containing the 1,3,4-oxadiazol core combined with the sulfanyl-ethanone connection were selected and screened for anti-virulence properties, cytoprotection of infected host cells, but no growth inhibition of *Mtb* in broth. Positive hits were then tested in a newly established, ELISA-based experimental setup in order to identify inhibition of ESX-1. The SARS resulted in two slightly more active compounds, S3_100 and S3_106. These close analogues of S3 only differ slightly on either side of the above-described structural core. Nonetheless, investigation of ethionamide booster activity yielded a distinct profile for each of the three ESX-1 inhibitors. Although S3_100 exhibited ethionamide booster activity, further investigation using targeted qRT-PCR and biological assays involving an EthA-deficient *Mtb* strain revealed that this effect was attributed to another monooxygenase. The upregulated gene *mymA* encodes the monooxygenase MymA, which is an alternative enzyme utilized in the prodrug activation of ethionamide⁸³. In contrast, the final analogue, S3_106, did not exhibit any ethionamide booster.

Unfortunately, this thesis did not unveil the mode of action by which S3, S3_100 or S3_106 inhibit ESX-1. To further elucidate this molecular interaction, the next step could involve a comparative RNA Seq analysis of *Mtb* exposed to either S3 or S3_106. In addition to the upregulation of *ethA*, exposure to S3 also led to differential regulation of multiple

oxidoreductases, hydrolases and other proteins involved in the clearing of xenobiotics. Therefore, it is conceivable that transcriptional changes caused by exposure to S3_106, which in contrast to S3 has not been attributed a secondary effect, might provide a clearer picture. Reducing the transcriptional footprint may potentially reveal differentially regulated genes associated with ESX 1 that were less distinguishable following exposure to S3. An alternative approach to identify potential proteins or genes that interact with S3 and result in ESX-1 inhibition could involve affinity-based pulldown. In this experimental setup, the compound is used as a molecular probe to capture proteins or nucleic acids from *Mtb* cell lysates. The compound is immobilized on a solid support, such as a (magnetic) bead, which is then exposed to *Mtb* lysates²¹⁶. The beads are subsequently washed and the interaction partner is eluted by a pH shift. Subsequently, the eluates can be subjected to mass spectrometry analysis to identify the respective interaction partners²¹⁶. As a prerequisite, this assumes that the potential target directly interacts with the test compound and is not denatured in the preceding lysis process, which remains to be determined.

Overall, the research conducted in this thesis on compounds with anti-virulence activity has yielded three promising ESX-1 inhibitors: S3, S3_100 and S3_106. All three small molecules show potential for further investigation as anti-*Mtb* drugs. This may entail further optimization of specific physiochemical properties, such as stability and solubility, through directed medical chemistry methods²¹⁷. The next crucial step in this process will involve *in vivo* pharmacokinetics to initiate the characterization of these compounds with respect to their ADME (absorption, distribution, metabolism and excretion) properties.

6.4 Concluding Remarks

This thesis contributes to the ongoing global battle against *Mtb* by screening, identifying and characterizing novel compounds with anti-mycobacterial activity. The application of a complementary screening setup, which combines examination of growth inhibitory effects and cytoprotection of infected host cells, has revealed several interesting compounds with diverse structures and putative molecular modes of actions. This includes a more detailed investigation of two compounds with antibiotic activity and one compound with anti-virulence activity, for which the putative molecular targets were successfully identified. The described antibiotic targets, while not unique, represent interesting starting points for further optimization. In particular, the potential application of B6 in combination with the well-developed antibiotic drug Q203 lays the foundation for extensive combinatorial testing. Additionally, with S3 and its

6 Discussion

two analogues (S3_100 and S3_106), a structural scaffold could be identified with an interesting ESX-1 inhibitory property. Furthermore, simple structural modifications to this scaffold led to a second effect with great application potential: the boosting of the clinically relevant antibiotic drug ethionamide. The combination of both effects has not yet been described for an anti-mycobacterial compound and could thus provide a significant advancement in dealing with drug-resistant *Mtb*.

7 Literature

1. Bussi, C., and Gutierrez, M.G. (2019). Mycobacterium tuberculosis infection of host cells in space and time. *FEMS Microbiol Rev* 43, 341-361. 10.1093/femsre/fuz006.
2. Lee, J.Y. (2015). Diagnosis and treatment of extrapulmonary tuberculosis. *Tuberc Respir Dis (Seoul)* 78, 47-55. 10.4046/trd.2015.78.2.47.
3. WHO, W.H.O. (2022). Global tuberculosis report.
4. Murray, J.F., Rieder, H.L., and Finley-Croswhite, A. (2016). The King's Evil and the Royal Touch: the medical history of scrofula. *Int J Tuberc Lung Dis* 20, 713-716. 10.5588/ijtld.16.0229.
5. Barberis, I., Bragazzi, N.L., Galluzzo, L., and Martini, M. (2017). The history of tuberculosis: from the first historical records to the isolation of Koch's bacillus. *J Prev Med Hyg* 58, E9-E12.
6. Daniel, T.M. (2006). The history of tuberculosis. *Respir Med* 100, 1862-1870. 10.1016/j.rmed.2006.08.006.
7. Jay, S.J., Kirbiyik, U., Woods, J.R., Steele, G.A., Hoyt, G.R., Schwengber, R.B., and Gupta, P. (2018). Modern theory of tuberculosis: culturomic analysis of its historical origin in Europe and North America. *Int J Tuberc Lung Dis* 22, 1249-1257. 10.5588/ijtld.18.0239.
8. Gradmann, C. (2001). Robert Koch and the pressures of scientific research: tuberculosis and tuberculin. *Med Hist* 45, 1-32. 10.1017/s0025727300000028.
9. Cambau, E., and Drancourt, M. (2014). Steps towards the discovery of Mycobacterium tuberculosis by Robert Koch, 1882. *Clin Microbiol Infect* 20, 196-201. 10.1111/1469-0691.12555.
10. Smith, N.H., Kremer, K., Inwald, J., Dale, J., Driscoll, J.R., Gordon, S.V., van Soolingen, D., Hewinson, R.G., and Smith, J.M. (2006). Ecotypes of the Mycobacterium tuberculosis complex. *J Theor Biol* 239, 220-225. 10.1016/j.jtbi.2005.08.036.
11. Comas, I., Coscolla, M., Luo, T., Borrell, S., Holt, K.E., Kato-Maeda, M., Parkhill, J., Malla, B., Berg, S., Thwaites, G., et al. (2013). Out-of-Africa migration and Neolithic coexpansion of Mycobacterium tuberculosis with modern humans. *Nat Genet* 45, 1176-1182. 10.1038/ng.2744.
12. Cole, S.T., Brosch, R., Parkhill, J., Garnier, T., Churcher, C., Harris, D., Gordon, S.V., Eiglmeier, K., Gas, S., Barry, C.E., 3rd, et al. (1998). Deciphering the biology of Mycobacterium tuberculosis from the complete genome sequence. *Nature* 393, 537-544. 10.1038/31159.
13. Hartmans, S., de Bont, J.A.M., and Stackebrandt, E. (2006). The Genus Mycobacterium--Nonmedical. In *The Prokaryotes: Volume 3: Archaea. Bacteria: Firmicutes, Actinomycetes*, M. Dworkin, S. Falkow, E. Rosenberg, K.-H. Schleifer, and E. Stackebrandt, eds. (Springer New York), pp. 889-918. 10.1007/0-387-30743-5_33.
14. Baulard, A.R., Besra, G.S., and Brennan, P.J. (1999). The Cell-Wall Core of Mycobacterium: Structure, Biogenesis and Genetics. In *Mycobacteria*, pp. 240-259. <https://doi.org/10.1002/9781444311433.ch13>.
15. Hirayama, D., Iida, T., and Nakase, H. (2017). The Phagocytic Function of Macrophage-Enforcing Innate Immunity and Tissue Homeostasis. *Int J Mol Sci* 19. 10.3390/ijms19010092.
16. Kinchen, J.M., and Ravichandran, K.S. (2008). Phagosome maturation: going through the acid test. *Nat Rev Mol Cell Biol* 9, 781-795. 10.1038/nrm2515.
17. Bao, Y., Wang, L., and Sun, J. (2021). A Small Protein but with Diverse Roles: A Review of EsxA in Mycobacterium-Host Interaction. *Cells* 10. 10.3390/cells10071645.

18. Mitchell, G., Chen, C., and Portnoy, D.A. (2016). Strategies Used by Bacteria to Grow in Macrophages. *Microbiol Spectr* 4. 10.1128/microbiolspec.MCHD-0012-2015.
19. Bo, H., Moure, U.A.E., Yang, Y., Pan, J., Li, L., Wang, M., Ke, X., and Cui, H. (2023). Mycobacterium tuberculosis-macrophage interaction: Molecular updates. *Front Cell Infect Microbiol* 13, 1062963. 10.3389/fcimb.2023.1062963.
20. Conrad, M., Angeli, J.P., Vandenabeele, P., and Stockwell, B.R. (2016). Regulated necrosis: disease relevance and therapeutic opportunities. *Nat Rev Drug Discov* 15, 348-366. 10.1038/nrd.2015.6.
21. Abe, J., and Morrell, C. (2016). Pyroptosis as a Regulated Form of Necrosis: PI+/Annexin V-/High Caspase 1/Low Caspase 9 Activity in Cells = Pyroptosis? *Circ Res* 118, 1457-1460. 10.1161/CIRCRESAHA.116.308699.
22. Theobald, S.J., Grab, J., Fritsch, M., Suarez, I., Eisfeld, H.S., Winter, S., Koch, M., Holscher, C., Pasparakis, M., Kashkar, H., and Rybniker, J. (2021). Gasdermin D mediates host cell death but not interleukin-1beta secretion in Mycobacterium tuberculosis-infected macrophages. *Cell Death Discov* 7, 327. 10.1038/s41420-021-00716-5.
23. Stockwell, B.R., Friedmann Angeli, J.P., Bayir, H., Bush, A.I., Conrad, M., Dixon, S.J., Fulda, S., Gascon, S., Hatzios, S.K., Kagan, V.E., et al. (2017). Ferroptosis: A Regulated Cell Death Nexus Linking Metabolism, Redox Biology, and Disease. *Cell* 171, 273-285. 10.1016/j.cell.2017.09.021.
24. Nahid, P., Dorman, S.E., Alipanah, N., Barry, P.M., Brozek, J.L., Cattamanchi, A., Chaisson, L.H., Chaisson, R.E., Daley, C.L., Grzemska, M., et al. (2016). Executive Summary: Official American Thoracic Society/Centers for Disease Control and Prevention/Infectious Diseases Society of America Clinical Practice Guidelines: Treatment of Drug-Susceptible Tuberculosis. *Clin Infect Dis* 63, 853-867. 10.1093/cid/ciw566.
25. Dartois, V.A., and Rubin, E.J. (2022). Anti-tuberculosis treatment strategies and drug development: challenges and priorities. *Nat Rev Microbiol* 20, 685-701. 10.1038/s41579-022-00731-y.
26. Seung, K.J., Keshavjee, S., and Rich, M.L. (2015). Multidrug-Resistant Tuberculosis and Extensively Drug-Resistant Tuberculosis. *Cold Spring Harb Perspect Med* 5, a017863. 10.1101/cshperspect.a017863.
27. Vanino, E., Granozzi, B., Akkerman, O.W., Munoz-Torrico, M., Palmieri, F., Seaworth, B., Tiberi, S., and Tadolini, M. (2023). Update of drug-resistant tuberculosis treatment guidelines: A turning point. *Int J Infect Dis* 130 Suppl 1, S12-S15. 10.1016/j.ijid.2023.03.013.
28. Prasad, R., Singh, A., and Gupta, N. (2019). Adverse drug reactions in tuberculosis and management. *Indian J Tuberc* 66, 520-532. 10.1016/j.ijtb.2019.11.005.
29. Shee, S., Singh, S., Tripathi, A., Thakur, C., Kumar, T.A., Das, M., Yadav, V., Kohli, S., Rajmani, R.S., Chandra, N., et al. (2022). Moxifloxacin-Mediated Killing of Mycobacterium tuberculosis Involves Respiratory Downshift, Reductive Stress, and Accumulation of Reactive Oxygen Species. *Antimicrob Agents Chemother* 66, e0059222. 10.1128/aac.00592-22.
30. Campbell, E.A., Korzheva, N., Mustaev, A., Murakami, K., Nair, S., Goldfarb, A., and Darst, S.A. (2001). Structural mechanism for rifampicin inhibition of bacterial rna polymerase. *Cell* 104, 901-912. 10.1016/s0092-8674(01)00286-0.
31. Campbell, E.A., Pavlova, O., Zenkin, N., Leon, F., Irschik, H., Jansen, R., Severinov, K., and Darst, S.A. (2005). Structural, functional, and genetic analysis of sorangicin inhibition of bacterial RNA polymerase. *EMBO J* 24, 674-682. 10.1038/sj.emboj.7600499.

32. Mukhopadhyay, J., Das, K., Ismail, S., Koppstein, D., Jang, M., Hudson, B., Sarafianos, S., Tuske, S., Patel, J., Jansen, R., et al. (2008). The RNA polymerase "switch region" is a target for inhibitors. *Cell* *135*, 295-307. 10.1016/j.cell.2008.09.033.
33. Temiakov, D., Zenkin, N., Vassilyeva, M.N., Perederina, A., Tahirov, T.H., Kashkina, E., Savkina, M., Zorov, S., Nikiforov, V., Igarashi, N., et al. (2005). Structural basis of transcription inhibition by antibiotic streptolydigin. *Mol Cell* *19*, 655-666. 10.1016/j.molcel.2005.07.020.
34. Lin, J., Zhou, D., Steitz, T.A., Polikanov, Y.S., and Gagnon, M.G. (2018). Ribosome-Targeting Antibiotics: Modes of Action, Mechanisms of Resistance, and Implications for Drug Design. *Annu Rev Biochem* *87*, 451-478. 10.1146/annurev-biochem-062917-011942.
35. Rastogi, N., Goh, K.S., Berchel, M., and Bryskier, A. (2000). In vitro activities of the ketolides telithromycin (HMR 3647) and HMR 3004 compared to those of clarithromycin against slowly growing mycobacteria at pHs 6.8 and 7.4. *Antimicrob Agents Chemother* *44*, 2848-2852. 10.1128/AAC.44.10.2848-2852.2000.
36. Falzari, K., Zhu, Z., Pan, D., Liu, H., Hongmanee, P., and Franzblau, S.G. (2005). In vitro and in vivo activities of macrolide derivatives against *Mycobacterium tuberculosis*. *Antimicrob Agents Chemother* *49*, 1447-1454. 10.1128/AAC.49.4.1447-1454.2005.
37. Vianna, J.F., K, S.B., J, I.N.O., Albuquerque, E.L., and Fulco, U.L. (2019). Binding energies of the drugs capreomycin and streptomycin in complex with tuberculosis bacterial ribosome subunits. *Phys Chem Chem Phys* *21*, 19192-19200. 10.1039/c9cp03631h.
38. Alangaden, G.J., Kreiswirth, B.N., Aouad, A., Khetarpal, M., Igno, F.R., Moghazeh, S.L., Manavathu, E.K., and Lerner, S.A. (1998). Mechanism of resistance to amikacin and kanamycin in *Mycobacterium tuberculosis*. *Antimicrob Agents Chemother* *42*, 1295-1297. 10.1128/AAC.42.5.1295.
39. Cynamon, M.H., Klemens, S.P., Sharpe, C.A., and Chase, S. (1999). Activities of several novel oxazolidinones against *Mycobacterium tuberculosis* in a murine model. *Antimicrob Agents Chemother* *43*, 1189-1191. 10.1128/AAC.43.5.1189.
40. Abrahams, K.A., and Besra, G.S. (2018). Mycobacterial cell wall biosynthesis: a multifaceted antibiotic target. *Parasitology* *145*, 116-133. 10.1017/S0031182016002377.
41. Matsumoto, M., Hashizume, H., Tsubouchi, H., Sasaki, H., Itotani, M., Kuroda, H., Tomishige, T., Kawasaki, M., and Komatsu, M. (2007). Screening for novel antituberculosis agents that are effective against multidrug resistant tuberculosis. *Curr Top Med Chem* *7*, 499-507. 10.2174/156802607780059727.
42. Stover, C.K., Warrener, P., VanDevanter, D.R., Sherman, D.R., Arain, T.M., Langhorne, M.H., Anderson, S.W., Towell, J.A., Yuan, Y., McMurray, D.N., et al. (2000). A small-molecule nitroimidazopyran drug candidate for the treatment of tuberculosis. *Nature* *405*, 962-966. 10.1038/35016103.
43. Nuermberger, E.L., Martinez-Martinez, M.S., Sanz, O., Urones, B., Esquivias, J., Soni, H., Tasneen, R., Tyagi, S., Li, S.Y., Converse, P.J., et al. (2022). GSK2556286 Is a Novel Antitubercular Drug Candidate Effective In Vivo with the Potential To Shorten Tuberculosis Treatment. *Antimicrob Agents Chemother* *66*, e0013222. 10.1128/aac.00132-22.
44. Yelamanchi, S.D., and Surolia, A. (2021). Targeting amino acid metabolism of *Mycobacterium tuberculosis* for developing inhibitors to curtail its survival. *IUBMB Life* *73*, 643-658. 10.1002/iub.2455.
45. Mahajan, R. (2013). Bedaquiline: First FDA-approved tuberculosis drug in 40 years. *Int J Appl Basic Med Res* *3*, 1-2. 10.4103/2229-516X.112228.

46. de Jager, V.R., Dawson, R., van Niekerk, C., Hutchings, J., Kim, J., Vanker, N., van der Merwe, L., Choi, J., Nam, K., and Diacon, A.H. (2020). Telacebec (Q203), a New Antituberculosis Agent. *N Engl J Med* 382, 1280-1281. 10.1056/NEJMc1913327.
47. Rybniker, J., Vocat, A., Sala, C., Busso, P., Pojer, F., Benjak, A., and Cole, S.T. (2015). Lansoprazole is an antituberculous prodrug targeting cytochrome bc1. *Nat Commun* 6, 7659. 10.1038/ncomms8659.
48. WHO (2023). Global tuberculosis report 2022 digital content: TB research and innovation. <https://www.who.int/teams/global-tuberculosis-programme/tb-reports/global-tuberculosis-report-2022/tb-research-and-innovation>.
49. Robertson, G.T., Ramey, M.E., Massoudi, L.M., Carter, C.L., Zimmerman, M., Kaya, F., Graham, B.G., Gruppo, V., Hastings, C., Woolhiser, L.K., et al. (2021). Comparative Analysis of Pharmacodynamics in the C3HeB/FeJ Mouse Tuberculosis Model for DprE1 Inhibitors TBA-7371, PBTZ169, and OPC-167832. *Antimicrob Agents Chemother* 65, e0058321. 10.1128/AAC.00583-21.
50. Guieu, B., Jourdan, J.P., Dreneau, A., Willand, N., Rochais, C., and Dallemagne, P. (2021). Desirable drug-drug interactions or when a matter of concern becomes a renewed therapeutic strategy. *Drug Discov Today* 26, 315-328. 10.1016/j.drudis.2020.11.026.
51. Brown, K.L., Wilburn, K.M., Montague, C.R., Grigg, J.C., Sanz, O., Perez-Herran, E., Barros, D., Ballell, L., VanderVen, B.C., and Eltis, L.D. (2023). Cyclic AMP-Mediated Inhibition of Cholesterol Catabolism in Mycobacterium tuberculosis by the Novel Drug Candidate GSK2556286. *Antimicrob Agents Chemother* 67, e0129422. 10.1128/aac.01294-22.
52. Xu, J., Converse, P.J., Upton, A.M., Mdluli, K., Fotouhi, N., and Nuermberger, E.L. (2021). Comparative Efficacy of the Novel Diarylquinoline TBAJ-587 and Bedaquiline against a Resistant Rv0678 Mutant in a Mouse Model of Tuberculosis. *Antimicrob Agents Chemother* 65. 10.1128/AAC.02418-20.
53. Almeida, D., Converse, P.J., Li, S.Y., Upton, A.M., Fotouhi, N., and Nuermberger, E.L. (2021). Comparative Efficacy of the Novel Diarylquinoline TBAJ-876 and Bedaquiline against a Resistant Rv0678 Mutant in a Mouse Model of Tuberculosis. *Antimicrob Agents Chemother* 65, e0141221. 10.1128/AAC.01412-21.
54. Lu, Y., Zheng, M., Wang, B., Fu, L., Zhao, W., Li, P., Xu, J., Zhu, H., Jin, H., Yin, D., et al. (2011). Clofazimine analogs with efficacy against experimental tuberculosis and reduced potential for accumulation. *Antimicrob Agents Chemother* 55, 5185-5193. 10.1128/AAC.00699-11.
55. Li, S.Y., Converse, P.J., Betoudji, F., Lee, J., Mdluli, K., Upton, A., Fotouhi, N., and Nuermberger, E.L. (2023). Next-Generation Diarylquinolines Improve Sterilizing Activity of Regimens with Pretomanid and the Novel Oxazolidinone TBI-223 in a Mouse Tuberculosis Model. *Antimicrob Agents Chemother* 67, e0003523. 10.1128/aac.00035-23.
56. Makarov, V., Manina, G., Mikusova, K., Mollmann, U., Ryabova, O., Saint-Joanis, B., Dhar, N., Pasca, M.R., Buroni, S., Lucarelli, A.P., et al. (2009). Benzothiazinones kill Mycobacterium tuberculosis by blocking arabinan synthesis. *Science* 324, 801-804. 10.1126/science.1171583.
57. Li, X., Hernandez, V., Rock, F.L., Choi, W., Mak, Y.S.L., Mohan, M., Mao, W., Zhou, Y., Easom, E.E., Plattner, J.J., et al. (2017). Discovery of a Potent and Specific M. tuberculosis Leucyl-tRNA Synthetase Inhibitor: (S)-3-(Aminomethyl)-4-chloro-7-(2-hydroxyethoxy)benzo[c][1,2]oxaborol-1(3H)-ol (GSK656). *J Med Chem* 60, 8011-8026. 10.1021/acs.jmedchem.7b00631.
58. Hariguchi, N., Chen, X., Hayashi, Y., Kawano, Y., Fujiwara, M., Matsuba, M., Shimizu, H., Ohba, Y., Nakamura, I., Kitamoto, R., et al. (2020). OPC-167832, a Novel

- Carbostyryl Derivative with Potent Antituberculosis Activity as a DprE1 Inhibitor. *Antimicrob Agents Chemother* 64. 10.1128/AAC.02020-19.
59. Talley, A.K., Thurston, A., Moore, G., Gupta, V.K., Satterfield, M., Manyak, E., Stokes, S., Dane, A., and Melnick, D. (2021). First-in-Human Evaluation of the Safety, Tolerability, and Pharmacokinetics of SPR720, a Novel Oral Bacterial DNA Gyrase (GyrB) Inhibitor for Mycobacterial Infections. *Antimicrob Agents Chemother* 65, e0120821. 10.1128/AAC.01208-21.
 60. Pethe, K., Bifani, P., Jang, J., Kang, S., Park, S., Ahn, S., Jiricek, J., Jung, J., Jeon, H.K., Cechetto, J., et al. (2013). Discovery of Q203, a potent clinical candidate for the treatment of tuberculosis. *Nat Med* 19, 1157-1160. 10.1038/nm.3262.
 61. Shirude, P.S., Shandil, R., Sadler, C., Naik, M., Hosagrahara, V., Hameed, S., Shinde, V., Bathula, C., Humnabadkar, V., Kumar, N., et al. (2013). Azaindoles: noncovalent DprE1 inhibitors from scaffold morphing efforts, kill *Mycobacterium tuberculosis* and are efficacious in vivo. *J Med Chem* 56, 9701-9708. 10.1021/jm401382v.
 62. Jeong, J.W., Jung, S.J., Lee, H.H., Kim, Y.Z., Park, T.K., Cho, Y.L., Chae, S.E., Baek, S.Y., Woo, S.H., Lee, H.S., and Kwak, J.H. (2010). In vitro and in vivo activities of LCB01-0371, a new oxazolidinone. *Antimicrob Agents Chemother* 54, 5359-5362. 10.1128/AAC.00723-10.
 63. Sacksteder, K.A., Protopopova, M., Barry, C.E., 3rd, Andries, K., and Nacy, C.A. (2012). Discovery and development of SQ109: a new antitubercular drug with a novel mechanism of action. *Future Microbiol* 7, 823-837. 10.2217/fmb.12.56.
 64. Barbachyn, M.R., Hutchinson, D.K., Brickner, S.J., Cynamon, M.H., Kilburn, J.O., Klemens, S.P., Glickman, S.E., Grega, K.C., Hendges, S.K., Toops, D.S., et al. (1996). Identification of a novel oxazolidinone (U-100480) with potent antimycobacterial activity. *J Med Chem* 39, 680-685. 10.1021/jm950956y.
 65. Yao, R., Wang, B., Fu, L., Li, L., You, K., Li, Y.G., and Lu, Y. (2022). Sudapyridine (WX-081), a Novel Compound against *Mycobacterium tuberculosis*. *Microbiol Spectr* 10, e0247721. 10.1128/spectrum.02477-21.
 66. Grzegorzewicz, A.E., de Sousa-d'Auria, C., McNeil, M.R., Huc-Claustre, E., Jones, V., Petit, C., Angala, S.K., Zemanova, J., Wang, Q., Belardinelli, J.M., et al. (2016). Assembling of the *Mycobacterium tuberculosis* Cell Wall Core. *J Biol Chem* 291, 18867-18879. 10.1074/jbc.M116.739227.
 67. Jacobo-Delgado, Y.M., Rodriguez-Carlos, A., Serrano, C.J., and Rivas-Santiago, B. (2023). *Mycobacterium tuberculosis* cell-wall and antimicrobial peptides: a mission impossible? *Front Immunol* 14, 1194923. 10.3389/fimmu.2023.1194923.
 68. Singh, P., Rameshwaram, N.R., Ghosh, S., and Mukhopadhyay, S. (2018). Cell envelope lipids in the pathophysiology of *Mycobacterium tuberculosis*. *Future Microbiol* 13, 689-710. 10.2217/fmb-2017-0135.
 69. Bajeli, S., Baid, N., Kaur, M., Pawar, G.P., Chaudhari, V.D., and Kumar, A. (2020). Terminal Respiratory Oxidases: A Targetable Vulnerability of Mycobacterial Bioenergetics? *Front Cell Infect Microbiol* 10, 589318. 10.3389/fcimb.2020.589318.
 70. Alderwick, L.J., Harrison, J., Lloyd, G.S., and Birch, H.L. (2015). The Mycobacterial Cell Wall--Peptidoglycan and Arabinogalactan. *Cold Spring Harb Perspect Med* 5, a021113. 10.1101/cshperspect.a021113.
 71. Vollmer, W., Blanot, D., and de Pedro, M.A. (2008). Peptidoglycan structure and architecture. *FEMS Microbiol Rev* 32, 149-167. 10.1111/j.1574-6976.2007.00094.x.
 72. Jarlier, V., and Nikaido, H. (1994). Mycobacterial cell wall: structure and role in natural resistance to antibiotics. *FEMS Microbiol Lett* 123, 11-18. 10.1111/j.1574-6968.1994.tb07194.x.

73. Jankute, M., Cox, J.A., Harrison, J., and Besra, G.S. (2015). Assembly of the Mycobacterial Cell Wall. *Annu Rev Microbiol* 69, 405-423. 10.1146/annurev-micro-091014-104121.
74. Kieser, K.J., and Rubin, E.J. (2014). How sisters grow apart: mycobacterial growth and division. *Nat Rev Microbiol* 12, 550-562. 10.1038/nrmicro3299.
75. Yadav, S., Soni, A., Tanwar, O., Bhadane, R., Besra, G.S., and Kawathekar, N. (2023). DprE1 Inhibitors: Enduring Aspirations for Future Antituberculosis Drug Discovery. *ChemMedChem* 18, e202300099. 10.1002/cmdc.202300099.
76. Batt, S.M., Burke, C.E., Moorey, A.R., and Besra, G.S. (2020). Antibiotics and resistance: the two-sided coin of the mycobacterial cell wall. *Cell Surf* 6, 100044. 10.1016/j.tcs.2020.100044.
77. Sammartino, J.C., Morici, M., Stelitano, G., Degiacomi, G., Riccardi, G., and Chiarelli, L.R. (2022). Functional investigation of the antitubercular drug target Decaprenylphosphoryl-beta-D-ribofuranose-2-epimerase DprE1/DprE2 complex. *Biochem Biophys Res Commun* 607, 49-53. 10.1016/j.bbrc.2022.03.091.
78. Vilcheze, C., Weisbrod, T.R., Chen, B., Kremer, L., Hazbon, M.H., Wang, F., Alland, D., Sacchettini, J.C., and Jacobs, W.R., Jr. (2005). Altered NADH/NAD⁺ ratio mediates coresistance to isoniazid and ethionamide in mycobacteria. *Antimicrob Agents Chemother* 49, 708-720. 10.1128/AAC.49.2.708-720.2005.
79. Rayasam, G.V. (2014). MmpL3 a potential new target for development of novel anti-tuberculosis drugs. *Expert Opin Ther Targets* 18, 247-256. 10.1517/14728222.2014.859677.
80. Portevin, D., De Sousa-D'Auria, C., Houssin, C., Grimaldi, C., Chami, M., Daffe, M., and Guilhot, C. (2004). A polyketide synthase catalyzes the last condensation step of mycolic acid biosynthesis in mycobacteria and related organisms. *Proc Natl Acad Sci U S A* 101, 314-319. 10.1073/pnas.0305439101.
81. Zhang, L., Zhao, Y., Gao, Y., Wu, L., Gao, R., Zhang, Q., Wang, Y., Wu, C., Wu, F., Gurucha, S.S., et al. (2020). Structures of cell wall arabinosyltransferases with the anti-tuberculosis drug ethambutol. *Science* 368, 1211-1219. 10.1126/science.aba9102.
82. Cole, S.T. (2016). Inhibiting Mycobacterium tuberculosis within and without. *Philos Trans R Soc Lond B Biol Sci* 371. 10.1098/rstb.2015.0506.
83. Grant, S.S., Wellington, S., Kawate, T., Desjardins, C.A., Silvis, M.R., Wivagg, C., Thompson, M., Gordon, K., Kazyanskaya, E., Nietupski, R., et al. (2016). Baeyer-Villiger Monooxygenases EthA and MymA Are Required for Activation of Replicating and Non-replicating Mycobacterium tuberculosis Inhibitors. *Cell Chem Biol* 23, 666-677. 10.1016/j.chembiol.2016.05.011.
84. Blondiaux, N., Moune, M., Desroses, M., Frita, R., Flippe, M., Mathys, V., Soetaert, K., Kiass, M., Delorme, V., Djaout, K., et al. (2017). Reversion of antibiotic resistance in Mycobacterium tuberculosis by spiroisoxazoline SMART-420. *Science* 355, 1206-1211. 10.1126/science.aag1006.
85. Li, W., Upadhyay, A., Fontes, F.L., North, E.J., Wang, Y., Crans, D.C., Grzegorzewicz, A.E., Jones, V., Franzblau, S.G., Lee, R.E., et al. (2014). Novel insights into the mechanism of inhibition of MmpL3, a target of multiple pharmacophores in Mycobacterium tuberculosis. *Antimicrob Agents Chemother* 58, 6413-6423. 10.1128/AAC.03229-14.
86. Dal Molin, M., Selchow, P., Schafle, D., Tschumi, A., Ryckmans, T., Laage-Witt, S., and Sander, P. (2019). Identification of novel scaffolds targeting Mycobacterium tuberculosis. *J Mol Med (Berl)* 97, 1601-1613. 10.1007/s00109-019-01840-7.
87. Imran, M., Arora, M.K., Chaudhary, A., Khan, S.A., Kamal, M., Alshammari, M.M., Alharbi, R.M., Althomali, N.A., Alzimam, I.M., Alshammari, A.A., et al. (2022). MmpL3 Inhibition as a Promising Approach to Develop Novel Therapies against

- Tuberculosis: A Spotlight on SQ109, Clinical Studies, and Patents Literature. *Biomedicines* 10. 10.3390/biomedicines10112793.
88. Shao, M., McNeil, M., Cook, G.M., and Lu, X. (2020). MmpL3 inhibitors as antituberculosis drugs. *Eur J Med Chem* 200, 112390. 10.1016/j.ejmech.2020.112390.
 89. Gavalda, S., Bardou, F., Laval, F., Bon, C., Malaga, W., Chalut, C., Guilhot, C., Mourey, L., Daffe, M., and Quemard, A. (2014). The polyketide synthase Pks13 catalyzes a novel mechanism of lipid transfer in mycobacteria. *Chem Biol* 21, 1660-1669. 10.1016/j.chembiol.2014.10.011.
 90. Wilson, R., Kumar, P., Parashar, V., Vilcheze, C., Veyron-Churlet, R., Freundlich, J.S., Barnes, S.W., Walker, J.R., Szymonifka, M.J., Marchiano, E., et al. (2013). Antituberculosis thiophenes define a requirement for Pks13 in mycolic acid biosynthesis. *Nat Chem Biol* 9, 499-506. 10.1038/nchembio.1277.
 91. Ioerger, T.R., O'Malley, T., Liao, R., Guinn, K.M., Hickey, M.J., Mohaideen, N., Murphy, K.C., Boshoff, H.I., Mizrahi, V., Rubin, E.J., et al. (2013). Identification of new drug targets and resistance mechanisms in *Mycobacterium tuberculosis*. *PLoS One* 8, e75245. 10.1371/journal.pone.0075245.
 92. Amin, A.G., Goude, R., Shi, L., Zhang, J., Chatterjee, D., and Parish, T. (2008). EmbA is an essential arabinosyltransferase in *Mycobacterium tuberculosis*. *Microbiology (Reading)* 154, 240-248. 10.1099/mic.0.2007/012153-0.
 93. Goude, R., Amin, A.G., Chatterjee, D., and Parish, T. (2009). The arabinosyltransferase EmbC is inhibited by ethambutol in *Mycobacterium tuberculosis*. *Antimicrob Agents Chemother* 53, 4138-4146. 10.1128/AAC.00162-09.
 94. Negatu, D.A., Yamada, Y., Xi, Y., Go, M.L., Zimmerman, M., Ganapathy, U., Dartois, V., Gengenbacher, M., and Dick, T. (2019). Gut Microbiota Metabolite Indole Propionic Acid Targets Tryptophan Biosynthesis in *Mycobacterium tuberculosis*. *mBio* 10. 10.1128/mBio.02781-18.
 95. Nurul Islam, M., Hitchings, R., Kumar, S., Fontes, F.L., Lott, J.S., Kruh-Garcia, N.A., and Crick, D.C. (2019). Mechanism of Fluorinated Anthranilate-Induced Growth Inhibition in *Mycobacterium tuberculosis*. *ACS Infect Dis* 5, 55-62. 10.1021/acscinfecdis.8b00092.
 96. Dunn, M.F. (2012). Allosteric regulation of substrate channeling and catalysis in the tryptophan synthase holoenzyme complex. *Arch Biochem Biophys* 519, 154-166. 10.1016/j.abb.2012.01.016.
 97. Kashket, E.R. (1985). The proton motive force in bacteria: a critical assessment of methods. *Annu Rev Microbiol* 39, 219-242. 10.1146/annurev.mi.39.100185.001251.
 98. Cook, G.M., Berney, M., Gebhard, S., Heinemann, M., Cox, R.A., Danilchanka, O., and Niederweis, M. (2009). Physiology of mycobacteria. *Adv Microb Physiol* 55, 81-182, 318-189. 10.1016/S0065-2911(09)05502-7.
 99. Bald, D., Vilellas, C., Lu, P., and Koul, A. (2017). Targeting Energy Metabolism in *Mycobacterium tuberculosis*, a New Paradigm in Antimycobacterial Drug Discovery. *mBio* 8. 10.1128/mBio.00272-17.
 100. Andries, K., Verhasselt, P., Guillemont, J., Gohlmann, H.W., Neefs, J.M., Winkler, H., Van Gestel, J., Timmerman, P., Zhu, M., Lee, E., et al. (2005). A diarylquinoline drug active on the ATP synthase of *Mycobacterium tuberculosis*. *Science* 307, 223-227. 10.1126/science.1106753.
 101. Tantry, S.J., Markad, S.D., Shinde, V., Bhat, J., Balakrishnan, G., Gupta, A.K., Ambady, A., Raichurkar, A., Kedari, C., Sharma, S., et al. (2017). Discovery of Imidazo[1,2-a]pyridine Ethers and Squaramides as Selective and Potent Inhibitors of Mycobacterial Adenosine Triphosphate (ATP) Synthesis. *J Med Chem* 60, 1379-1399. 10.1021/acs.jmedchem.6b01358.

102. Yano, T., Kassovska-Bratinova, S., Teh, J.S., Winkler, J., Sullivan, K., Isaacs, A., Schechter, N.M., and Rubin, H. (2011). Reduction of clofazimine by mycobacterial type 2 NADH:quinone oxidoreductase: a pathway for the generation of bactericidal levels of reactive oxygen species. *J Biol Chem* 286, 10276-10287. 10.1074/jbc.M110.200501.
103. Zhang, Y., Wade, M.M., Scorpio, A., Zhang, H., and Sun, Z. (2003). Mode of action of pyrazinamide: disruption of Mycobacterium tuberculosis membrane transport and energetics by pyrazinoic acid. *J Antimicrob Chemother* 52, 790-795. 10.1093/jac/dkg446.
104. Li, K., Schurig-Briccio, L.A., Feng, X., Upadhyay, A., Pujari, V., Lechartier, B., Fontes, F.L., Yang, H., Rao, G., Zhu, W., et al. (2014). Multitarget drug discovery for tuberculosis and other infectious diseases. *J Med Chem* 57, 3126-3139. 10.1021/jm500131s.
105. Gries, R., Sala, C., and Rybniker, J. (2020). Host-Directed Therapies and Anti-Virulence Compounds to Address Anti-Microbial Resistant Tuberculosis Infection. *Applied Sciences-Basel* 10. ARTN 2688 10.3390/app10082688.
106. Jeong, E.K., Lee, H.J., and Jung, Y.J. (2022). Host-Directed Therapies for Tuberculosis. *Pathogens* 11. 10.3390/pathogens11111291.
107. Rasko, D.A., and Sperandio, V. (2010). Anti-virulence strategies to combat bacteria-mediated disease. *Nat Rev Drug Discov* 9, 117-128. 10.1038/nrd3013.
108. Raught, B., Gingras, A.C., and Sonenberg, N. (2001). The target of rapamycin (TOR) proteins. *Proc Natl Acad Sci U S A* 98, 7037-7044. 10.1073/pnas.121145898.
109. Singhal, A., Jie, L., Kumar, P., Hong, G.S., Leow, M.K., Paleja, B., Tsenova, L., Kurepina, N., Chen, J., Zolezzi, F., et al. (2014). Metformin as adjunct antituberculosis therapy. *Sci Transl Med* 6, 263ra159. 10.1126/scitranslmed.3009885.
110. An, X., Tiwari, A.K., Sun, Y., Ding, P.R., Ashby, C.R., Jr., and Chen, Z.S. (2010). BCR-ABL tyrosine kinase inhibitors in the treatment of Philadelphia chromosome positive chronic myeloid leukemia: a review. *Leuk Res* 34, 1255-1268. 10.1016/j.leukres.2010.04.016.
111. Rook, G.A., Steele, J., Fraher, L., Barker, S., Karmali, R., O'Riordan, J., and Stanford, J. (1986). Vitamin D3, gamma interferon, and control of proliferation of Mycobacterium tuberculosis by human monocytes. *Immunology* 57, 159-163.
112. Dallenga, T., Repnik, U., Corleis, B., Eich, J., Reimer, R., Griffiths, G.W., and Schaible, U.E. (2017). M. tuberculosis-Induced Necrosis of Infected Neutrophils Promotes Bacterial Growth Following Phagocytosis by Macrophages. *Cell Host Microbe* 22, 519-530 e513. 10.1016/j.chom.2017.09.003.
113. Amaral, E.P., Costa, D.L., Namasivayam, S., Riteau, N., Kamenyeva, O., Mittereder, L., Mayer-Barber, K.D., Andrade, B.B., and Sher, A. (2019). A major role for ferroptosis in Mycobacterium tuberculosis-induced cell death and tissue necrosis. *J Exp Med* 216, 556-570. 10.1084/jem.20181776.
114. Liu, X., Zhang, Z., Ruan, J., Pan, Y., Magupalli, V.G., Wu, H., and Lieberman, J. (2016). Inflammasome-activated gasdermin D causes pyroptosis by forming membrane pores. *Nature* 535, 153-158. 10.1038/nature18629.
115. Wallis, R.S., Kyambadde, P., Johnson, J.L., Horter, L., Kittle, R., Pohle, M., Ducar, C., Millard, M., Mayanja-Kizza, H., Whalen, C., and Okwera, A. (2004). A study of the safety, immunology, virology, and microbiology of adjunctive etanercept in HIV-1-associated tuberculosis. *AIDS* 18, 257-264. 10.1097/00002030-200401230-00015.
116. Grab, J., Suarez, I., van Gumpel, E., Winter, S., Schreiber, F., Esser, A., Holscher, C., Fritsch, M., Herb, M., Schramm, M., et al. (2019). Corticosteroids inhibit Mycobacterium tuberculosis-induced necrotic host cell death by abrogating mitochondrial membrane permeability transition. *Nat Commun* 10, 688. 10.1038/s41467-019-08405-9.

117. Grab, J., and Rybniker, J. (2019). The Expanding Role of p38 Mitogen-Activated Protein Kinase in Programmed Host Cell Death. *Microbiol Insights* *12*, 1178636119864594. 10.1177/1178636119864594.
118. Holscher, C., Grab, J., Holscher, A., Muller, A.L., Schafer, S.C., and Rybniker, J. (2020). Chemical p38 MAP kinase inhibition constrains tissue inflammation and improves antibiotic activity in *Mycobacterium tuberculosis*-infected mice. *Sci Rep* *10*, 13629. 10.1038/s41598-020-70184-x.
119. Dehbanipour, R., and Ghalavand, Z. (2022). Anti-virulence therapeutic strategies against bacterial infections: recent advances. *Germs* *12*, 262-275. 10.18683/germs.2022.1328.
120. Ramon-Luing, L.A., Palacios, Y., Ruiz, A., Tellez-Navarrete, N.A., and Chavez-Galan, L. (2023). Virulence Factors of *Mycobacterium tuberculosis* as Modulators of Cell Death Mechanisms. *Pathogens* *12*. 10.3390/pathogens12060839.
121. Paharik, A.E., Schreiber, H.L.t., Spaulding, C.N., Dodson, K.W., and Hultgren, S.J. (2017). Narrowing the spectrum: the new frontier of precision antimicrobials. *Genome Med* *9*, 110. 10.1186/s13073-017-0504-3.
122. Spaulding, C.N., Klein, R.D., Schreiber, H.L.t., Janetka, J.W., and Hultgren, S.J. (2018). Precision antimicrobial therapeutics: the path of least resistance? *NPJ Biofilms Microbiomes* *4*, 4. 10.1038/s41522-018-0048-3.
123. Johnson, B.K., Colvin, C.J., Needle, D.B., Mba Medie, F., Champion, P.A., and Abramovitch, R.B. (2015). The Carbonic Anhydrase Inhibitor Ethoxzolamide Inhibits the *Mycobacterium tuberculosis* PhoPR Regulon and Esx-1 Secretion and Attenuates Virulence. *Antimicrob Agents Chemother* *59*, 4436-4445. 10.1128/AAC.00719-15.
124. Gupta, S., Sinha, A., and Sarkar, D. (2006). Transcriptional autoregulation by *Mycobacterium tuberculosis* PhoP involves recognition of novel direct repeat sequences in the regulatory region of the promoter. *FEBS Lett* *580*, 5328-5338. 10.1016/j.febslet.2006.09.004.
125. Khan, H., Paul, P., Sevalkar, R.R., Kachhap, S., Singh, B., and Sarkar, D. (2022). Convergence of two global regulators to coordinate expression of essential virulence determinants of *Mycobacterium tuberculosis*. *Elife* *11*. 10.7554/eLife.80965.
126. Solans, L., Gonzalo-Asensio, J., Sala, C., Benjak, A., Uplekar, S., Rougemont, J., Guilhot, C., Malaga, W., Martin, C., and Cole, S.T. (2014). The PhoP-dependent ncRNA Mcr7 modulates the TAT secretion system in *Mycobacterium tuberculosis*. *PLoS Pathog* *10*, e1004183. 10.1371/journal.ppat.1004183.
127. Gonzalo Asensio, J., Maia, C., Ferrer, N.L., Barilone, N., Laval, F., Soto, C.Y., Winter, N., Daffe, M., Gicquel, B., Martin, C., and Jackson, M. (2006). The virulence-associated two-component PhoP-PhoR system controls the biosynthesis of polyketide-derived lipids in *Mycobacterium tuberculosis*. *J Biol Chem* *281*, 1313-1316. 10.1074/jbc.C500388200.
128. Frigui, W., Bottai, D., Majlessi, L., Monot, M., Josselin, E., Brodin, P., Garnier, T., Gicquel, B., Martin, C., Leclerc, C., et al. (2008). Control of *M. tuberculosis* ESAT-6 secretion and specific T cell recognition by PhoP. *PLoS Pathog* *4*, e33. 10.1371/journal.ppat.0040033.
129. Vickers, C.F., Silva, A.P.G., Chakraborty, A., Fernandez, P., Kurepina, N., Saville, C., Naranjo, Y., Pons, M., Schnettger, L.S., Gutierrez, M.G., et al. (2018). Structure-Based Design of MptpB Inhibitors That Reduce Multidrug-Resistant *Mycobacterium tuberculosis* Survival and Infection Burden in Vivo. *J Med Chem* *61*, 8337-8352. 10.1021/acs.jmedchem.8b00832.
130. Fernandez-Soto, P., Bruce, A.J.E., Fielding, A.J., Cavet, J.S., and Taberner, L. (2019). Mechanism of catalysis and inhibition of *Mycobacterium tuberculosis* SapM,

- implications for the development of novel antivirulence drugs. *Sci Rep* 9, 10315. 10.1038/s41598-019-46731-6.
131. Paolino, M., Brindisi, M., Vallone, A., Butini, S., Campiani, G., Nannicini, C., Giuliani, G., Anzini, M., Lamponi, S., Giorgi, G., et al. (2018). Development of Potent Inhibitors of the Mycobacterium tuberculosis Virulence Factor Zmp1 and Evaluation of Their Effect on Mycobacterial Survival inside Macrophages. *ChemMedChem* 13, 422-430. 10.1002/cmdc.201700759.
132. Rybniker, J., Chen, J.M., Sala, C., Hartkoorn, R.C., Vocat, A., Benjak, A., Boy-Rottger, S., Zhang, M., Szekely, R., Greff, Z., et al. (2014). Anticytolytic screen identifies inhibitors of mycobacterial virulence protein secretion. *Cell Host Microbe* 16, 538-548. 10.1016/j.chom.2014.09.008.
133. Simeone, R., Bottai, D., and Brosch, R. (2009). ESX/type VII secretion systems and their role in host-pathogen interaction. *Curr Opin Microbiol* 12, 4-10. 10.1016/j.mib.2008.11.003.
134. Houben, E.N., Korotkov, K.V., and Bitter, W. (2014). Take five - Type VII secretion systems of Mycobacteria. *Biochim Biophys Acta* 1843, 1707-1716. 10.1016/j.bbamcr.2013.11.003.
135. Pym, A.S., Brodin, P., Brosch, R., Huerre, M., and Cole, S.T. (2002). Loss of RD1 contributed to the attenuation of the live tuberculosis vaccines Mycobacterium bovis BCG and Mycobacterium microti. *Mol Microbiol* 46, 709-717. 10.1046/j.1365-2958.2002.03237.x.
136. Brodin, P., Majlessi, L., Marsollier, L., de Jonge, M.I., Bottai, D., Demangel, C., Hinds, J., Neyrolles, O., Butcher, P.D., Leclerc, C., et al. (2006). Dissection of ESAT-6 system 1 of Mycobacterium tuberculosis and impact on immunogenicity and virulence. *Infect Immun* 74, 88-98. 10.1128/IAI.74.1.88-98.2006.
137. Lewis, K.N., Liao, R., Guinn, K.M., Hickey, M.J., Smith, S., Behr, M.A., and Sherman, D.R. (2003). Deletion of RD1 from Mycobacterium tuberculosis mimics bacille Calmette-Guerin attenuation. *J Infect Dis* 187, 117-123. 10.1086/345862.
138. Guinn, K.M., Hickey, M.J., Mathur, S.K., Zakel, K.L., Grotzke, J.E., Lewinsohn, D.M., Smith, S., and Sherman, D.R. (2004). Individual RD1-region genes are required for export of ESAT-6/CFP-10 and for virulence of Mycobacterium tuberculosis. *Mol Microbiol* 51, 359-370. 10.1046/j.1365-2958.2003.03844.x.
139. Chirakos, A.E., Balaram, A., Conrad, W., and Champion, P.A. (2020). Modeling Tubercular ESX-1 Secretion Using Mycobacterium marinum. *Microbiol Mol Biol Rev* 84. 10.1128/MMBR.00082-19.
140. Groschel, M.I., Sayes, F., Simeone, R., Majlessi, L., and Brosch, R. (2016). ESX secretion systems: mycobacterial evolution to counter host immunity. *Nat Rev Microbiol* 14, 677-691. 10.1038/nrmicro.2016.131.
141. Rosenberg, O.S., Dovala, D., Li, X., Connolly, L., Bendebury, A., Finer-Moore, J., Holton, J., Cheng, Y., Stroud, R.M., and Cox, J.S. (2015). Substrates Control Multimerization and Activation of the Multi-Domain ATPase Motor of Type VII Secretion. *Cell* 161, 501-512. 10.1016/j.cell.2015.03.040.
142. Fortune, S.M., Jaeger, A., Sarracino, D.A., Chase, M.R., Sasseti, C.M., Sherman, D.R., Bloom, B.R., and Rubin, E.J. (2005). Mutually dependent secretion of proteins required for mycobacterial virulence. *Proc Natl Acad Sci U S A* 102, 10676-10681. 10.1073/pnas.0504922102.
143. Champion, P.A., Champion, M.M., Manzanillo, P., and Cox, J.S. (2009). ESX-1 secreted virulence factors are recognized by multiple cytosolic AAA ATPases in pathogenic mycobacteria. *Mol Microbiol* 73, 950-962. 10.1111/j.1365-2958.2009.06821.x.

144. Arend, S.M., Andersen, P., van Meijgaarden, K.E., Skjot, R.L., Subronto, Y.W., van Dissel, J.T., and Ottenhoff, T.H. (2000). Detection of active tuberculosis infection by T cell responses to early-secreted antigenic target 6-kDa protein and culture filtrate protein 10. *J Infect Dis* *181*, 1850-1854. 10.1086/315448.
145. Meher, A.K., Bal, N.C., Chary, K.V., and Arora, A. (2006). Mycobacterium tuberculosis H37Rv ESAT-6-CFP-10 complex formation confers thermodynamic and biochemical stability. *FEBS J* *273*, 1445-1462. 10.1111/j.1742-4658.2006.05166.x.
146. Renshaw, P.S., Panagiotidou, P., Whelan, A., Gordon, S.V., Hewinson, R.G., Williamson, R.A., and Carr, M.D. (2002). Conclusive evidence that the major T-cell antigens of the Mycobacterium tuberculosis complex ESAT-6 and CFP-10 form a tight, 1:1 complex and characterization of the structural properties of ESAT-6, CFP-10, and the ESAT-6*CFP-10 complex. Implications for pathogenesis and virulence. *J Biol Chem* *277*, 21598-21603. 10.1074/jbc.M201625200.
147. Houben, D., Demangel, C., van Ingen, J., Perez, J., Baldeon, L., Abdallah, A.M., Caleechurn, L., Bottai, D., van Zon, M., de Punder, K., et al. (2012). ESX-1-mediated translocation to the cytosol controls virulence of mycobacteria. *Cell Microbiol* *14*, 1287-1298. 10.1111/j.1462-5822.2012.01799.x.
148. van der Wel, N., Hava, D., Houben, D., Fluittsma, D., van Zon, M., Pierson, J., Brenner, M., and Peters, P.J. (2007). M. tuberculosis and M. leprae translocate from the phagolysosome to the cytosol in myeloid cells. *Cell* *129*, 1287-1298. 10.1016/j.cell.2007.05.059.
149. Kellar, K.L., Gehrke, J., Weis, S.E., Mahmutovic-Mayhew, A., Davila, B., Zajdowicz, M.J., Scarborough, R., LoBue, P.A., Lardizabal, A.A., Daley, C.L., et al. (2011). Multiple cytokines are released when blood from patients with tuberculosis is stimulated with Mycobacterium tuberculosis antigens. *PLoS One* *6*, e26545. 10.1371/journal.pone.0026545.
150. Drever, K., Lim, Z.L., Zriba, S., and Chen, J.M. (2021). Protein Synthesis and Degradation Inhibitors Potently Block Mycobacterium tuberculosis type-7 Secretion System ESX-1 Activity. *ACS Infect Dis* *7*, 273-280. 10.1021/acsinfecdis.0c00741.
151. Chen, J.M., Boy-Rottger, S., Dhar, N., Sweeney, N., Buxton, R.S., Pojer, F., Rosenkrands, I., and Cole, S.T. (2012). EspD is critical for the virulence-mediating ESX-1 secretion system in Mycobacterium tuberculosis. *J Bacteriol* *194*, 884-893. 10.1128/JB.06417-11.
152. Perez, E., Samper, S., Bordas, Y., Guilhot, C., Gicquel, B., and Martin, C. (2001). An essential role for phoP in Mycobacterium tuberculosis virulence. *Mol Microbiol* *41*, 179-187. 10.1046/j.1365-2958.2001.02500.x.
153. Bosserman, R.E., Nguyen, T.T., Sanchez, K.G., Chirakos, A.E., Ferrell, M.J., Thompson, C.R., Champion, M.M., Abramovitch, R.B., and Champion, P.A. (2017). WhiB6 regulation of ESX-1 gene expression is controlled by a negative feedback loop in Mycobacterium marinum. *Proc Natl Acad Sci U S A* *114*, E10772-E10781. 10.1073/pnas.1710167114.
154. Sanchez, K.G., Ferrell, M.J., Chirakos, A.E., Nicholson, K.R., Abramovitch, R.B., Champion, M.M., and Champion, P.A. (2020). EspM Is a Conserved Transcription Factor That Regulates Gene Expression in Response to the ESX-1 System. *mBio* *11*. 10.1128/mBio.02807-19.
155. Blasco, B., Chen, J.M., Hartkoorn, R., Sala, C., Uplekar, S., Rougemont, J., Pojer, F., and Cole, S.T. (2012). Virulence regulator EspR of Mycobacterium tuberculosis is a nucleoid-associated protein. *PLoS Pathog* *8*, e1002621. 10.1371/journal.ppat.1002621.
156. Pang, X., Samten, B., Cao, G., Wang, X., Tvinnereim, A.R., Chen, X.L., and Howard, S.T. (2013). MprAB regulates the espA operon in Mycobacterium tuberculosis and

- modulates ESX-1 function and host cytokine response. *J Bacteriol* 195, 66-75. 10.1128/JB.01067-12.
157. Gordon, B.R., Li, Y., Wang, L., Sintsova, A., van Bakel, H., Tian, S., Navarre, W.W., Xia, B., and Liu, J. (2010). Lsr2 is a nucleoid-associated protein that targets AT-rich sequences and virulence genes in *Mycobacterium tuberculosis*. *Proc Natl Acad Sci U S A* 107, 5154-5159. 10.1073/pnas.0913551107.
158. Ates, L.S., and Brosch, R. (2017). Discovery of the type VII ESX-1 secretion needle? *Mol Microbiol* 103, 7-12. 10.1111/mmi.13579.
159. van Embden, J.D., Cave, M.D., Crawford, J.T., Dale, J.W., Eisenach, K.D., Gicquel, B., Hermans, P., Martin, C., McAdam, R., Shinnick, T.M., and et al. (1993). Strain identification of *Mycobacterium tuberculosis* by DNA fingerprinting: recommendations for a standardized methodology. *J Clin Microbiol* 31, 406-409. 10.1128/jcm.31.2.406-409.1993.
160. Kohl, T.A., Utpatel, C., Schleusener, V., De Filippo, M.R., Beckert, P., Cirillo, D.M., and Niemann, S. (2018). MTBseq: a comprehensive pipeline for whole genome sequence analysis of *Mycobacterium tuberculosis* complex isolates. *PeerJ* 6, e5895. 10.7717/peerj.5895.
161. Schneider, C.A., Rasband, W.S., and Eliceiri, K.W. (2012). NIH Image to ImageJ: 25 years of image analysis. *Nat Methods* 9, 671-675. 10.1038/nmeth.2089.
162. Tylutki, Z., Polak, S., and Wisniowska, B. (2016). Top-down, Bottom-up and Middle-out Strategies for Drug Cardiac Safety Assessment via Modeling and Simulations. *Curr Pharmacol Rep* 2, 171-177. 10.1007/s40495-016-0060-3.
163. Palomino, J.C., Martin, A., Camacho, M., Guerra, H., Swings, J., and Portaels, F. (2002). Resazurin microtiter assay plate: simple and inexpensive method for detection of drug resistance in *Mycobacterium tuberculosis*. *Antimicrob Agents Chemother* 46, 2720-2722. 10.1128/AAC.46.8.2720-2722.2002.
164. Ford, C.B., Lin, P.L., Chase, M.R., Shah, R.R., Iartchouk, O., Galagan, J., Mohaideen, N., Ioerger, T.R., Sacchettini, J.C., Lipsitch, M., et al. (2011). Use of whole genome sequencing to estimate the mutation rate of *Mycobacterium tuberculosis* during latent infection. *Nat Genet* 43, 482-486. 10.1038/ng.811.
165. Liu, Q., Wei, J., Li, Y., Wang, M., Su, J., Lu, Y., Lopez, M.G., Qian, X., Zhu, Z., Wang, H., et al. (2020). *Mycobacterium tuberculosis* clinical isolates carry mutational signatures of host immune environments. *Sci Adv* 6, eaba4901. 10.1126/sciadv.aba4901.
166. Te Brake, L.H.M., de Knegt, G.J., de Steenwinkel, J.E., van Dam, T.J.P., Burger, D.M., Russel, F.G.M., van Crevel, R., Koenderink, J.B., and Aarnoutse, R.E. (2018). The Role of Efflux Pumps in Tuberculosis Treatment and Their Promise as a Target in Drug Development: Unraveling the Black Box. *Annu Rev Pharmacol Toxicol* 58, 271-291. 10.1146/annurev-pharmtox-010617-052438.
167. Ismail, N., Omar, S.V., Ismail, N.A., and Peters, R.P.H. (2018). In vitro approaches for generation of *Mycobacterium tuberculosis* mutants resistant to bedaquiline, clofazimine or linezolid and identification of associated genetic variants. *J Microbiol Methods* 153, 1-9. 10.1016/j.mimet.2018.08.011.
168. Chang, C., Michalska, K., Bigelow, L., Jedrzejczak, R., ANDERSON, W.F., JOACHIMIAK, A. (2016). Crystal structure of tryptophan synthase alpha beta complex from *Streptococcus pneumoniae*. https://www.wwpdb.org/pdb?id=pdb_00005kin.
169. Michalska, K., Gale, J., Joachimiak, G., Chang, C., Hatzos-Skintges, C., Nocek, B., Johnston, S.E., Bigelow, L., Bajrami, B., Jedrzejczak, R.P., et al. (2019). Conservation of the structure and function of bacterial tryptophan synthases. *IUCrJ* 6, 649-664. 10.1107/S2052252519005955.

170. Dickey, S.W., Cheung, G.Y.C., and Otto, M. (2017). Different drugs for bad bugs: antivirulence strategies in the age of antibiotic resistance. *Nat Rev Drug Discov* *16*, 457-471. 10.1038/nrd.2017.23.
171. Zhang, M., Chen, J.M., Sala, C., Rybniker, J., Dhar, N., and Cole, S.T. (2014). EspI regulates the ESX-1 secretion system in response to ATP levels in *Mycobacterium tuberculosis*. *Mol Microbiol* *93*, 1057-1065. 10.1111/mmi.12718.
172. Sotgiu, G., Centis, R., D'Ambrosio, L., and Migliori, G.B. (2015). Tuberculosis treatment and drug regimens. *Cold Spring Harb Perspect Med* *5*, a017822. 10.1101/cshperspect.a017822.
173. Grace, A.G., Mittal, A., Jain, S., Tripathy, J.P., Satyanarayana, S., Tharyan, P., and Kirubakaran, R. (2019). Shortened treatment regimens versus the standard regimen for drug-sensitive pulmonary tuberculosis. *Cochrane Database Syst Rev* *12*, CD012918. 10.1002/14651858.CD012918.pub2.
174. Luo, Y., Cobb, R.E., and Zhao, H. (2014). Recent advances in natural product discovery. *Curr Opin Biotechnol* *30*, 230-237. 10.1016/j.copbio.2014.09.002.
175. Haniff, H.S., Knerr, L., Chen, J.L., Disney, M.D., and Lightfoot, H.L. (2020). Target-Directed Approaches for Screening Small Molecules against RNA Targets. *SLAS Discov* *25*, 869-894. 10.1177/2472555220922802.
176. Huszar, S., Chibale, K., and Singh, V. (2020). The quest for the holy grail: new antitubercular chemical entities, targets and strategies. *Drug Discov Today* *25*, 772-780. 10.1016/j.drudis.2020.02.003.
177. Abrahams, K.A., and Besra, G.S. (2020). Mycobacterial drug discovery. *RSC Med Chem* *11*, 1354-1365. 10.1039/d0md00261e.
178. Collins, L., and Franzblau, S.G. (1997). Microplate alamar blue assay versus BACTEC 460 system for high-throughput screening of compounds against *Mycobacterium tuberculosis* and *Mycobacterium avium*. *Antimicrob Agents Chemother* *41*, 1004-1009. 10.1128/AAC.41.5.1004.
179. Ekins, S., Reynolds, R.C., Franzblau, S.G., Wan, B., Freundlich, J.S., and Bunin, B.A. (2013). Enhancing hit identification in *Mycobacterium tuberculosis* drug discovery using validated dual-event Bayesian models. *PLoS One* *8*, e63240. 10.1371/journal.pone.0063240.
180. Mak, P.A., Rao, S.P., Ping Tan, M., Lin, X., Chyba, J., Tay, J., Ng, S.H., Tan, B.H., Cherian, J., Duraiswamy, J., et al. (2012). A high-throughput screen to identify inhibitors of ATP homeostasis in non-replicating *Mycobacterium tuberculosis*. *ACS Chem Biol* *7*, 1190-1197. 10.1021/cb2004884.
181. Manjunatha, U.H., and Smith, P.W. (2015). Perspective: Challenges and opportunities in TB drug discovery from phenotypic screening. *Bioorg Med Chem* *23*, 5087-5097. 10.1016/j.bmc.2014.12.031.
182. Stefan, M.A., Velazquez, G.M., and Garcia, G.A. (2020). High-throughput screening to discover inhibitors of the CarD.RNA polymerase protein-protein interaction in *Mycobacterium tuberculosis*. *Sci Rep* *10*, 21309. 10.1038/s41598-020-78269-3.
183. Herrmann, J., Rybniker, J., and Muller, R. (2017). Novel and revisited approaches in antituberculosis drug discovery. *Curr Opin Biotechnol* *48*, 94-101. 10.1016/j.copbio.2017.03.023.
184. von Amburen, J., Schreiber, F., Fischer, J., Winter, S., van Gumpel, E., Simonis, A., and Rybniker, J. (2020). Comprehensive Host Cell-Based Screening Assays for Identification of Anti-Virulence Drugs Targeting *Pseudomonas aeruginosa* and *Salmonella Typhimurium*. *Microorganisms* *8*. 10.3390/microorganisms8081096.
185. Malin, J.J., Winter, S., van Gumpel, E., Plum, G., and Rybniker, J. (2019). Extremely Low Hit Rate in a Diverse Chemical Drug Screen Targeting *Mycobacterium abscessus*. *Antimicrob Agents Chemother* *63*. 10.1128/AAC.01008-19.

186. Bloemberg, G.V., Keller, P.M., Stucki, D., Trauner, A., Borrell, S., Latshang, T., Coscolla, M., Rothe, T., Homke, R., Ritter, C., et al. (2015). Acquired Resistance to Bedaquiline and Delamanid in Therapy for Tuberculosis. *N Engl J Med* *373*, 1986-1988. 10.1056/NEJMc1505196.
187. Willby, M., Sikes, R.D., Malik, S., Metchock, B., and Posey, J.E. (2015). Correlation between GyrA substitutions and ofloxacin, levofloxacin, and moxifloxacin cross-resistance in *Mycobacterium tuberculosis*. *Antimicrob Agents Chemother* *59*, 5427-5434. 10.1128/AAC.00662-15.
188. Li, M.C., Lu, J., Lu, Y., Xiao, T.Y., Liu, H.C., Lin, S.Q., Xu, D., Li, G.L., Zhao, X.Q., Liu, Z.G., et al. (2021). rpoB Mutations and Effects on Rifampin Resistance in *Mycobacterium tuberculosis*. *Infect Drug Resist* *14*, 4119-4128. 10.2147/IDR.S333433.
189. Torres, J.N., Paul, L.V., Rodwell, T.C., Victor, T.C., Amallraja, A.M., Elghraoui, A., Goodmanson, A.P., Ramirez-Busby, S.M., Chawla, A., Zadorozhny, V., et al. (2015). Novel katG mutations causing isoniazid resistance in clinical *M. tuberculosis* isolates. *Emerg Microbes Infect* *4*, e42. 10.1038/emi.2015.42.
190. Dover, L.G., Alahari, A., Gratraud, P., Gomes, J.M., Bhowruth, V., Reynolds, R.C., Besra, G.S., and Kremer, L. (2007). EthA, a common activator of thiocarbamide-containing drugs acting on different mycobacterial targets. *Antimicrob Agents Chemother* *51*, 1055-1063. 10.1128/AAC.01063-06.
191. Mabhula, A., and Singh, V. (2019). Drug-resistance in *Mycobacterium tuberculosis*: where we stand. *Medchemcomm* *10*, 1342-1360. 10.1039/c9md00057g.
192. Di, L., and Kerns, E.H. (2009). Stability challenges in drug discovery. *Chem Biodivers* *6*, 1875-1886. 10.1002/cbdv.200900061.
193. Portelli, S., Phelan, J.E., Ascher, D.B., Clark, T.G., and Furnham, N. (2018). Understanding molecular consequences of putative drug resistant mutations in *Mycobacterium tuberculosis*. *Sci Rep* *8*, 15356. 10.1038/s41598-018-33370-6.
194. Amado, P.S.M., Woodley, C., Cristiano, M.L.S., and O'Neill, P.M. (2022). Recent Advances of DprE1 Inhibitors against *Mycobacterium tuberculosis*: Computational Analysis of Physicochemical and ADMET Properties. *ACS Omega* *7*, 40659-40681. 10.1021/acsomega.2c05307.
195. Shetye, G.S., Franzblau, S.G., and Cho, S. (2020). New tuberculosis drug targets, their inhibitors, and potential therapeutic impact. *Transl Res* *220*, 68-97. 10.1016/j.trsl.2020.03.007.
196. Sethiya, J.P., Sowards, M.A., Jackson, M., and North, E.J. (2020). MmpL3 Inhibition: A New Approach to Treat Nontuberculous Mycobacterial Infections. *Int J Mol Sci* *21*. 10.3390/ijms21176202.
197. Kapp, E., Calitz, H., Streicher, E.M., Dippenaar, A., Egieyeh, S., Jordaan, A., Warner, D.F., Joubert, J., Malan, S.F., and Sampson, S.L. (2023). Discovery and biological evaluation of an adamantyl-amide derivative with likely MmpL3 inhibitory activity. *Tuberculosis (Edinb)* *141*, 102350. 10.1016/j.tube.2023.102350.
198. Abrahams, K.A., Cox, J.A.G., Futterer, K., Rullas, J., Ortega-Muro, F., Loman, N.J., Moynihan, P.J., Perez-Herran, E., Jimenez, E., Esquivias, J., et al. (2017). Inhibiting mycobacterial tryptophan synthase by targeting the inter-subunit interface. *Sci Rep* *7*, 9430. 10.1038/s41598-017-09642-y.
199. Wellington, S., Nag, P.P., Michalska, K., Johnston, S.E., Jedrzejczak, R.P., Kaushik, V.K., Clatworthy, A.E., Siddiqi, N., McCarren, P., Bajrami, B., et al. (2017). A small-molecule allosteric inhibitor of *Mycobacterium tuberculosis* tryptophan synthase. *Nat Chem Biol* *13*, 943-950. 10.1038/nchembio.2420.
200. Michalska, K., Chang, C., Maltseva, N.I., Jedrzejczak, R., Robertson, G.T., Gusovsky, F., McCarren, P., Schreiber, S.L., Nag, P.P., and Joachimiak, A. (2020). Allosteric

- inhibitors of Mycobacterium tuberculosis tryptophan synthase. *Protein Sci* 29, 779-788. 10.1002/pro.3825.
201. Rhee, S., Parris, K.D., Ahmed, S.A., Miles, E.W., and Davies, D.R. (1996). Exchange of K⁺ or Cs⁺ for Na⁺ induces local and long-range changes in the three-dimensional structure of the tryptophan synthase alpha2beta2 complex. *Biochemistry* 35, 4211-4221. 10.1021/bi952506d.
 202. Rowlett, R., Yang, L.H., Ahmed, S.A., McPhie, P., Jhee, K.H., and Miles, E.W. (1998). Mutations in the contact region between the alpha and beta subunits of tryptophan synthase alter subunit interaction and intersubunit communication. *Biochemistry* 37, 2961-2968. 10.1021/bi972286z.
 203. Ngo, H., Harris, R., Kimmich, N., Casino, P., Niks, D., Blumenstein, L., Barends, T.R., Kulik, V., Weyand, M., Schlichting, I., and Dunn, M.F. (2007). Synthesis and characterization of allosteric probes of substrate channeling in the tryptophan synthase henzyme complex. *Biochemistry* 46, 7713-7727. 10.1021/bi700385f.
 204. Niks, D., Hilario, E., Dierkers, A., Ngo, H., Borchardt, D., Neubauer, T.J., Fan, L., Mueller, L.J., and Dunn, M.F. (2013). Allostery and substrate channeling in the tryptophan synthase henzyme complex: evidence for two subunit conformations and four quaternary states. *Biochemistry* 52, 6396-6411. 10.1021/bi400795e.
 205. Chang, C., Michalska, K., Maltseva, N.I., Jedrzejczak, R., McCarren, P., Nag, P.P., Joachimiak, A., Center for Structural Genomics of Infectious Diseases (CSGID) (2019). Crystal structure of tryptophan synthase from *M. tuberculosis* - aminoacrylate- and GSK1-bound form. <https://www.rcsb.org/structure/6USA>.
 206. Rybniker, J., Kohl, T.A., Barilar, I., and Niemann, S. (2019). No Evidence for Acquired Mutations Associated with Cytochrome bc(1) Inhibitor Resistance in 13,559 Clinical Mycobacterium tuberculosis Complex Isolates. *Antimicrob Agents Chemother* 63. 10.1128/AAC.01317-18.
 207. Santajit, S., and Indrawattana, N. (2016). Mechanisms of Antimicrobial Resistance in ESKAPE Pathogens. *Biomed Res Int* 2016, 2475067. 10.1155/2016/2475067.
 208. Ford, C.A., Hurford, I.M., and Cassat, J.E. (2020). Antivirulence Strategies for the Treatment of Staphylococcus aureus Infections: A Mini Review. *Front Microbiol* 11, 632706. 10.3389/fmicb.2020.632706.
 209. Sharma, A.K., Dhasmana, N., Dubey, N., Kumar, N., Gangwal, A., Gupta, M., and Singh, Y. (2017). Bacterial Virulence Factors: Secreted for Survival. *Indian J Microbiol* 57, 1-10. 10.1007/s12088-016-0625-1.
 210. Kim, J.K., Silwal, P., and Jo, E.K. (2020). Host-Pathogen Dialogues in Autophagy, Apoptosis, and Necrosis during Mycobacterial Infection. *Immune Netw* 20, e37. 10.4110/in.2020.20.e37.
 211. Laborde, J., Deraeve, C., and Bernardes-Genisson, V. (2017). Update of Antitubercular Prodrugs from a Molecular Perspective: Mechanisms of Action, Bioactivation Pathways, and Associated Resistance. *ChemMedChem* 12, 1657-1676. 10.1002/cmdc.201700424.
 212. Tanina, A., Wohlkonig, A., Soror, S.H., Flipo, M., Villemagne, B., Prevez, H., Deprez, B., Moune, M., Peree, H., Meyer, F., et al. (2019). A comprehensive analysis of the protein-ligand interactions in crystal structures of Mycobacterium tuberculosis EthR. *Biochim Biophys Acta Proteins Proteom* 1867, 248-258. 10.1016/j.bbapap.2018.12.003.
 213. Frenois, F., Engohang-Ndong, J., Locht, C., Baulard, A.R., and Villeret, V. (2004). Structure of EthR in a ligand bound conformation reveals therapeutic perspectives against tuberculosis. *Mol Cell* 16, 301-307. 10.1016/j.molcel.2004.09.020.
 214. Flipo, M., Desroses, M., Lecat-Guillet, N., Villemagne, B., Blondiaux, N., Leroux, F., Piveteau, C., Mathys, V., Flament, M.P., Siepmann, J., et al. (2012). Ethionamide

- boosters. 2. Combining bioisosteric replacement and structure-based drug design to solve pharmacokinetic issues in a series of potent 1,2,4-oxadiazole EthR inhibitors. *J Med Chem* *55*, 68-83. 10.1021/jm200825u.
215. Flipo, M., Frita, R., Bourotte, M., Martinez-Martinez, M.S., Boesche, M., Boyle, G.W., Derimanov, G., Drewes, G., Gamallo, P., Ghidelli-Disse, S., et al. (2022). The small-molecule SMART751 reverses *Mycobacterium tuberculosis* resistance to ethionamide in acute and chronic mouse models of tuberculosis. *Sci Transl Med* *14*, eaaz6280. 10.1126/scitranslmed.aaz6280.
216. McFedries, A., Schwaid, A., and Saghatelian, A. (2013). Methods for the elucidation of protein-small molecule interactions. *Chem Biol* *20*, 667-673. 10.1016/j.chembiol.2013.04.008.
217. Meanwell, N.A. (2011). Improving drug candidates by design: a focus on physicochemical properties as a means of improving compound disposition and safety. *Chem Res Toxicol* *24*, 1420-1456. 10.1021/tx200211v.

8 Summary

Tuberculosis (TB) is a communicable disease that is responsible for serious health problems around the globe. TB is caused by *Mycobacterium tuberculosis* (*Mtb*) and can be effectively treated with an extensive treatment regimen. However, incompetent application of this regimen is the cause for the prevalent emergence of multidrug-resistant *Mtb* strains, which are no longer sensitive to first-line antibiotics. Furthermore, the current drug development pipeline for novel antibiotics targeting *Mtb*, while promising, still lacks the diversity of targets needed to introduce a variety of novel mechanisms of action. This circumstance is partly caused by the robustness of *Mtb* against bioactive compounds. The major reason for this is the unique, impermeable cell wall containing additional layers of mycolic acids. An alternative approach to conventional antibiotics is the adjunct application of anti-virulence drugs. These compounds target specific mycobacterial components or substrates (virulence factors) that are essential for the host cell infection by *Mtb*. As a result, the pathogen's efficacy in infection is compromised and it can potentially be more easily cleared by the host. The most notable virulence factor of *Mtb* is the type VII secretion system ESX-1 and its substrates EsxA and EsxB.

In this thesis, 60,000 compounds were tested in a medium-throughput screening for anti-*Mtb* activity. This screening utilized different combinatorial applications of the screening platform by combining testing for growth inhibitory activity and host cell survival (cytoprotection) during *Mtb* infection. This includes both conventionally antibiotically active compounds as well as anti-virulence compounds, which show no antibiotic activity but still exhibit cytoprotective activity against *Mtb*. Investigation of the genome of *Mtb* mutants resistant to the antibiotics revealed putative modes of action associated with cell wall biogenesis, amino acid production and the respiratory chain. One notable compound (B6) inhibited the respiratory chain and additionally demonstrated great potential for combinatorial application with the frontrunner drug Q203, due to a unique cross-resistance pattern. Furthermore, several anti-virulence compounds exhibited inhibitory activity against ESX-1. Transcriptional analysis suggests that the compound S3 boosts the efficacy of the antibiotic prodrug ethionamide, which was subsequently confirmed by synergistic activity testing. Consequent analysis of structural analogues of this compound identified two similar molecules that also inhibit ESX-1 but differ in their respective booster effect. While one analogue (S3_106) did not exert this effect, the other (S3_100) similarly enhances the efficacy of ethionamide by utilizing a different molecular pathway for prodrug activation.

This thesis describes an early stage of drug discovery for two different, but potentially synergistic, classes of compounds with activity against *Mtb*, either antibiotic or anti-virulence. The discovered molecules and the deciphering of their modes of action show great potential and represent an important step progressing from drug discovery towards clinical application for combating multidrug-resistant *Mtb*.

9 Zusammenfassung

Tuberkulose (TB) ist eine Infektionskrankheit, die weltweit für ernsthafte Gesundheitsproblemen sorgt. TB wird durch *Mycobacterium tuberculosis* (*Mtb*) verursacht und kann effektiv mit einem aufwendigen Behandlungsschema behandelt werden. Allerdings kann die unsachgemäße Anwendung dieses Schemas zur Entstehung von multiresistenten *Mtb* Stämmen, welche nicht mehr auf First-Line-Antibiotika ansprechen, beitragen. Darüber hinaus fehlt es derzeit im Bereich der Wirkstoffentwicklung für neuartige Antibiotika gegen *Mtb* trotz vielversprechender Ansätze noch an der benötigten Vielfalt neuer Wirkungsmechanismen. Dieser Umstand ist teilweise auf die Robustheit von *Mtb* gegenüber bioaktiven Substanzen zurückzuführen. Der Hauptgrund dafür ist die einzigartige, undurchlässige Zellwand von *Mtb*, welche zusätzliche Schichten von Mykolsäuren enthält. Neben der Forschung an konventionellen Antibiotika werden aktuell auch alternative Ansätze verfolgt, wie zum Beispiel die adjunkte Anwendung von Anti-Virulenz-Wirkstoffen. Diese zielen auf spezifische mykobakterielle Komponenten oder Substrate (Virulenzfaktoren) ab, welche essentiell für die erfolgreiche Infektion der Wirtszelle durch *Mtb* sind. Durch die Hemmung von Virulenzfaktoren wird die Wirksamkeit des Erregers bei der Infektion stark beeinträchtigt und das Pathogen kann möglicherweise leichter vom Wirt bekämpft werden.

In dieser Arbeit wurde ein Screening mit medium-throughput durchgeführt, bei dem 60.000 Verbindungen auf ihre anti-*Mtb*-Aktivität getestet wurden. Dabei wurden die Substanzen auf verschiedene Eigenschaften geprüft, indem Tests auf wachstumshemmende Aktivität und Überleben der Wirtszellen (Zytoprotektion) während der *Mtb*-Infektion kombiniert wurden. Somit konnten sowohl herkömmliche antibiotisch wirksame Verbindungen als auch anti-Virulenz-Verbindungen identifiziert werden. Letztere zeichnen sich dadurch aus, dass sie explizit nicht das Wachstum von *MtB* hemmen, aber trotzdem Wirtszellen während der Infektion mit *Mtb* vor dem Zelltod schützen.

Um dem Wirkmechanismus der antibiotisch aktiven Substanzen auf den Grund zu gehen, wurde das Genom von *Mtb*-Mutanten, die gegen die jeweilige Verbindung resistent waren, analysiert. Diese Genomuntersuchung identifizierte verschiedene Proteine, welche im Zusammenhang mit der Zellwandbiogenese, der Aminosäureproduktion und mit der Atmungskette stehen, als mutmaßliche Ziele. Eine dieser Verbindungen (B6), welche die Atmungskette hemmt, zeigte auch großes Potenzial für eine kombinierte Anwendung mit dem Wirkstoff Q203. Darüber hinaus zeigten mehrere anti-Virulenz-Verbindungen eine hemmende Wirkung gegenüber dem Typ VII-Sekretionssystem ESX-1, welches einen der wichtigsten Virulenzfaktoren von *Mtb* darstellt. Eine folgende Transkriptionsanalyse ergab außerdem, dass die Verbindung S3 die Wirksamkeit des Antibiotikums Ethionamid verstärkt, was durch entsprechende synergistische Wachstumsexperimente nachgewiesen werden konnte. Bei der anschließenden Analyse von Strukturanaloga dieser Verbindung wurden Moleküle identifiziert, die ebenfalls ESX-1 hemmen, sich aber in ihrer jeweiligen verstärkenden Wirkung unterscheiden. Während das eine Analogon (S3_106) diese Wirkung nicht ausübte, verstärkte das andere (S3_100) die Wirksamkeit von Ethionamid in ähnlicher Weise, allerdings durch ein alternatives Enzym.

Insgesamt beschreibt diese Arbeit eine frühe Phase der Arzneimittelentdeckung für zwei unterschiedliche, aber potenziell synergistische Klassen von Verbindungen mit Aktivität, entweder antibiotisch oder anti-virulent, gegen *Mtb*. Die hier entdeckten Moleküle und die Entschlüsselung ihrer Wirkmechanismen zeigen großes Potenzial und stellen einen wichtigen Schritt auf dem Weg von der Arzneimittelentdeckung zur klinischen Anwendung gegen multiresistente *Mtb* dar.

10 List of Abbreviations

Abbreviation	Description
%	Percent
°C	Degree Celsius
µg, mg, g	Microgram, milligram, gram
µL, mL, L	Microliter, milliliter, litre
µM, mM, M	Micromolar/millimolar/molar
ACP	Acyl carrier protein reductase
ADME	Absorption, distribution, metabolism and excretion
ADP	Adenosine diphosphate
Ag85	Antigen 85 complex
AmbA/B/C	Arabinosyltransferase A/B/C
ANOVA	Analysis of variance
ATP	Adenosine triphosphate
BCG	Bacillus Calmette-Guérin
BDQ	Bedaquiline
BTZ	Benzothiazinone
BWA-MEM	Burrow-Wheeler Aligner algorithm
cDNA	Complementary DNA
CFP-10	Culture filtrate protein 10 kDa
CO ₂	Carbon dioxide
COVID-19	Coronavirus disease 2019
CTAB	Cetyltrimethylammonium bromide
cydB	Subunit II of the cytochrome bd-I complex
DAPI	4',6-diamidino-2-phenylindole
DMSO	Dimethyl sulfoxide
DNA	Desoxyribonucleic acid
DprE1	Decaprenylphosphoryl-β-D-ribofuranose-2-epimerase 1/2
dsred2	Discosoma Red Fluorescent Protein
DUF	Domain of unknown function
EC	Effective concentration
EC ₅₀	Half maximal effective concentration
EccA/B/Ca/Cb/D/E	ESX conserved components B/Ca/Cb/D/E

10 List of Abbreviations

Abbreviation	Description
EDTA	Ethylenediaminetetraacetic acid
eGFP	Enhanced green fluorescent protein
ELISA	Enzyme-linked immunosorbent assay
embA/B/C	Probable arabinosyltransferase A/B/C
EMSA	Electrophoretic mobility shift assay
ESAT-6	Early secreted antigenic target 6 kDa <i>Enterococcus faecium</i> , <i>Staphylococcus aureus</i> , <i>Klebsiella</i>
ESKAPE	<i>pneumoniae</i> , <i>Acinetobacter baumannii</i> , <i>Pseudomonas aeruginosa</i> and <i>Enterobacter</i> species
EspA/B/C/D/E/G/J/K/M/R	ESX-1 secretion-associated protein A/B/C/D/G/M/R
ETH	Ethionamide
ETH-NAD	Ethionamide NAD adduct
FBS	Fetal bovine serum
FSA	Fibroblast survival assay
gDNA	Genomic DNA
Genta	Gentamycin
Gpx4	Glutathione peroxidase-4
gyrA/B	Gyrase A/B
h	Hours
HIV	Human immunodeficiency virus
HSP65	Heat shock protein 65
IFN- γ	Interferon γ
IL-1 β /2/6/8/10/18	Interleukin-1 β /2/6/8/10/18
indels	Insertions and deletions
INH	Isoniazid
INH-NAD	Isoniazid NAD adduct
kDa	Kilo dalton
LPZS	Lansoprazole sulfide
<i>M caprae</i>	<i>Mycobacterium caprae</i>
<i>M. africanum</i>	<i>Mycobacterium africanum</i>
<i>M. bovis</i>	<i>Mycobacterium bovis</i>
<i>M. canetti</i>	<i>Mycobacterium canetti</i>
<i>M. microti</i>	<i>Mycobacterium microti</i>

10 List of Abbreviations

Abbreviation	Description
<i>M. pinnipedii</i>	<i>Mycobacterium pinnipedii</i>
<i>Mabs</i>	<i>Mycobacterium abscessus</i>
MCP-1	Monocyte chemoattractant protein-1
MDR	Multidrug-resistant
MIC	Minimal inhibitory concentration
MIC ₉₀	90% minimal inhibitory concentration
MIP-1 α	Macrophage inflammatory protein-1 α
MLKL	Mixed lineage kinase domain-like protein
MmpL3	Mycobacterial membrane protein large 3
MOI	Multiplicity of infection
MptpB	<i>Mtb</i> protein-tyrosine-phosphatase B
mRNA	Messenger ribnucleic acid
<i>Mtb</i>	<i>Mycobacterium tuberculosis</i>
NAD	Nicotinamide adenine dinucleotide; oxidierte Form
NADH	Nicotinamide adenine dinucleotide; reduzierte Form
NGS	Next-generation sequencing
NLRP3	NLR family pyrin domain containing 3
nm/ μ m/mm/m	Nanometer/micrometer/millimeter/meter
OD ₅₆₀	Optical density at 560 nm
PBMC	Peripheral blood mononuclear cell
PBS	Phosphate-buffered saline
PCR	Polymerase chain reaction
PE35	Pro-Glu family protein 35
Pks13	Polyketide synthase 13
PMA	Phorbol 12-myristate 13-acetate
PGRS genes	Polymorphic GC-rich gene sequences
PPE68	Pro-Pro-Glu family protein 68
Q203	Imidazopyridine
QcrB	Cytochrome bc1 complex cytochrome b subunit
qRT-PCR	Quantitative real-time PCR
RD1	Region of difference 1
REMA	Resazurin microtiter assay
RIF	Rifampicin

10 List of Abbreviations

Abbreviation	Description
RIPK1/3	Receptor-interacting protein kinase 1/3
RNA	Ribonucleic acid
RNA-Seq	Sequencing of transcriptome (total RNA)
RND	Resistance-nodulation-division superfamily
RPMI	Roswell Park Memorial Institute medium
RR	Rifampicin resistant
SapM	Secreted acid phosphatase M
SARS	Structure activity relationship study
SDS-PAGE	Sodium dodecyl-sulfate polyacrylamide gel electrophoresis
Sec2	Sec-mediated secretory pathways
SNP	Single nucleotide polymorphism
ST	<i>Salmonella enterica</i> subsp. <i>enterica</i> ser. Typhimurium
TAT	Twin-arginine translocation
TB	Tuberculosis
TNF- α	Tumor necrosis factor α
TNFR1	Tumor necrosis factor receptor 1
tRNA	Transfer ribonucleic acid
TSA	Thermal shift assay
WGS	Whole genome sequencing
WHO	World Health Organisation
WT	Wildtype
XDR	Extensively drug-resistant
Zmp1	Zinc peptidase

11 List of Tables

Table 1: Overview of the global clinical development pipeline for new anti- <i>Mtb</i> drugs in 2022.	11
Table 2: Overview of hit compounds with growth inhibitory activity.....	32
Table 3: Overview of hit compounds with anti-virulence activity.....	51

12 List of Figures

Figure 1: Estimated number of incident cases of MDR/RR-TB in 2021 for countries with at least 1000 incident cases.	8
Figure 2: Schematic overview of antibiotic targets in <i>Mycobacterium tuberculosis</i>	10
Figure 3: Schematic overview of the plasma membrane, cell wall and cell envelope of <i>Mycobacterium tuberculosis</i>	12
Figure 4: Schematic overview of the respiratory chain of <i>Mycobacterium tuberculosis</i>	15
Figure 5: Schematic overview of anti-virulence targets in <i>Mycobacterium tuberculosis</i>	17
Figure 6: Conserved aspects of ESX-1 protein transport in <i>M. tuberculosis</i>	20
Figure 7: Schematic overview of the utilized screening approaches.	28
Figure 8: Schematic overview of utilized pipeline for target identification.....	30
Figure 9: MIC shift of compounds after pre-incubation at 37°C.	31
Figure 10: Compound B5 shows potential anti-mycobacterial activity by inhibiting L-tryptophan biosynthesis.	34
Figure 11: Screening for anti-virulence compounds.	49
Figure 12: Representative Western blots of samples taken from <i>Mtb</i> cultures after exposure to anti-virulence compounds.	52

13 Affidavit / Eidesstattliche Erklärung

Hiermit versichere ich an Eides statt, dass ich die vorliegende Dissertation selbstständig und ohne die Benutzung anderer als der angegebenen Hilfsmittel und Literatur angefertigt habe. Alle Stellen, die wörtlich oder sinngemäß aus veröffentlichten und nicht veröffentlichten Werken dem Wortlaut oder dem Sinn nach entnommen wurden, sind als solche kenntlich gemacht. Ich versichere an Eides statt, dass diese Dissertation noch keiner anderen Fakultät oder Universität zur Prüfung vorgelegen hat; dass sie - abgesehen von unten angegebenen Teilpublikationen und eingebundenen Artikeln und Manuskripten - noch nicht veröffentlicht worden ist sowie, dass ich eine Veröffentlichung der Dissertation vor Abschluss der Promotion nicht ohne Genehmigung des Promotionsausschusses vornehmen werde. Die Bestimmungen dieser Ordnung sind mir bekannt. Darüber hinaus erkläre ich hiermit, dass ich die Ordnung zur Sicherung guter wissenschaftlicher Praxis und zum Umgang mit wissenschaftlichem Fehlverhalten der Universität zu Köln gelesen und sie bei der Durchführung der Dissertation zugrundeliegenden Arbeiten und der schriftlich verfassten Dissertation beachtet habe und verpflichte mich hiermit, die dort genannten Vorgaben bei allen wissenschaftlichen Tätigkeiten zu beachten und umzusetzen. Ich versichere, dass die eingereichte elektronische Fassung der eingereichten Druckfassung vollständig entspricht.



Raphael Gries

Included Publications

- **Gries, R.**, Dal Molin, M., Chhen, J., van Gumpel, E., Dreyer, V., Niemann, S., and Rybniker, J. (2023). Characterization of Two Novel Inhibitors of the Mycobacterium tuberculosis Cytochrome bc(1) Complex. *Antimicrob Agents Chemother* 67, e0025123. 10.1128/aac.00251-23.
- **Gries, R.**, Chhen, J., van Gumpel, E., Theobald, S., Sonnenkalb, L., Utpatel, C., Metzen, F., Koch, M., Dallenga, T., Djaout, K., Baulard, A., Dal Molin, M., Rybniker, J (2023). Discovery of dual-active ethionamide boosters inhibiting the Mycobacterium tuberculosis ESX-1 secretion system. *Cell Chem Biol.* 10.1016/j.chembiol.2023.12.007.

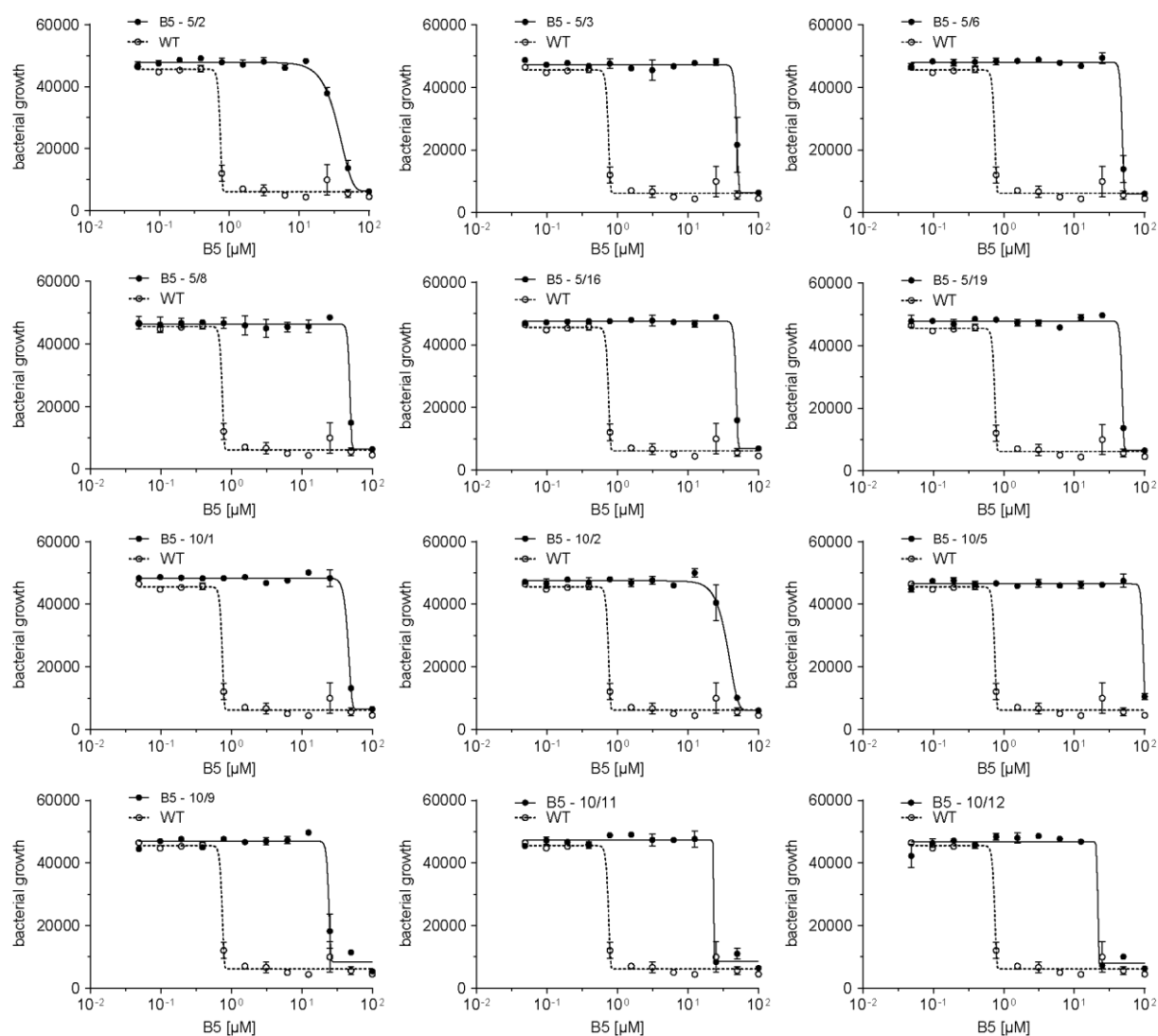
Additional Publications

- **Gries, R.**, Sala, C., and Rybniker, J. (2020). Host-Directed Therapies and Anti-Virulence Compounds to Address Anti-Microbial Resistant Tuberculosis Infection. *Applied Sciences-Basel* 10. ARTN 2688.

Conference Contributions

- DGI-DZIF Joint Annual Meeting 2022; Scientific Poster
- Internal Med I Retreat 2020; Scientific Poster
- Internal Med I Retreat 2022; Scientific Poster

14 Appendix



Appendix Figure 1: Shift of MIC of mutants resistant to B5. Shown is bacterial growth (REMA) of the *Mtb* parental wild type strain and of selected strains with spontaneous mutations exhibiting increased resistance to the compound B5, in the presence of different concentrations of the compound B5.